

**Willard Spur Nutrient Cycling**  
**Report January 2014**  
**to the Willard Spur Science Panel**

**Investigators:**

**Heidi Hoven, William Johnson, David Richards,  
Sam Rushforth, Sarah Rushforth, Ramesh Goel**

**Graduate Researchers:**

**Mitch Hogsett, Sarah Kissell, Ramin Nasrabadi, Joel Pierson**

## Table of Contents

<b>List of Figures</b> .....	<b>5</b>
<b>List of Tables</b> .....	<b>9</b>
<b>1. INTRODUCTION</b> .....	<b>10</b>
<b>1.1 Great Salt Lake Wetlands</b> .....	<b>10</b>
<b>2. WILLARD SPUR NUTRIENT CYCLING</b> .....	<b>12</b>
<b>2.1 Background: Willard Spur Nutrient Cycling</b> .....	<b>12</b>
<b>2.2 Methods</b> .....	<b>14</b>
2.2.1 Experimental Design.....	14
2.2.1.1 2012 Nutrient Cycling Plots .....	14
2.2.1.1.1 Plot Location and Dimensions.....	14
2.2.1.1.2 Amendment Ranges .....	15
2.2.1.1.3 Fertilizer Amendments.....	16
2.2.1.1.4 Sample Schedule.....	16
2.2.1.2 2013 Nutrient Cycling Plots .....	16
2.2.1.2.1 Plot Location and Dimensions.....	16
2.2.1.2.2 Amendment Ranges .....	17
2.2.1.2.3 Fertilizer Amendments.....	17
2.2.1.2.4 Sample Schedule.....	19
2.2.2 Field Methods .....	19
2.2.3 Laboratory Methods .....	20
2.2.3.1 Surface Water Methods.....	20
2.2.3.2 Sediment Methods.....	21
2.2.4 Release Rate Experiments.....	21
2.2.4.1 Bucket Release Rate Tests .....	21
2.2.4.2 Mesocosm Release Rate Tests.....	22
<b>2.3 Sediment and Surface Water Chemistry Results</b> .....	<b>22</b>
2.3.1 2012 Field Results .....	23
2.3.1.1 2012 Surface Water .....	23
2.3.1.1.1 Trace Elements.....	23
2.3.1.1.2 Nutrients .....	23
2.3.1.2 2012 Sediment.....	25
2.3.1.2.1 Trace Elements.....	26
2.3.1.2.2 Nutrients .....	26
2.3.1.2.3 C/N Isotopes.....	27
2.3.3 2013 Results.....	29
2.3.3.1 2013 Surface Water .....	29
2.3.3.2 2013 Sediment.....	31
2.3.3 Quantifying Nutrient Release Rates to Water Column .....	33
2.3.3.1 Bucket Test Results.....	33
2.3.3.2 Mesocosm Test Results .....	35
2.3.3.3 Determining Nutrient Release Rate Constants from Buckets and Mesocosms.....	36
2.3.3.4 Mesocosm Nutrient Removal Rates.....	42
2.3.3.5 Willard Spur Nutrient Removal Rates.....	43
<b>2.4 Water and Sediment Discussion</b> .....	<b>43</b>
<b>2.5 Water and Sediment Summary</b> .....	<b>48</b>

<b>3. 2013 VEGETATIVE RESPONSE .....</b>	<b>49</b>
<b>3.1. Summary of 2012 Significant Biological Indicators and 2013 Research Objectives .....</b>	<b>49</b>
<b>3.2 Vegetative Metric Methods .....</b>	<b>49</b>
3.2.1 Field Methods .....	49
3.2.2 Statistical Analyses .....	50
3.2.2.1 Bioindicators.....	50
3.2.2.2 Establishing an Ecological Time-frame for Statistical Comparisons .....	50
3.2.2.3 Thresholds .....	51
<b>3.3 2013 Vegetative Response Results .....</b>	<b>51</b>
3.3.1 Ambient data.....	51
3.3.2 Vegetation Metrics.....	52
3.3.3 2013 Plant Tissue Nutrients.....	60
<b>3.4 2013 Metric Analysis and Bioindicator Selection.....</b>	<b>71</b>
3.4.1 Metric Selection .....	71
3.4.4 Metric Response Thresholds.....	72
3.4.4.1 % Algae on SAV .....	72
3.4.4.2 %BDS on SAV.....	73
3.4.4.3 Total Alkalinity.....	74
3.4.4.4 Branch Density.....	75
3.4.4.5 Condition Index .....	76
<b>3.5 CART vs. Multiple Regression .....</b>	<b>77</b>
3.5.1 Relationships between metric predictors.....	78
<b>3.6 Bioindicator Metric Thresholds.....</b>	<b>78</b>
<b>3.7 Discussion .....</b>	<b>79</b>
<b>3.8 Summary of Project DQO's .....</b>	<b>81</b>
<b>APPENDIX A. Water and Sediment Chemistry .....</b>	<b>83</b>
<b>A.1 Methods .....</b>	<b>83</b>
<b>A.2 Rate Constant Regression .....</b>	<b>89</b>
<b>A.3 Results.....</b>	<b>97</b>
A.3.1 2012 Surface Water .....	97
A.3.2 2012 Sediment Results.....	106
A.3.3 2013 Surface Water .....	112
A.3.4 2013 Sediment Results.....	119
<b>APPENDIX B. Nutrient spiking experiment using “Square Chambers” in Willard Spur .....</b>	<b>122</b>
<b>B.1 Overall Objective .....</b>	<b>122</b>
<b>B.2 Chamber Details and Methodology.....</b>	<b>122</b>
B.2.1 Chamber Details and installation.....	122
B.2.2 Spiked nutrient concentrations .....	124
B.2.3 Sample collection and analysis.....	124
<b>B.3 Results and Discussion.....</b>	<b>125</b>
<b>B.4 Conclusions.....</b>	<b>128</b>
<b>APPENDIX C. Box plots of control and ambient metrics and H2O depth at eleven sampling dates 2013. ....</b>	<b>130</b>
<b>APPENDIX D. Metric Evaluation.....</b>	<b>132</b>
<b>APPENDIX E. Comparison between cumulative degree days and Julian Date</b>	<b>135</b>

<b>APPENDIX F. Correlation matrix (Pearson) of CART chemical and physical parameters of surface water samples .....</b>	<b>136</b>
<b>REFERENCES .....</b>	<b>137</b>

## List of Figures

Figure 2.1. Image provided by the Utah DWQ. URL: <a href="http://www.willardspur.utah.gov/images/maps/willardspurgenerallocation.jpg">http://www.willardspur.utah.gov/images/maps/willardspurgenerallocation.jpg</a>	12
Figure 2.2. False color images show the proliferation of vegetation (represented in red) in the Willard Spur, contrasted by Willard Bay and Great Salt Lake Minerals, Inc. to the south and impounded wetlands in the BRMBR to the north.	13
Figure 2.3. 2012 plots are shown in red and light blue; 2013 plots are shown in dark blue. Yellow circles indicate locations where PWRWTP effluent is discharged directly into the Willard Spur.	15
Figure 2.4. Amendment techniques for a) 2012: Plant debris collecting on ropes within the plots. The darker areas show where the mat was sufficiently dense enough to collapse onto the plants below. b) 2013: Underwater photo of submerged fertilizer bags attached to a stake and embedded in the sediment.	18
Figure 2.5. Sediment squeezer apparatus with attached syringe filters and syringes.	20
Figure 2.6. Surface water concentrations for a) dissolved $\text{NO}_2\text{-N} + \text{NO}_3\text{-N}$ correspond with b) dissolved phosphate concentrations showing elevated levels in the high water column plot during 2012. Error bars represent one standard deviation ( $n=3$ except for June samples where $n=4$ , excluding Control Water Column where $n=3$ ). All bar plots that show concentrations in plots through time are arranged chronologically from left to right (e.g. bars in Figure 6 in the High Sediment plot represent 26-Jun, 24-Jul, 28-Aug, 25-Sep, and 30-Oct from left to right).	24
Figure 2.7. Significant variation between amendments and controls was observed in 2012 for a) dissolved $\text{NO}_2\text{-N} + \text{NO}_3\text{-N}$ and b) dissolved P averages from June and July. Error bars represent one standard deviation ( $n=12$ for all locations except for Ambient where $n=4$ ).	25
Figure 2.8. Elevated concentrations are observed in sediment-amended plots of a) nitrate and b) available phosphorus and nitrate. Error bars for June results represent one standard deviation ( $n=3$ ).	27
Figure 2.9. Isotope ratio mass spectrometry (IRMS) sediment results show enriched $\delta^{15}\text{N}$ values in the amended sediment plots. Error bars for June and November results represent one standard deviation ( $n=3$ ).	28
Figure 2.10. Average $\Delta^{15}\text{N}$ values indicate fractionation in the sediment amendment plots. For each month, $\delta^{15}\text{N}$ values from control plots were subtracted from $\delta^{15}\text{N}$ values from sediment amendments during 2012 ( $n=3$ for SAV leaves and $n=7$ for sediment).	28
Figure 2.11. 2013 surface water concentrations for dissolved a) $\text{NO}_2\text{-N} + \text{NO}_3\text{-N}$ and b) dissolved P do not show a clear trend between amendment and control plots.	30
Figure 2.12. Significant variation between amendments and controls was not observed in 2013 for a) dissolved $\text{NO}_2\text{-N} + \text{NO}_3\text{-N}$ and b) dissolved P averages from June and July. Error bars represent one standard deviation ( $n=12$ for all locations except for Ambient where $n=4$ ).	31
Figure 2.13. In 2013 total $\delta^{15}\text{N}$ values were similar between amended and control plots.	32
Figure 2.14. $\delta^{15}\text{N}$ values from 2013 high water column plots in sediment horizons between 0 and 10 cm.	32
Figure 2.15. Results from bucket dissolution tests for a) $\text{NO}_3\text{-N}$ and b) $\text{PO}_4\text{-P}$ . White areas indicate temperatures averaging 13 °C (volume of water for test = 11.3 L). Red shading indicates outdoor tests and temperatures averaging 29 °C (volume = 9.5 L).	34
Figure 2.16. Mass of nutrients in the water column for a) the Osmocote™ amendment and b) the 2013 mix amendment.	36
Figure 2.17. Release rate constants for $\text{NO}_3\text{-N}$ and $\text{PO}_4\text{-P}$ for the range of times fertilizer is submerged and water temperatures. Open circles represent discrete rate constants from the bucket and mesocosm tests. Note the different scale on the 2012 $\text{NO}_3\text{-N}$ rate constant color bar.	39
Figure 2.18. Release rate constants for $\text{NO}_3\text{-N}$ and $\text{PO}_4\text{-P}$ for each day during the 2012 and 2013 sampling periods.	40
Figure 2.19. Daily release rates of $\text{NO}_3\text{-N}$ and $\text{PO}_4\text{-P}$ into the water column from the nutrient amendments during the 2012 and 2013 sampling periods.	41
Figure 2.20. Summary of delivery of $\text{NO}_3\text{-N}$ and TP to the water column from fertilizer amendments estimated using release rates ( $k_{\text{release}}$ ). Shaded area indicates 2012 plots.	42
Figure 2.21. Comparison of estimated $\text{NO}_3\text{-N}$ and TP loads from 2012 nutrient amendments and PWRWTP.	44

Figure 2.22. Surface SAV branch coverage in a) high water column plot and b) low water column plot. Areal SAV coverage and color of SAV varied significantly between c) the high water column plot and d) the low water column plot. _____	47
Figure 3.1. Average water depth at the UUWS research plots during 2013. Box plots include median (line) and 25 <sup>th</sup> and 75 <sup>th</sup> percentiles. n = 5. _____	52
Figure 3.2. Mean percent total SAV in UUWS research plots during 2013. Box plots include median (line) and 25 <sup>th</sup> and 75 <sup>th</sup> percentiles. n = 5. _____	53
Figure 3.3. Mean percent forageable SAV in UUWS research plots during 2013. Box plots include median (line) and 25 <sup>th</sup> and 75 <sup>th</sup> percentiles. n = 5. _____	54
Figure 3.4. Branch density of SAV in UUWS research plots during 2013. Box plots include median (line) and 25 <sup>th</sup> and 75 <sup>th</sup> percentiles. n = 5. _____	55
Figure 3.5. Percent algal mat in UUWS research plots during 2013. Box plots include median (line) and 25 <sup>th</sup> and 75 <sup>th</sup> percentiles. n = 5. _____	56
Figure 3.6. Percent cover other mat in the UUWS research plots, consisting primarily of drift SAV, during 2013. Box plots include median (line) and 25 <sup>th</sup> and 75 <sup>th</sup> percentiles. n = 5. _____	57
Figure 3.7. Percent cover BDS on SAV leaves in the UUWS research plots during 2013. Box plots include median (line) and 25 <sup>th</sup> and 75 <sup>th</sup> percentiles. n = 5. _____	58
Figure 3.8. Percent algae on SAV in UUWS research plots during 2013. Box plots include median (line) and 25 <sup>th</sup> and 75 <sup>th</sup> percentiles. n = 5. _____	59
Figure 3.9. Condition index (CI) of SAV in the UUWS research plots during 2013. Box plots include median (line) and 25 <sup>th</sup> and 75 <sup>th</sup> percentiles. n = 5. _____	60
Figure 3.10. Comparison of $\delta^{15}\text{N}$ values by three dates and four treatments, 2013. Box plots include median (line) and 25 <sup>th</sup> and 75 <sup>th</sup> percentiles. _____	61
Figure 3.11. Comparison of percent weight nitrogen (Wt%N) in <i>Stuckenia filiformis</i> leaves by three dates and four treatments, 2013. Box plots include median (line) and 25 <sup>th</sup> and 75 <sup>th</sup> percentiles. _____	62
Figure 3.12. Percent N by weight in algae samples collected from SAV during the week of June 13 <sup>th</sup> , 2013. Box plots include median (line) and 25 <sup>th</sup> and 75 <sup>th</sup> percentiles; n = 3. _____	63
Figure 3.13. <i>S. filiformis</i> leaf phosphorous levels during 2013. Box plots include median (line) and 25 <sup>th</sup> and 75 <sup>th</sup> percentiles. n = 3. _____	64
Figure 3.14. Phosphorous levels of algae collected from SAV in UUWS research plots, during the week of June 13 <sup>th</sup> , 2013. Box plots include median (line) and 25 <sup>th</sup> and 75 <sup>th</sup> percentiles. n = 3. If the letters are different then there was a significant difference. If there are two letters together then there were ties. _____	65
Figure 3.15. Comparison of percent weight carbon (Wt%C) in <i>S. filiformis</i> leaves by three dates and four treatments, 2013. Box plots include median (line) and 25 <sup>th</sup> and 75 <sup>th</sup> percentiles. _____	67
Figure 3.16. Surface water pH during late morning to early afternoon, May 30 (May C), June 13 (June A), and June 27 (June B), in high, medium, low, control and ambient plots, 2013. _____	67
Figure 3.17. Total bicarbonate, aqueous phase from UUWS research plots during 2013. Red line indicates 30 mg·L <sup>-1</sup> HCO <sub>3</sub> <sup>-</sup> compensation point for <i>S. pectinatus</i> (Huebert & Gorham 1983). _____	68
Figure 3.18. Comparison of $\delta^{13}\text{C}$ ratios ( <sup>13</sup> C/ <sup>12</sup> C VPDB) by three dates and four treatments, 2013. Box plots include median (line) and 25 <sup>th</sup> and 75 <sup>th</sup> percentiles. _____	69
Figure 3.19. C:N ratios by three dates and four treatments, 2013. Box plots include median (line) and 25 <sup>th</sup> and 75 <sup>th</sup> percentiles. _____	71
Figure 3.20. CART model of percent macroalgae associated with SAV (as % Algae on SAV) at UU Willard Spur research plots, 2012 – 2013. _____	73
Figure 3.21. CART model of percent BDS (biofilm, diatoms, and / or sediment) associated with SAV (as % Algae on SAV) at UU Willard Spur research plots, 2012 – 2013. _____	74
Figure 3.22. CART model of percent total SAV, at UU Willard Spur research plots, 2012 – 2013. _____	75
Figure 3.23. CART model of branch density, at UU Willard Spur research plots, 2012 – 2013. (Note: Estimated branch density results in figure are back transformed log +1 values). _____	76
Figure 3.24. CART model of condition index (CI), at UU Willard Spur research plots, 2012 – 2013. _____	77
Figure A.1. The area of plots where sediment and water column was amended with Osmocote Smart Release™ fertilizer. _____	83
Figure A.2: Distribution of stakes and fertilizer in 2013 water column plots _____	88
Figure A.3. Dissolved trace element concentrations in for all elements measured. Error bars represent one standard deviation (n=4 excluding Control Water Column where n=3). _____	97

Figure A.4. Dissolved Nitrite + Nitrate and Dissolved P 2D plots for filtered surface water samples. Boundary values were set at 90% of lowest value measured in the plot (n=3 except for June samples where n=4, excluding June Control Water Column where n=3).	99
Figure A.5. Total Dissolved Solids for unfiltered surface water samples. Error bars represent one standard deviation (n=3 except for June samples where n=4, excluding June Control Water Column where n=3).	100
Figure A.6. Total Volatile Solids for unfiltered surface water samples. Error bars represent one standard deviation (n=3 except for June samples where n=4, excluding June Control Water Column where n=3).	101
Figure A.7. Dissolved Total Nitrogen for filtered surface water samples. Error bars represent one standard deviation (n=3 except for June samples where n=4, excluding June Control Water Column where n=3).	102
Figure A.8. Total ammonia for unfiltered surface water samples. Error bars represent one standard deviation (n=3 except for June samples where n=4, excluding June Control Water Column where n=3).	103
Figure A.9. TKN for unfiltered surface water samples. Error bars represent one standard deviation (n=3 except for June samples where n=4, excluding June Control Water Column where n=3).	104
Figure A.10. Unfiltered total phosphate (n=3 except for June samples where n=4, excluding June Control Water Column where n=3).	105
Figure A.11. Sediment trace metals represented by the concentration of trace elements in the extract. Error bars represent one standard deviation (n=3).	106
Figure A.12. Sediment nitrate and available phosphorus in amended sediment plots. Three samples were collected in random locations. Boundary values were set at 90% of lowest value measured in the plot (n=3 except for June samples where n=4, excluding June Control Water Column where n=3).	108
Figure A.13. Sediment C:N ratio. Error bars represent one standard deviation (n=3).	109
Figure A.14. Total weight percent nitrogen. Error bars represent one standard deviation (n=3).	110
Figure A.15. Total $\delta^{13}C_{PDB}$ . Error bars represent one standard deviation (n=3).	111
Figure A.16. Dissolved nitrite + nitrate and dissolved P 2D plots for filtered surface water samples. Error bars represent one standard deviation (n=3 except for June samples where n=4, excluding June Control Water Column where n=3).	112
Figure A.17. Total Dissolved Solids for unfiltered surface water samples. Error bars represent one standard deviation (n=3 except for June samples where n=4, excluding June Control Water Column where n=3).	113
Figure A.18. Total Volatile Solids for unfiltered surface water samples. Error bars represent one standard deviation (n=3 except for June samples where n=4, excluding June Control Water Column where n=3).	114
Figure A.19. Dissolved Total Nitrogen for filtered surface water samples. Error bars represent one standard deviation (n=3 except for June samples where n=4, excluding June Control Water Column where n=3).	115
Figure A.20. Total ammonia for unfiltered surface water samples. Error bars represent one standard deviation (n=3 except for June samples where n=4, excluding June Control Water Column where n=3).	116
Figure A.21. TKN for unfiltered surface water samples. Error bars represent one standard deviation (n=3 except for June samples where n=4, excluding June Control Water Column where n=3).	117
Figure A.22. Unfiltered total phosphate (n=3 except for June samples where n=4, excluding June Control Water Column where n=3).	118
Figure A.23. Sediment C:N ratio. Error bars represent one standard deviation (n=3).	119
Figure A.24. Total weight percent nitrogen. Error bars represent one standard deviation (n=3).	120
Figure A.25. Total $\delta^{13}C_{PDB}$ . Error bars represent one standard deviation (n=3).	121
Figure B.1. Site and Chamber Details; (A) site location, (B) sample photo showing installed chambers (WC chamber tied to stake to prevent falling over due to wind (left) and sediment chamber (right))	122
Figure B.2. Chambers installed for daytime and nighttime sampling	123
Figure B.3. NH <sub>3</sub> -N expressed as g/m <sup>3</sup> /day for water column and as g/m <sup>2</sup> /day for sediments in all chambers under low and high spikes.	126

<i>Figure B.4. NO<sub>3</sub>-N expressed as g/m<sup>3</sup>/day for water column and as g/m<sup>2</sup>/day for sediments in all chambers under low and high spikes.</i>	<i>127</i>
<i>Figure B.5. PO<sub>4</sub>-P expressed as g/m<sup>3</sup>/day for water column and as g/m<sup>2</sup>/day for sediments in all chambers under low and high spikes.</i>	<i>128</i>
<i>Figure C.1 Box plots of control and ambient metrics and H<sub>2</sub>O depth at eleven sampling dates 2013.</i>	<i>131</i>

## List of Tables

Table 2.1. Mass of nutrients in 2012 sediment and water column amendments.	16
Table 2.2. Nutrient mass in each amended water column plots.	17
Table 2.3. Release rate constants from bucket and mesocosm tests.	37
Table 2.4. Equations describing nutrient release rates ( $k_{\text{release}}$ ) for the 2012 and 2013 fertilizer mixtures.	38
Table 2.5. Comparison of nutrient release and removal rate constants in mesocosms.	43
Table 3.4.1 Response direction, seasonality and sensitivity of five bioindicators of nutrient enrichment based on on Kruskal-Wallis tests and box plot examination.	72
Table 3.5.1 OLS multiple regressions on variables used in CART	77
Table 3.6.1. Five proposed bioindicators; environmental variables most related to changes in each; approximate threshold levels; and the direction of change (based on CART)	78
Table A.1. Mass of fertilizer in 2012 sediment and water column plots.	85
Table A.2. Mass of fertilizer in 2013 water column amendment plots.	85
Table A.3. 2012 water and sediment chemistry and number of samples per metric, per treatment plot by month and total sample number for all 6 plots. The number of samples collected each month per plot is provided for each metric. ‡ = up to six plots.	86
Table A.4. 2013 water and sediment chemistry and number of samples per metric, per treatment plot and total sample number for the four plots. The number of samples collected each month is provided for each metric. Three samples were collected per plot one sample was collected at the ambient site.	87
Table B.1. Matrix of experiments with low concentrations of nutrients (Total 8 chambers)	124
Table B.2: Matrix of experiments with high concentrations of nutrients (total 8 chambers)	124
Table D.1. Kruskal-Wallis Tests for SAV and isotope metrics* (Date = Julian Date; Treatment = High, Medium, Low, and Control; DF = degrees of freedom; alpha = 0.05). Note: calendar dates are shown in Table D.2.	132
Table D.2. Multiple pairwise comparisons of treatment dates, 2013 on all metrics examined using the Steel-Dwass-Critchlow-Fligner (1984) two tailed test No algae comparisons were possible because there was only one collection date. (If upper case letters are the same then there was no significant difference between treatments at alpha = 0.05. If letters are different then there were significant differences. All metrics that were measured as percentages were arcsine transformed and Branch Density $m^2$ was log + 1 transformed prior to comparisons).	133
Table D.3. Multiple pairwise comparisons of the 2013 four nutrient treatments; high, medium, low, and control on all metrics examined using the Steel-Dwass-Critchlow-Fligner (1984) two- tailed test (If upper case letters are the same then there was no significant difference between treatments at alpha = 0.05. If letters are different then there were significant differences. All metrics that were measured as percentages were arcsine transformed and Branch Density/ $m^2$ was log + 1 transformed prior to comparisons.)	134
Table E.1 Comparison between cumulative degree days and Julian Date. Lower Threshold was set at 10 °C.	135
Table E.2. Pearson's correlation matrix of cumulative degree days vs. weekly Julian date	135
Table F.1 Correlation matrix (Pearson) of CART chemical and physical parameters of surface water samples	136

# 1. INTRODUCTION

## 1.1 Great Salt Lake Wetlands

Small wetlands and ponds are increasingly recognized in the scientific community as significant contributors to developing models of global cycles. Despite the small size of individual wetlands compared to larger inland lakes, recently updated inventories show that small lakes and ponds make up over half of the areal extent of inland water bodies, covering an estimated 4.2 million km<sup>2</sup> (Downing, 2010). The collective rate of carbon burial in impounded wetland and pond sediment is up to three orders of magnitude greater than large lakes and oceans (Downing, 2010). Additionally, this author notes that small water bodies support a higher concentration of species per area than large water bodies

The wetlands surrounding the Great Salt Lake are no exception. Over the past century the wetlands of the Great Salt Lake (GSL) have been recognized as dynamic and essential ecosystem for migratory waterfowl. An estimated 3-5 million waterfowl (Vest and Conover, 2011) and approximately 500,000 shore birds (Gorrell et al., 2005) rely on the GSL and its wetlands for food during migration each year. For several decades, research has been directed towards maximizing the GSL wetlands for waterfowl habitat and population (Bellrose and Low, 1978).

The Great Salt Lake has approximately 250,000 ha of freshwater wetlands on its north and east shorelines. Over 50,000 ha are managed, approximately 20,000 by private owners and 32,000 ha by federal and local government (Johnson, 2008). Managing freshwater inflows and water quality of these small water bodies is crucial for maintaining waterfowl habitat (Aldrich and Paul, 2002). Anthropogenic influences on the Great Salt Lake wetlands are extensive and, thus far, seem to be localized in the southeastern portion of the Lake where highest human population densities occur. The Jordan River is the primary input to Farmington Bay. Well over 1 million people live in the Jordan River watershed. Salt Lake County is home to 10 Superfund sites designated under Comprehensive Environmental Response, Compensation, and Liability Act (CERCLA). Most contamination is related to high trace metal content in soil and groundwater that is attributed to historic mining and smelting operations in the Salt Lake Valley (Waddell and Giddings, 2004). Agricultural runoff has also posed problems to the wetlands with high surface water nutrient concentrations measured in impounded wetlands throughout Farmington Bay (Hoven and Miller, 2009). As human communities expand in the northeastern region of the Lake's shores, additional pressures related to anthropogenic inputs to the Lake may have undesirable impacts on its wildlife and wetland resources.

The north end of the Lake is home to the U.S. Fish and Wildlife Service Bear River Migratory Bird Refuge (BRMBR, or Refuge) and includes approximately 74K acres, 41K of which is managed as wetland habitat. The Refuge attracts hundreds of thousands of shorebirds and water birds each year with its nesting and staging resources. Shorebird habitat is managed to support critical life stages of breeding birds such as American avocet, black-necked stilt, and snowy plover, among many others (Wildlife and Habitat). Up to 75 percent of the western population of tundra swans (more than 30,000 birds) use the Refuge for fall staging and wintering in mild years. The Refuge

is positioned in the Bear River Delta and extends into Willard Spur of Great Salt Lake. Willard Spur has been identified by the National Audubon Society as an Important Bird Area as its aquatic resources are used extensively by shorebirds, water birds and waterfowl (Paul and Manning 2002).

## 2. WILLARD SPUR NUTRIENT CYCLING

### 2.1 Background: Willard Spur Nutrient Cycling

The Willard Spur makes up the northeast arm of Bear River Bay (Figure 2.1). A series of dykes form the southern boundary of the Spur, separating it from the Willard Bay Reservoir, Harold Crane Waterfowl Management Area, and Great Salt Lake Minerals, Inc.. The northern boundary of the Spur is formed by the system of dykes that separate the Willard Spur from impounded wetlands of BRMBR to the north and the Spur lies partially within the boundaries of the BRMBR. The areas of the Willard Spur outside the BRMBR are hunted extensively for waterfowl.

In 2010 the Utah DWQ granted a Utah pollutant discharge elimination system (UPDES) permit to the newly constructed Perry/Willard Regional Wastewater Treatment Plant (PWRWTP). The decision met significant resistance from multiple groups, including the Utah Waterfowl Association and the Utah Airboat Association. In response to a petition from Western Resources Advocates to the Water Quality Board, the DWQ undertook a study to evaluate possible deleterious effects of the PWRWTP effluent on the Willard Spur. The prevalence of vegetation in the open water of the Willard Spur highlights its capacity to support forageable plants for waterfowl and its importance to the Bear River Bay ecosystem. The false color image in Figure 2.2 represents vegetation in red.

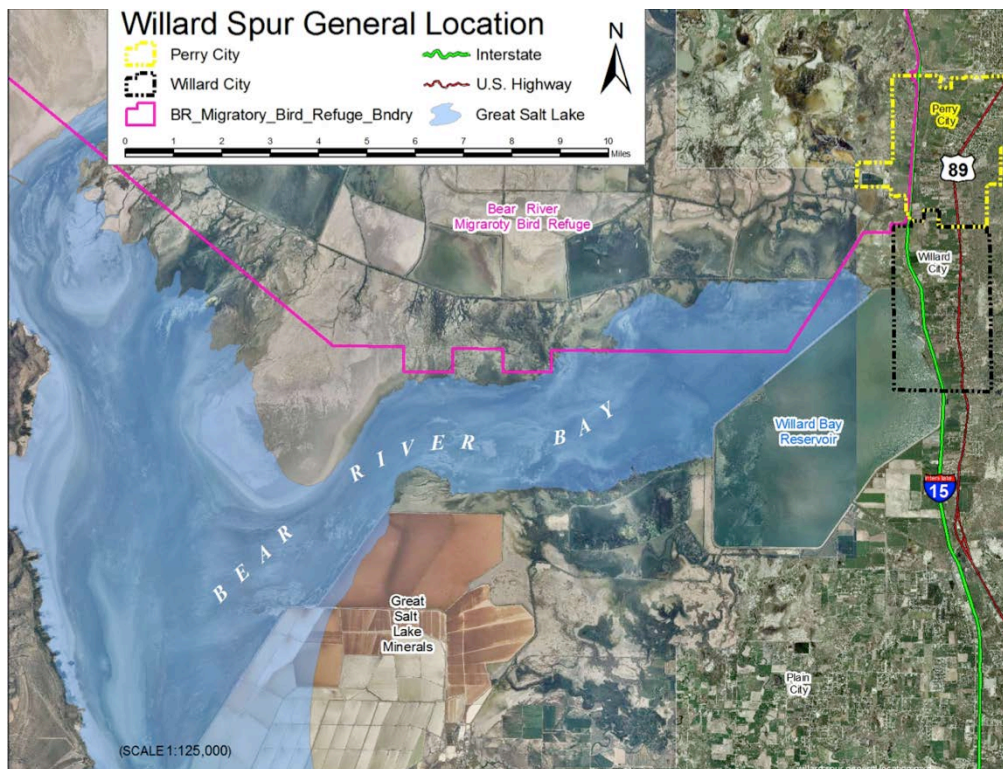


Figure 2.1. Image provided by the Utah DWQ. URL: <http://www.willardspur.utah.gov/images/maps/willardspurgenerallocation.jpg>

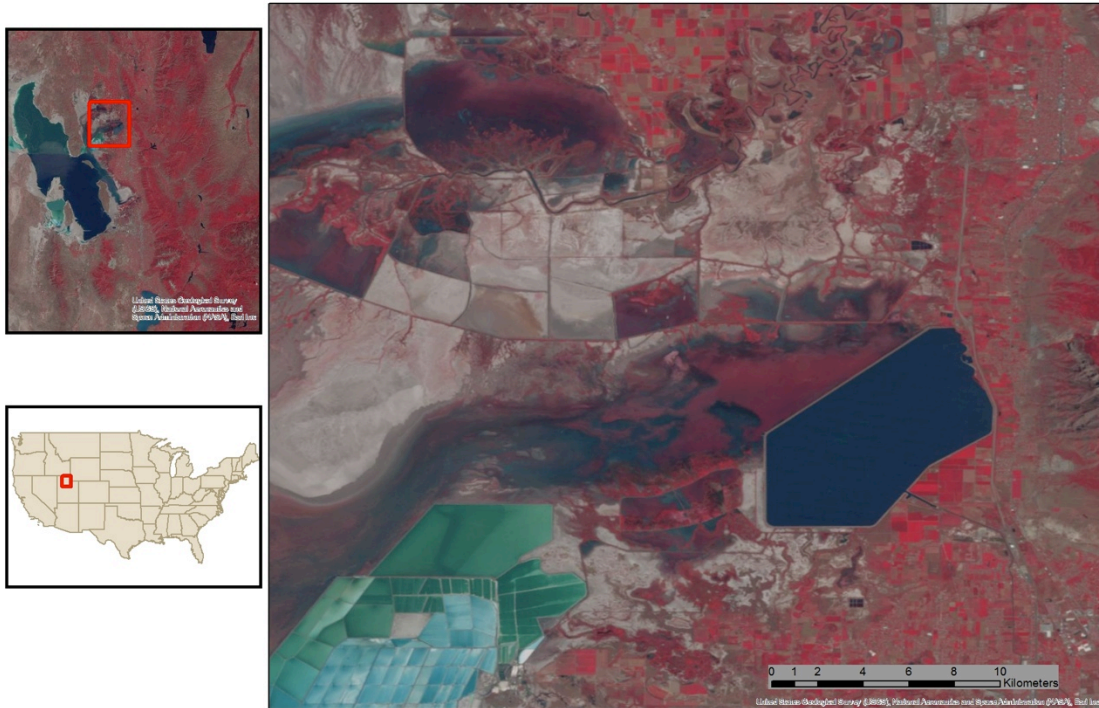


Figure 2.2. False color images show the proliferation of vegetation (represented in red) in the Willard Spur, contrasted by Willard Bay and Great Salt Lake Minerals, Inc. to the south and impounded wetlands in the BRMBR to the north.

The two main questions to be answered by the Willard Spur project were:

- 1) What are the potential impacts of the PWRWTP on the Willard Spur?
- 2) What will be required to provide long-term protection of Willard Spur?

The Utah DWQ put out requests for proposals to answer these and subsidiary questions associated with the Willard Spur study, including understanding the assimilative capacity of the Willard Spur and identifying sensitive biological indicators that respond to nutrient loading.

A proposal to study nutrient cycling from the research group from the University of Utah was funded by the Utah DWQ. This group includes Dr. William P. Johnson, Dr. Heidi Hoven, Dr. Ramesh Goel, Dr. Sam Rushforth, and Dr. David Richards. The primary goals of the nutrient cycling proposal were to:

- 1) Provide an understanding of the natural variability of biological processes and productivity related to nutrient cycling in the Willard Spur; and
- 2) Identify thresholds for nutrient response using biological indicators.

The research questions addressed by this proposal included:

- 1) How does the Willard Spur respond to nutrient loading in the water column and sediment?
- 2) What constitutes a negative or unacceptable response to nutrients by the submerged aquatic vegetation (SAV), macroinvertebrate community, phytoplankton, and macroalgae?
- 3) What threshold(s) to nutrient enrichment could be established relative to responses of the biological indicator(s)?

During the spring of 2012 and 2013 the research group constructed *in-situ* plots in the Willard Spur in order to utilize wetland response metrics developed by Dr. Hoven in the presence of varying nutrient loads. The vegetation metrics are intended to assess the health of a wetland and “identify thresholds of significant change (impairment) that can be attributed to nutrients” (Hoven and Miller, 2009).

The response of the water column, sediment, and SAV to increased nutrient loading in the Willard Spur was observed from June through October in 2012 and April through July in 2013. Vegetation metrics were measured throughout the plots to characterize the response of the system under varying degrees of nutrient loading (Hoven et al., in preparation).

## 2.2 Methods

In the spring of 2012 and 2013 *in-situ* plots were constructed in a perennially submerged area of the Willard Spur. The plots were designed to mimic nutrient loading from the PWRWTP from April to October.

### 2.2.1 Experimental Design

Experimental design was established in 2012 and appropriate changes were implemented in 2013.

#### 2.2.1.1 2012 Nutrient Cycling Plots

The 2012 plots included sediment and water column fertilizer amendments, as described below.

##### 2.2.1.1.1 Plot Location and Dimensions

Following acceptance of the proposal in March 2012, six *in-situ* plots were constructed in the Willard Spur perpendicular to surface water flow in April 2012. *Ex-situ* mesocosms were considered however it is impossible to replicate seasonal and daily temperature cycles in *ex-situ* experiments. Conditions in the Willard Spur, specifically temperature and water depth, can also vary significantly throughout the season. In dry years, the Willard Spur is cut off from the main body of the Great Salt Lake by a prominent sand bar. Figure 2.3 shows the location of the 2012 and 2013 plots. The location of the plots was selected using historical satellite photos that indicated areas of the Willard Spur were more likely to remain water covered throughout the course of the year.



Figure 2.3. 2012 plots are shown in red and light blue; 2013 plots are shown in dark blue. Yellow circles indicate locations where PWRWTP effluent is discharged directly into the Willard Spur.

The plots were organized into two transects (Figure 2.3). Three water column-amended plots (WS4, WS5, WS6) were installed 350 m upstream (northeast) of three sediment-amended plots (WS1, WS2, WS3). The three plots on each transect were spaced 20 m apart. The amended area of the water column plots was 6 m by 20 m and the amended area of the sediment plots was 2.5 m by 20 m. Appendix A shows the amended areas of each plot. The orientation, size, and spacing of the plots were intended to minimize influences from adjacent plots and ensure that all plots had similar plant communities. Galvanized steel posts were used to delineate the borders of the plots. The posts provided a way to secure kayaks and canoes during sampling in order to avoid disturbing the plants and sediment during the study.

#### 2.2.1.1.2 Amendment Ranges

The water and sediment amendments were intended to simulate ambient, mid-range, and high range nutrient loading to the water column and sediment Willard Spur. In 2012, high and low target concentrations for dissolved phosphorus ( $\text{PO}_4\text{-P}$ ) in the water column were 0.4 mg/L and 0.1 mg/L, respectively. The high and low target concentrations of available phosphorus in the sediment were 200 mg/kg and 100 mg/kg, respectively. Water column and sediment target concentrations for phosphorus were established relative to phosphorus concentrations in Willard Spur surface water and sediment measured in 2011 by the Utah DWQ (Ostermiller, 2012).

### 2.2.1.1.3 Fertilizer Amendments

Osmocote Smart Release™ fertilizer was deployed in April 2012. Woven nylon bags were filled with 0.4 kg of fertilizer and suspended in the water column or buried in the sediment. [Table 2.1](#) shows the approximate mass of fertilizer in each plot in 2012.

*Table 2.1. Mass of nutrients in 2012 sediment and water column amendments.*

	kg/plot			
	P	NO <sub>3</sub> -N	NH <sub>4</sub> -N	Urea-N
<b>2012 High Sediment</b>	9.6	16.0	14.4	0.0
<b>2012 Low Sediment</b>	4.8	8.0	7.2	0.0
<b>2012 High</b>	8.0	13.4	12.1	0.0
<b>2012 Low</b>	2.0	3.4	3.1	0.0

To amend water column nutrient concentrations, bags of Osmocote™ were suspended about 10 cm below the water surface from five ropes extending between posts 20 m across the plots. The ropes were lowered as the water level dropped throughout the summer.

To amend the sediment nutrient concentrations, bags of Osmocote™ fertilizer were pushed 10-20 cm into the sediment, which was sufficiently soft (mud) to deform and cover each bag. The mass of fertilizer placed in the sediment was calculated by estimating the volume of sediment affected by each bag of fertilizer and a bulk density for the sediment.

### 2.2.1.1.4 Sample Schedule

Following site set up and monitoring, regular sample events were conducted monthly between June and October. [Appendix A](#) contains tables describing the samples collected for water and sediment chemistry, nutrient flux, and biota in more detail. Biweekly monitoring of dissolved nutrients occurred between monthly sample events in 2012.

### 2.2.1.2 2013 Nutrient Cycling Plots

The 2013 experimental design only included fertilizer amendments in the water column. In addition, improvements from the 2012 design were worked into the experimental design in order to avoid complications encountered during the 2012 field season.

#### 2.2.1.2.1 Plot Location and Dimensions

Several changes to the experimental design were implemented for the 2013 experiment. Nutrient amendments in 2013 only targeted the water column in order to reflect the waterborne loads from the PWRWTP. The 2013 plots included three water column amendments and one control. Four 6 m x 20 m water amendment plots were constructed in April 2013, about 70 m northeast of the location of the 2012 plots.

Just as in 2012, satellite photos were used to orient the 2013 plots with their widest dimension perpendicular to the direction of surface water flow and in a location perennially submerged. One transect was formed by the high, medium, and low water column plots ([Figure 2.3](#): WS7, WS8, WS9). These three plots were separated by 20 m, just as in 2012. The control plot was

located about 90 m upstream (northeast) of the amended plots. In addition to the control plot, ambient sediment and water column samples were collected outside of the constructed plots. For the ambient site, a single post (identical to the posts used to delineate the borders of the four plots) was placed 30 m northwest of the control plot, forming a second transect (Figure 2.3: WS10, WS11). This post provided an attachment for kayaks and canoes during sampling.

#### 2.2.1.2.2 Amendment Ranges

A larger range of water column amendments was possible in 2013 with the elimination of sediment plots from the experimental design. Three levels of nutrient loading in the water column were planned for the 2013 plots. In 2012, plant response to nutrient loading was observed for high and low water column plots, though differences in nutrient concentrations between plots was minimal and well below the target concentrations (See results in Section 2.3). Therefore three water column amendments were constructed in 2013.

The high water column plot had approximately the same amount fertilizer in 2012 and 2013. Likewise, the amount of fertilizer in the 2013 medium water column plot was similar to the low water column amendment in 2012. The low water column plot in 2013 contained half the fertilizer that was contained in the 2012 low and 2103 medium water column amendments in order to further bracket the nutrient load ranges potentially driving the condition of macrophyte health.

#### 2.2.1.2.3 Fertilizer Amendments

The type of fertilizer used in 2013 was different from 2012 in order to promote dissolution during the relatively cold water period of April and May, which ranged between 40 °F and 55 °F in 2012. Based on PO<sub>4</sub>-P and NO<sub>3</sub>-N data from 2012 amendment plots, the Osmocote Smart Release™ fertilizer did not release significant amounts of nutrients until June, which may be expected since the polymer coating is designed to release nutrients above 60 °F.

In order to promote dissolution of nutrients into the water column during both colder and warmer temperatures, a different mixture of fertilizers was used in the 2013 amendment. Table 2.2 shows the mass of nutrients added to the water column amendments in 2013. The mixture was made up of approximately 60% Osmocote™ (the same fertilizer used in 2012), approximately 37% coated urea, and about 3% soluble urea. The urea fertilizers were designed to provide nutrient release during the cool water temperatures expected during the first 90 days of the experiment.

Table 2.2. Nutrient mass in each amended water column plots.

	kg/plot			
	P	NO <sub>3</sub> -N	NH <sub>4</sub> -N	Urea-N
<b>2013 High</b>	5.6	9.3	10.2	23.4
<b>2013 Medium</b>	1.3	2.2	2.4	5.5
<b>2013 Low</b>	0.7	1.1	1.2	2.8

A different method for deploying bags of fertilizer was used in 2013 in order to remove artifacts from the fertilizer deployment in the water column in 2012. The 2012 experiment was complicated by the ropes and posts used to construct the plots. The floating ropes used to suspend the bags of fertilizer in the water column trapped drifting SAV debris. This debris consisted of plants uprooted during wind events and grazing as well as branches and leaves that are released naturally throughout the growing season. The debris formed mats above the plots with a thickness of up to 35 cm, at which point the mat became dense enough to sink and collapse onto the SAV below (Figures 2.4a). This debris was removed from the plot weekly until a fence was constructed around the plots to exclude additional debris from entering the plot areas.

a.



b.



*Figure 2.4. Amendment techniques for a) 2012: Plant debris collecting on ropes within the plots. The darker areas show where the mat was sufficiently dense enough to collapse onto the plants below. b) 2013: Underwater photo of submerged fertilizer bags attached to a stake and embedded in the sediment.*

In 2013, rather than suspending fertilizer bags in the water column from ropes strung across the plots, wooden stakes were embedded in the sediment (Figure 2.4b). Between 1 and 4 bags of fertilizer were attached to the top of each stake about 10 cm to 25 cm above the surface of the sediment. The lines of stakes followed the same pattern as the ropes, five lines extending 20 m across the plots. The number of stakes on each line varied between 9 and 19, depending on the mass of fertilizer placed in the plot. Appendix A shows the patterns of stakes and bags for each plot. Because of the variation in the number of stakes in each plot, half of the control plot reflected the pattern of the stakes in the low and medium treatment plots while the other half reflected the pattern of stakes in the high treatment plot.

#### 2.2.1.2.4 Sample Schedule

The timing of intensive sampling events in 2013 was scheduled for the early months of high growth observed between April and July of 2012. Capturing the conditions leading up to plant senescence observed during late May and June of 2012 was a primary objective for the 2013 sampling season. Plots were installed in early April 2013 and sampling began in mid-April. Between mid-April and the end of July water samples were collected every two weeks and sediment samples were collected every month. Sampling ended in late July after plant senescence was observed and water levels had dropped, making canoe access to the sites impossible. Additional squeezer core sediment samples described in Section 2.1.3 were collected in 2013 to supplement the information from homogenized sediment samples collected in 2012.

#### 2.2.2 Field Methods

Surface water and sediment samples were collected by canoe, transported on ice, and stored in the refrigerator or freezer until analysis. Unfiltered samples for carbonaceous BOD, general chemistry, and nutrients were collected in plastic bottles supplied by the Utah State Health Laboratory. Filtered and unfiltered samples for nutrient analysis were preserved with 0.5% H<sub>2</sub>SO<sub>4</sub>. Filtered trace metal samples were collected in acid-leached LDPE bottles and acidified using 2.4% trace metal grade HNO<sub>3</sub>.

For most sample events in 2012 and 2013, three samples were collected per plot. More detail describing the number of samples during each sample event collected and the specific analyses run is found in [Appendix A](#). Filtered samples were collected using a GeoTech™ peristaltic pump. Teflon™ tubing was submerged into the middle of the water column. Water was forced through the high-capacity capsule filters (0.45 μm GeoTech Dispose-a-filter™). Both the tubing and capsule filters were rinsed with 10% HCl prior to use in the field. At least two volumes of water were flushed through Teflon™ tubing and filter system between sample sites within a plot. The Teflon™ tubing was rinsed between plots with 10% HCl and flushed with sample water and a new filter was used for each plot.

Field parameters were measured using YSI Professional Plus multimeter probe. Temperature, dissolved oxygen (DO), pH, and conductivity were collected for each plot. Prior to each sample event the probe was calibrated for conductivity and pH using commercial standards (GeoTech). DO was calibrated using a one-point calibration method in water-saturated air.

Sediment samples were collected using a 1-inch copper pipe in three to four random areas throughout the plots. The top 10 cm of the sediment was retained and 8-10 samples per plot were homogenized in a plastic bag. In 2013 squeezer core samples were collected in 2-inch plastic core and kept on ice until squeezed on shore. The squeezer core is outfitted with threaded holes to allow for extraction of pore water from the sediment. Porex™ rods were inserted into the sediment core and attached to syringe filters (Whatman 0.45 μm PES) and syringes ([Figure 2.5](#)). Pistons compressed the core from both sides, forcing pore water into the syringes (method modified from [Carling et al., 2013](#)).



*Figure 2.5. Sediment squeezer apparatus with attached syringe filters and syringes.*

### **2.2.3 Laboratory Methods**

Samples were processed according to standard operating procedures developed by laboratories at the University of Utah, Utah State University, and the Utah State Health Laboratory, as described below.

#### **2.2.3.1 Surface Water Methods**

The laboratories and associated methods for each parameter are provided in [Appendix A](#). Quantification limits were established for each sample batch run following regular sample events. The highest value of trip blank, field blank, method blanks, or established limits of detection for the instrument were used to set the quantification limit for sample runs. For all samples analyzed in the Johnson Lab at the University of Utah method blanks were run every ten samples and matrix spikes for every batch. Nutrient concentrations below the quantification limit were set at  $\frac{1}{2}$  the quantification limit for statistical analyses.

Trace element extractions were performed by digesting sediment subsample in 20 ml 5% (v/v) trace metal grade HCl for three days at room temperature, followed by centrifugation and analysis of supernatant as a water sample. A quadrupole inductively coupled plasma mass spectrometer (ICP-MS) with a collision cell was used to measure trace elements in surface water samples and sediment sample supernatant. A list of elements analyzed is provided in [Appendix A](#).

Most samples submitted to the Utah State Health Laboratory were analyzed within 30 days of collection, except for carbonaceous BOD samples that were analyzed within 2 days. Major anion

concentrations were measured within 72 hours of sampling using ion chromatography. Mercury samples were analyzed within 3 months of sampling.

### **2.2.3.2 Sediment Methods**

Sediment samples were sub sectioned to for analysis at the Johnson Lab, Utah State University Analytical Laboratory (USUAL), and the Stable Isotope Ratio Facility for Environmental Research (SIRFER). Samples for the USUAL lab refrigerated and submitted within 3 days of collection. USUAL provided analyzed for ammonia-N and nitrate-N (from 2N KCl extract) and available phosphorus using the Olsen NaHCO<sub>3</sub> method (Poulton et al., 2012). All sediment nutrient concentrations were above the analytical detection limit provided by the Utah State University Analytical Laboratory.

Sediment samples prepared for C/N analysis at SIRFER were dried overnight in an oven at 100 °C within 5 days of collection. Dried samples were crushed using a Retsch ball mill. Samples for organic carbon and nitrogen analysis were prepared by treating crushed and dried sediment with 0.5 N HCl until the pH of the mixture dropped below 5. The leftover sediment was rinsed with DI water and dried using a vacuum Buchner funnel and dried in an oven at 70°C. The SIRFER lab analyzed carbon and nitrogen isotopes using a Delta Plus isotope ratio mass spectrometer (Finnigan-MAT, Bremen Germany) interfaced with an Elemental Analyzer (model 1110, Carla Erba, Milan, Italy). Instrument precision for  $\delta^{13}\text{C}$  and  $\delta^{15}\text{N}$  is  $\pm 0.15$  ‰ and  $\pm 0.2$  ‰ respectively. Carbon and nitrogen isotope data met all quality assurance-quality control standards established by the SIRFER lab.

### **2.2.4 Release Rate Experiments**

Osmocote™ has been used with favorable results in other large-scale nutrient enrichment studies (Baggett et al., 2010; Furman and Heck, 2008; Heck et al., 2000) where nutrient release rates were measured in the laboratory and field. For this study, tests were conducted in laboratory and *in-situ* settings in order to characterize dissolution characteristics of the fertilizers used in 2012 and 2013. Multiple conditions were tested in order to expand on previous experiments described in the literature and increase the range of known release rates for different conditions.

#### **2.2.4.1 Bucket Release Rate Tests**

The bucket scale release rate test analyzed Osmocote™ dissolution in a relatively closed system in a laboratory setting. New and used bags containing approximately 0.4 kg of Osmocote™ were placed in 3 gallons of water in 5-gallon plastic buckets open to the atmosphere. Samples were collected over the course of four weeks and filtered using 0.45  $\mu\text{m}$  syringe filters. Because the release of nutrients from Osmocote™ is temperature dependent, tests were conducted at two temperatures that bracketed the expected temperatures in the field. During the first two weeks of the experiment, the buckets were kept indoors at temperatures near 60 °F. During the second two weeks, buckets were kept outdoors with daily high temperatures ranging between 70 and 85 °F.

#### **2.2.4.2 Mesocosm Release Rate Tests**

The mesocosm scale release rate experiments analyzed dissolution rates in the field from bags of Osmocote™ used in 2012 and from bags of the mixture of fertilizers used in 2013. Two mesocosms designed by the Utah Division of Water Quality were installed in the Turpin (GSLI-013) impounded wetland in Farmington Bay. Turpin was chosen for the location of the experiment as Willard Spur water levels dropped below 2 inches in August 2013. Rapid changes in the water levels were unlikely as the Utah Division of Wildlife Resources controls water levels in impounded wetlands in the Farmington Bay Waterfowl Management Area.

The source of water to Turpin Unit is the Jordan River. The Jordan River flows through industrial areas in the Salt Lake Valley and is heavily influenced by anthropogenic contaminants (Naftz et al., 2008). Background concentrations of dissolved phosphorus (0.75 mg/L) are more than one order of magnitude greater than those of the Willard Spur (0.035 mg/L).

The walls of the mesocosms were made of Lexan™ plastic and were pressed down into the sediment in order to avoid large amounts of flow in or out of the mesocosm. The mesocosms were not completely watertight, however, since a small gap in the mesocosm wall allowed the water levels inside to slowly equilibrate with water levels outside the mesocosm. This flux was not expected to lead to significant loss of nutrients during the experiment since flow was into the mesocosm. This is based on the observation that levels inside the enclosure gradually increased from 0.50 m to 0.54 m over the course of the experiment in response to the same increase outside the mesocosm.

Four bags containing 0.4 kg of fertilizer were attached to a wooden stake and placed in the center of each mesocosm. This deployment system was identical to the fertilizer deployment method in 2013 high water column test plot. Bags of Osmocote™ fertilizer, identical to those used in 2012, were placed in the center of one mesocosm and the 2013 mixture of fertilizers was placed in the other.

Filtered and unfiltered samples for nutrient analysis were collected periodically over 12 days. A GeoTech™ peristaltic pump was used to collect composite samples. Teflon™ tubing was submerged into the middle of the water column and moved in a uniform pattern throughout each mesocosm in order to collect a representative sample. The same method was used for filtered samples with the addition of forcing the water through high-capacity capsule filters (0.45 µm GeoTech Dispose-a-filter™). At least two volumes of water were flushed through the system between sample sites. Dissolved nutrients were measured in the Johnson Lab using ion chromatography. Total and dissolved nutrient samples were sent to the Utah State Health Laboratory for analysis.

### **2.3 Sediment and Surface Water Chemistry Results**

There are three sections of chemistry results: 2012 field results, 2013 field results, and subsidiary laboratory and field results designed to quantify nutrient release rates from the fertilizer amendments in the field.

### 2.3.1 2012 Field Results

2012 field results include concentration measurements from two phases, surface water and sediment, as described below.

#### 2.3.1.1 2012 Surface Water

Trace elements were measured to confirm concentrations in the six test plots were equivalent, and therefore not driving any observed differences between the plots, as described below. In addition nutrient concentrations were monitored to determine whether target concentrations were reached.

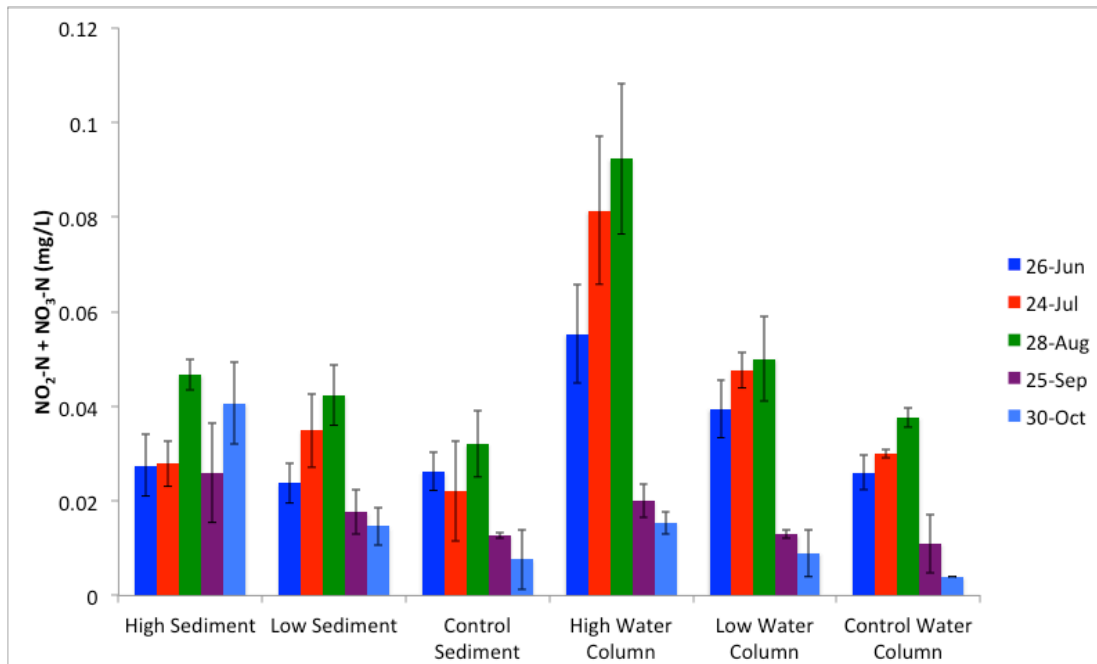
##### 2.3.2.1.1 Trace Elements

Water column trace element concentrations were similar between treatments and most likely were not responsible for any differences in observed biological responses among the test plots. This is shown by the equivalence of filtered trace element surface water concentrations in both water-amendment and sediment-amendment test plots ([Appendix A](#)). The samples were collected six weeks following deployment of Osmocote™ in 2012; hence, deployment of Osmocote™ did not significantly alter trace element concentrations among the plots.

##### 2.3.2.1.2 Nutrients

The highest surface water phosphate concentrations corresponded with the warmest months in terms of surface water temperatures; i.e., September and October were 7-12 °C cooler than August. Notably, the highest dissolved phosphorus concentrations were measured in the high water column plot for each sample event ([Figure 2.6b](#) and [2.7b](#)). The surface water concentrations for dissolved phosphate were far below the target concentrations of the high and low water column amendments, 0.4 mg/L and 0.1 mg/L, respectively.

a.



b.

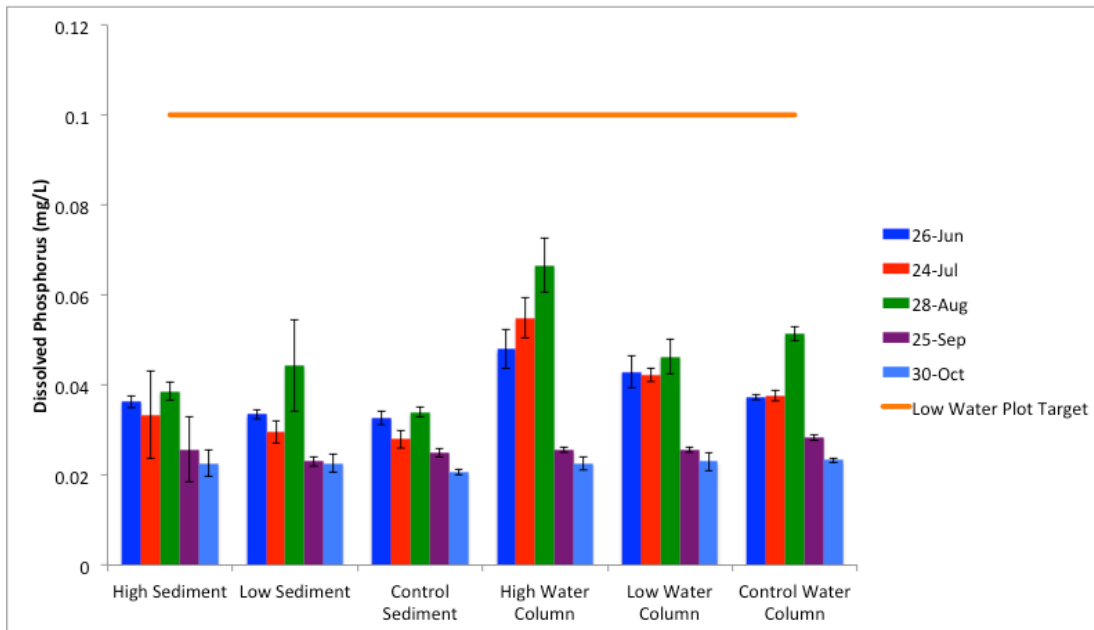


Figure 2.6. Surface water concentrations for a) dissolved  $\text{NO}_2\text{-N} + \text{NO}_3\text{-N}$  correspond with b) dissolved phosphate concentrations showing elevated levels in the high water column plot during 2012. Error bars represent one standard deviation ( $n=3$  except for June samples where  $n=4$ , excluding Control Water Column where  $n=3$ ). All bar plots that show concentrations in plots through time are arranged chronologically from left to right (e.g. bars in Figure 6 in the High Sediment plot represent 26-Jun, 24-Jul, 28-Aug, 25-Sep, and 30-Oct from left to right).

As was observed for phosphate, increased  $\text{NO}_2\text{-N} + \text{NO}_3\text{-N}$  concentrations corresponded with the warmest months. Again, the highest  $\text{NO}_2\text{-N} + \text{NO}_3\text{-N}$  concentrations occurred in the high water column plot for each sample event (Figures 2.6a and 2.7a), as was observed for dissolved phosphorus. In contrast to phosphate, a surface water target concentration for nitrate was not established. Additional surface water nutrient concentrations were measured and are available in [Appendix A](#).

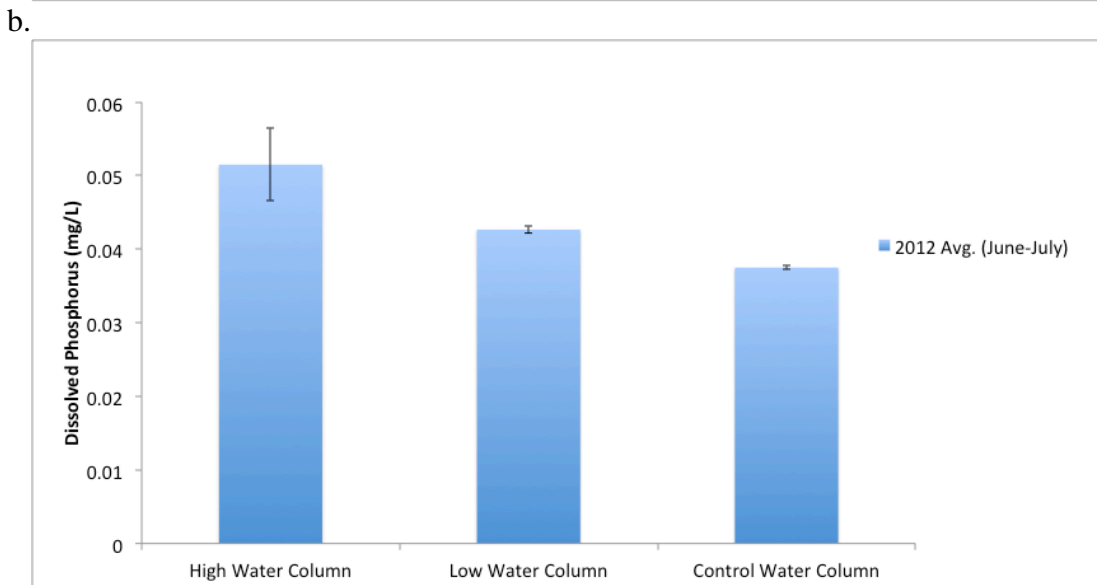
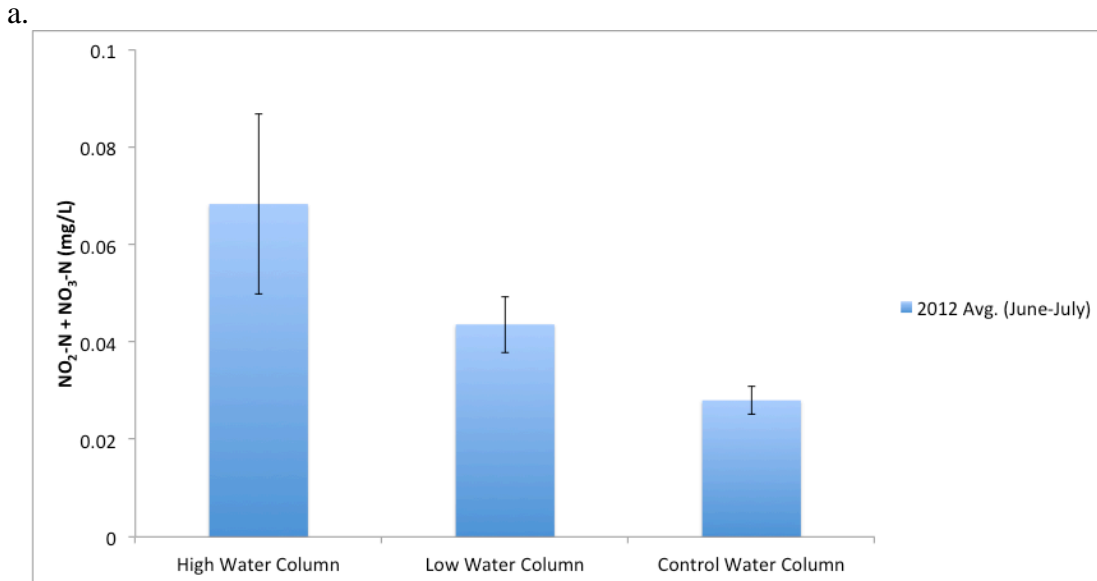


Figure 2.7. Significant variation between amendments and controls was observed in 2012 for a) dissolved  $\text{NO}_2\text{-N} + \text{NO}_3\text{-N}$  and b) dissolved P averages from June and July. Error bars represent one standard deviation ( $n=12$  for all locations except for Ambient where  $n=4$ ).

### 2.3.1.2 2012 Sediment

In 2012, several constituents were analyzed. Trace elements were measured to confirm concentrations in the six test plots were equivalent, and therefore not driving any observed differences between the plots, as described below. In addition, nutrient concentrations were monitored to determine whether target concentrations were reached. Carbon and nitrogen content and stable isotopes were measured in order to further examine potential propagation of nutrients into the sediment.

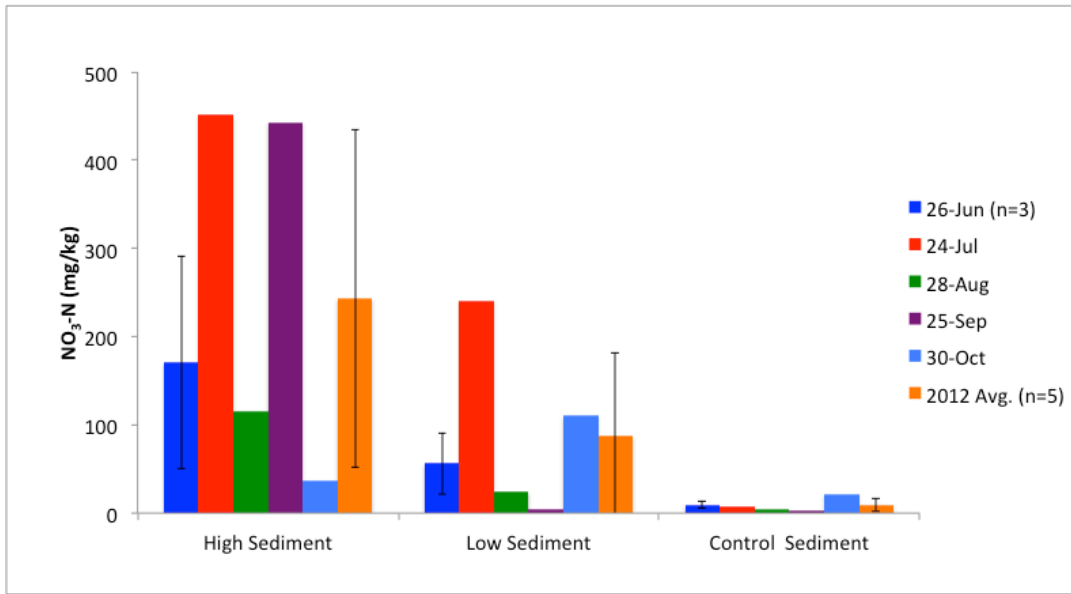
### 2.3.1.2.1 Trace Elements

Trace elements concentrations in the sediment were equivalent between plots. Sediment samples for trace element were collected six weeks after the Osmocote was deployed therefore the Osmocote did not significantly alter sediment trace element concentrations. Results indicate that trace elements in the sediment did not likely drive differences in biological responses between plots. Sediment trace element data is available in [Appendix A](#).

### 2.3.1.2.2 Nutrients

Sediment phosphorus concentrations in the high sediment plot were significantly higher than low sediment plots. Yearly averages for phosphorus concentrations in sediment-amended plots ([Figure 2.8b](#)) were approximately half of the target concentrations for the high and low amendments, 200 mg/kg and 100 mg/kg, respectively.

a.



b.

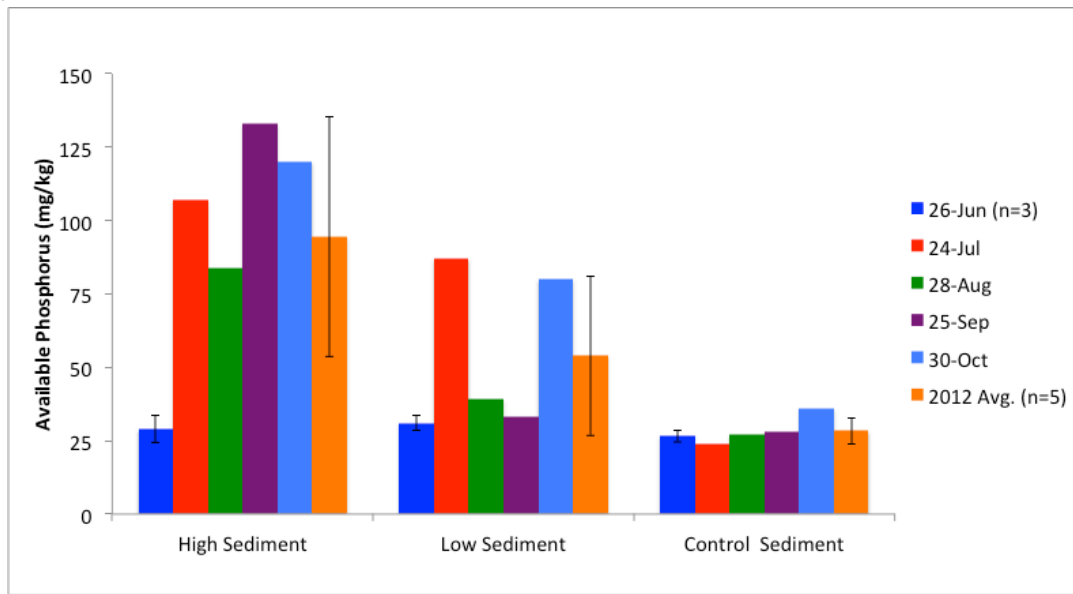


Figure 2.8. Elevated concentrations are observed in sediment-amended plots of a) nitrate and b) available phosphorus and nitrate. Error bars for June results represent one standard deviation ( $n=3$ ).

Sediment nitrate concentrations were elevated in high and low sediment-amended plots (Figure 2.8a). Temporal variability observed in sediment nitrate and phosphorus concentrations (Figure 2.8) may be attributed to the size of the sediment cores collected and collecting cores in discreet locations. Nutrient concentrations in the sediment collected in the core were dependent on proximity of sediment cores to bags of Osmocote and the rate of propagation of nutrients into the sediment. C:N ratios and % N also indicate increased nitrogen in the sediment in sediment amended plots. This information is available in the Appendix A.

#### 2.3.1.2.3 C/N Isotopes

Nitrogen isotope data for sediment and plant leaves show isotope effects in sediment amendments. Sediment  $\delta^{15}\text{N}$  values were enriched in the high and low sediment plots relative to the water column amendments and the sediment control plot (Figure 2.9).

Isotope differences ( $\Delta$ ) shown in Figure 2.10 represent the deviation of nitrogen isotope values for sediment and SAV leaves in amended sediment plots relative to the control sediment plot. The high sediment plot had  $\Delta^{15}\text{N}_{\text{amendment-control}}$  averaging approximately 1.5‰ in the sediment and -1.5‰ in SAV leaves.

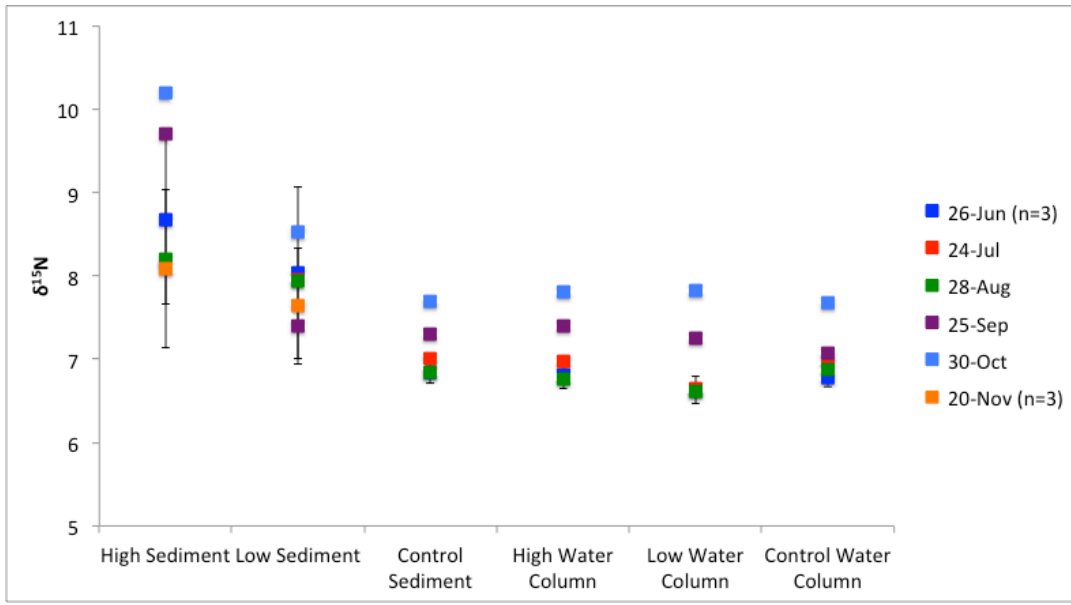


Figure 2.9. Isotope ratio mass spectrometry (IRMS) sediment results show enriched  $\delta^{15}\text{N}$  values in the amended sediment plots. Error bars for June and November results represent one standard deviation ( $n=3$ ).

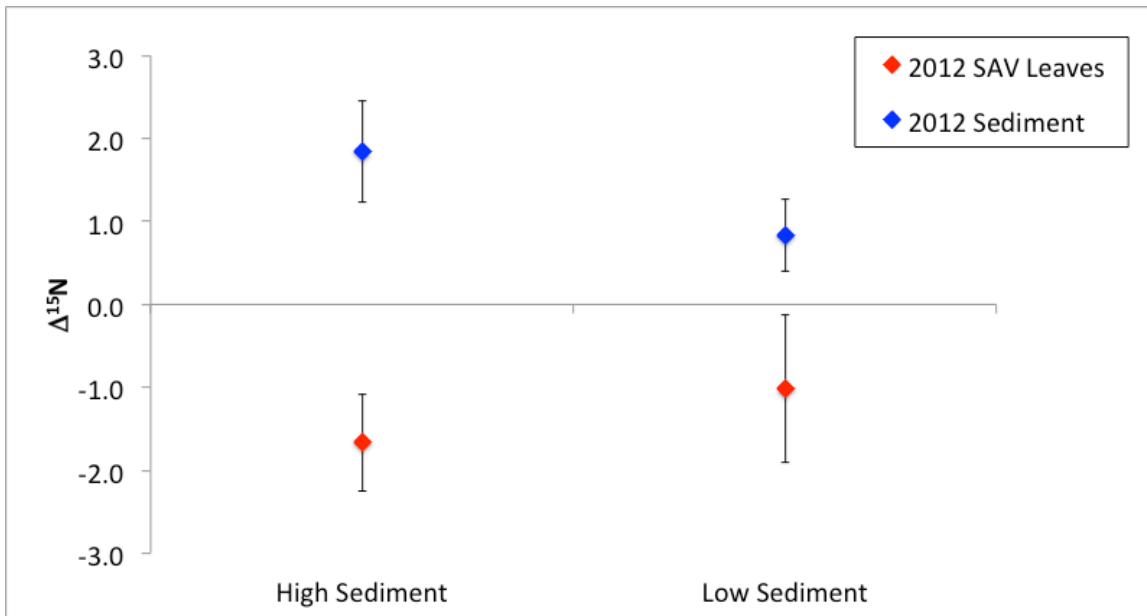


Figure 2.10. Average  $\Delta^{15}\text{N}$  values indicate fractionation in the sediment amendment plots. For each month,  $\delta^{15}\text{N}$  values from control plots were subtracted from  $\delta^{15}\text{N}$  values from sediment amendments during 2012 ( $n=3$  for SAV leaves and  $n=7$  for sediment).

### 2.3.3 2013 Results

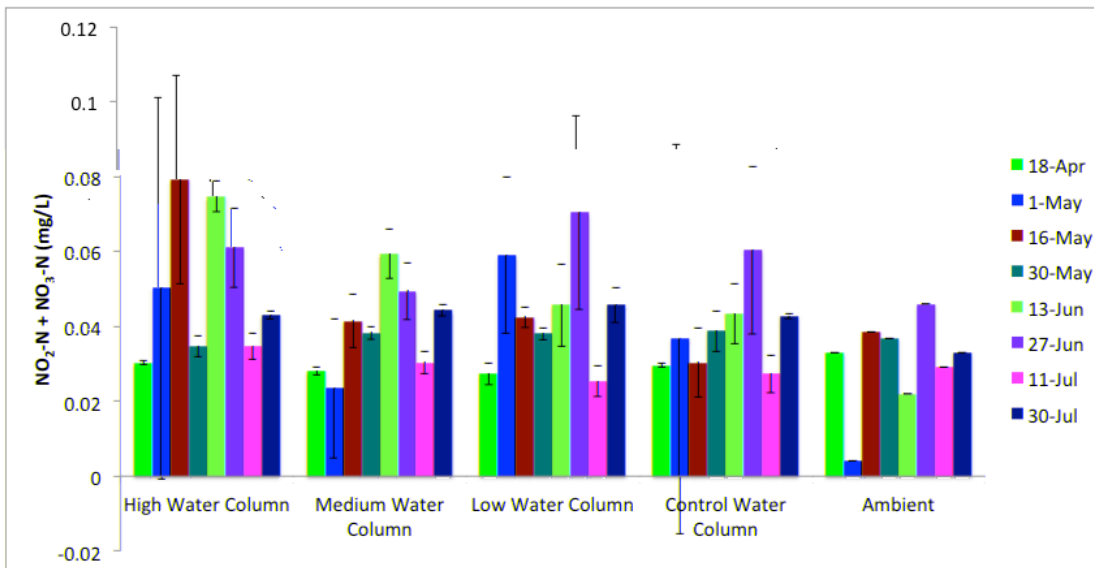
2013 field results also include concentration measurements from two phases, surface water and sediment, though only the water column was amended with fertilizer.

#### 2.3.3.1 2013 Surface Water

In 2013 average concentrations of dissolved  $\text{NO}_2\text{-N} + \text{NO}_3\text{-N}$  for all sample dates were approximately equal among all plots, regardless of amendment (Figure 2.11.a). The same was true for dissolved phosphorus (Figure 2.11.b).  $\text{NO}_2\text{-N} + \text{NO}_3\text{-N}$  concentrations are greatest in the high water column amendment for only two of eight sample events in 2013. There are no sample events where the highest dissolved phosphorus concentration was measured in the high water column amendment.

Dissolved  $\text{NO}_2\text{-N} + \text{NO}_3\text{-N}$  and dissolved P averages during the warmer months, June and July 2013 (Figures 2.12.a and 2.12.b), do not show significant amendment effects that were observed during the same months in 2012 (Figure 2.7.a and 2.7.b). Additional nutrient concentrations were measured and results are available in Appendix A.

a.



b.

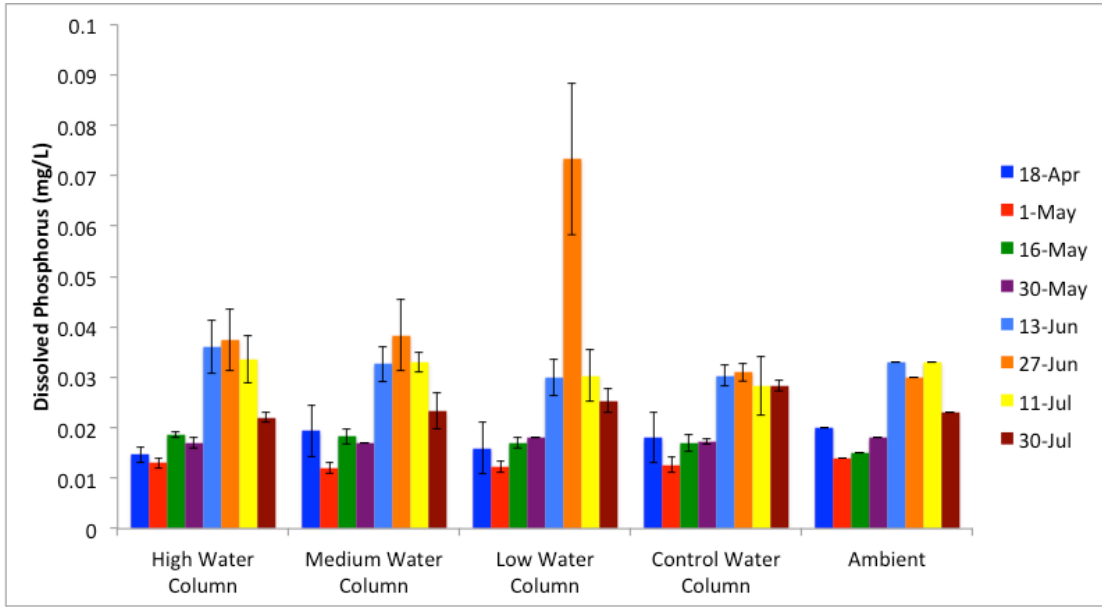
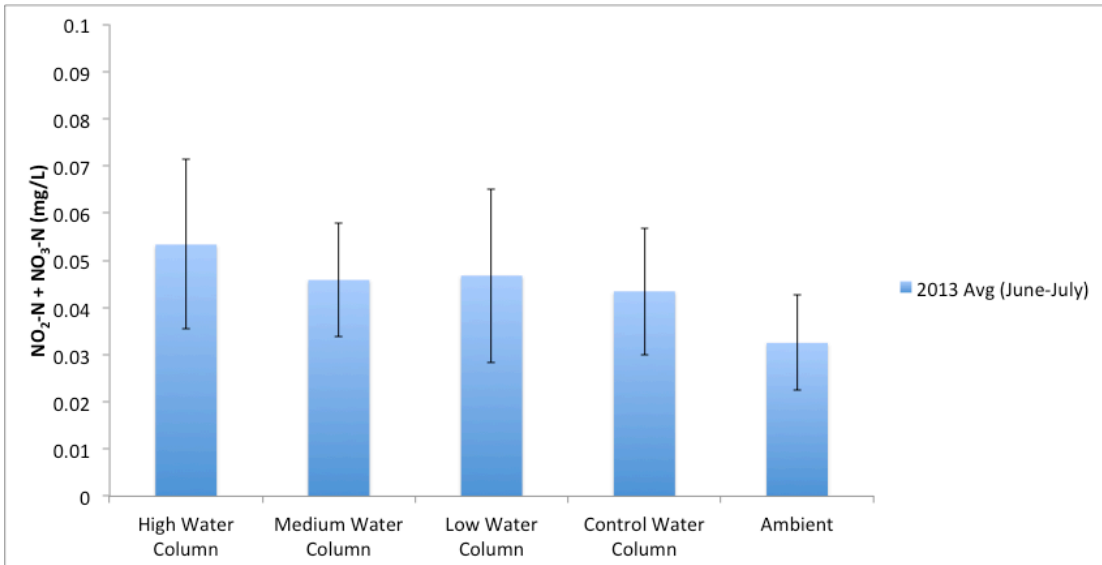


Figure 2.11. 2013 surface water concentrations for dissolved a)  $\text{NO}_2\text{-N} + \text{NO}_3\text{-N}$  and b) dissolved P do not show a clear trend between amendment and control plots.

a.



b.

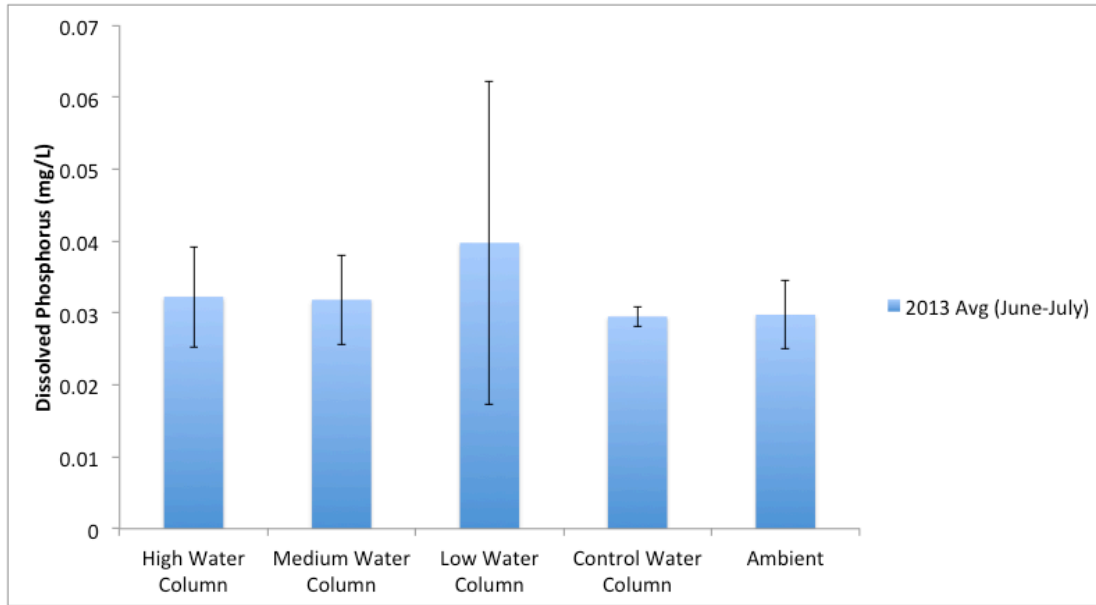


Figure 2.12. Significant variation between amendments and controls was not observed in 2013 for a) dissolved  $\text{NO}_2\text{-N}+\text{NO}_3\text{-N}$  and b) dissolved P averages from June and July. Error bars represent one standard deviation ( $n=12$  for all locations except for Ambient where  $n=4$ ).

Equivalent concentrations were observed among all amendments and control and ambient plots. This indicates that the release of nutrients into the water column was approximately balanced by dilution and loss of nutrients from the water column (e.g., nutrient removal by biota, precipitant settling, etc.). This is supported by nutrient flux chamber experiments described in [Appendix B](#). Nutrient fluxes for  $\text{NO}_3\text{-N}$  and  $\text{PO}_4\text{-P}$  are mostly negative for spiked chambers over 12 hours ([Figures B.4 and B.5](#)), indicating that dissolved nutrients are quickly removed from the Willard Spur water column.

### 2.3.3.2 2013 Sediment

Because the sediment was not amended in 2013, sediment phosphorus and nitrate were equivalent between plots. Sediment nutrient measurements from 2013 are available in [Appendix A](#). Likewise,  $\delta^{15}\text{N}$  values did not vary between plots ([Figure 2.13](#)).

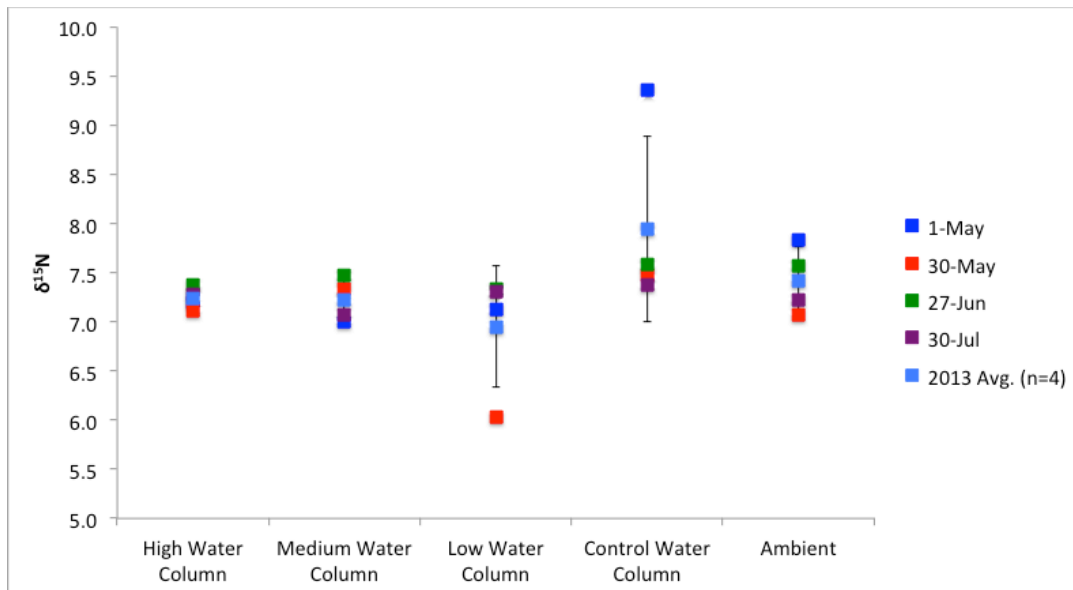


Figure 2.13. In 2013 total  $\delta^{15}\text{N}$  values were similar between amended and control plots.

Additional sediment cores were collected in 2013 in order to characterize variation of nitrogen isotopes with depth (Figure 2.14). Squeezer cores were used to remove sediment pore water and then extrude sediment in 2 cm sections. These sections represented horizons within the sediment from 0-12 cm.

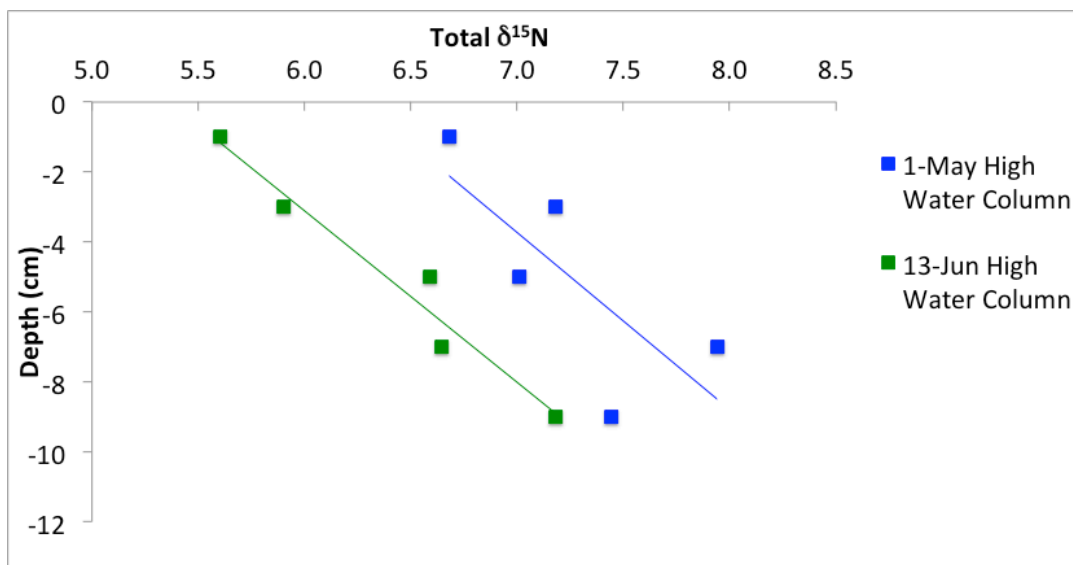


Figure 2.14.  $\delta^{15}\text{N}$  values from 2013 high water column plots in sediment horizons between 0 and 10 cm.

The average of  $\delta^{15}\text{N}$  values observed from the squeezer cores was similar to  $\delta^{15}\text{N}$  values of homogenized samples, approximately 7%. However the top horizon from the high water

column amendment collected in June has a  $\delta^{15}\text{N}$  value near 5.5‰, the lowest value measured in Willard Spur sediment in 2012 and 2013.

### 2.3.3 Quantifying Nutrient Release Rates to Water Column

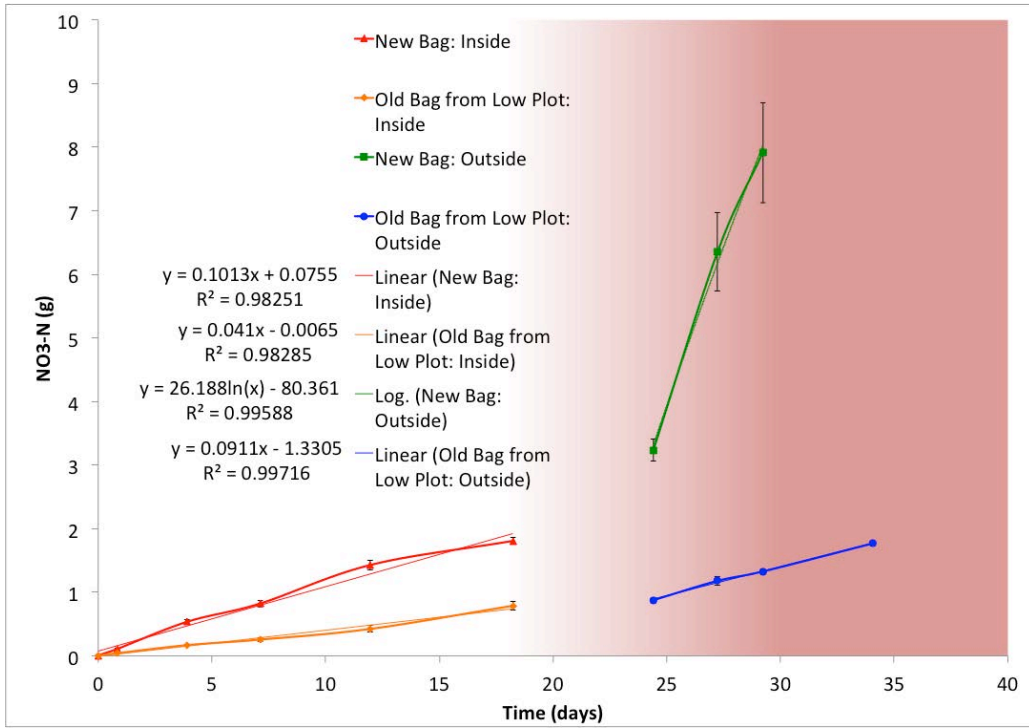
In order to estimate the nutrient release rates from the fertilizer amendments into the water column in amended plots, two types of release rate experiments were performed; small volume bucket tests which were portable to allow temperature control, and mesocosm tests involving much larger volumes in the field as well as biological response to nutrient addition.

#### 2.3.3.1 Bucket Test Results

The release rates for  $\text{NO}_3\text{-N}$  and  $\text{PO}_4\text{-P}$  were calculated using measured concentrations from the indoor and outdoor tests (Figure 2.15). Throughout the bucket test it was clear that the results were not significantly affected by potential depletion of the nutrient source or saturation limits of the solution, based on the fact that the release of nutrients was linear (Figure 2.15). This was true even for the fertilizer that had been in the field for approximately 3.5 months prior to the experiment. However, at warmer temperatures an “initial burst” was observed in other studies (Heck et al., 2000), most notably in bags that had not been previously used in the field.

The bucket tests indicate a significant difference in release rates of nutrients between temperatures near 60 °F and temperatures near 80 °F. Figure 2.15 shows nutrient release rates for  $\text{NO}_3\text{-N}$  and  $\text{PO}_4\text{-P}$  from bucket tests. New bags released  $\text{NO}_3\text{-N}$  into the water at a rate of about 0.101  $\text{g}\cdot\text{day}^{-1}$  in cool temperatures and 0.980  $\text{g}\cdot\text{day}^{-1}$  in warm temperatures. Likewise for  $\text{PO}_4\text{-P}$ , changes in concentration increased from 0.00530  $\text{g}\cdot\text{day}^{-1}$  in cool temperatures to 0.0855  $\text{g}\cdot\text{day}^{-1}$  in warm temperatures. Bags of Osmocote™ that were deployed in the field for four months and then used in buckets released  $\text{NO}_3\text{-N}$  and  $\text{PO}_4\text{-P}$  at 10% and 15%, respectively, of the rate of new bags at warmer temperatures.

a.



b.

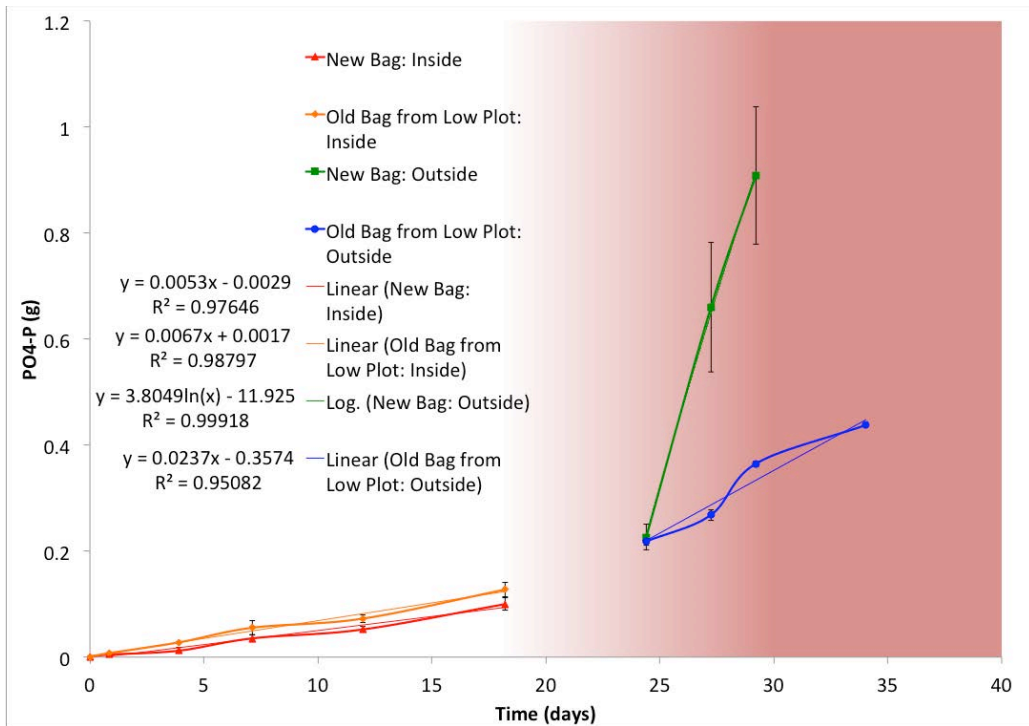


Figure 2.15. Results from bucket dissolution tests for a) NO<sub>3</sub>-N and b) PO<sub>4</sub>-P. White areas indicate temperatures averaging 13 °C (volume of water for test = 11.3 L). Red shading indicates outdoor tests and temperatures averaging 29 °C (volume = 9.5 L).

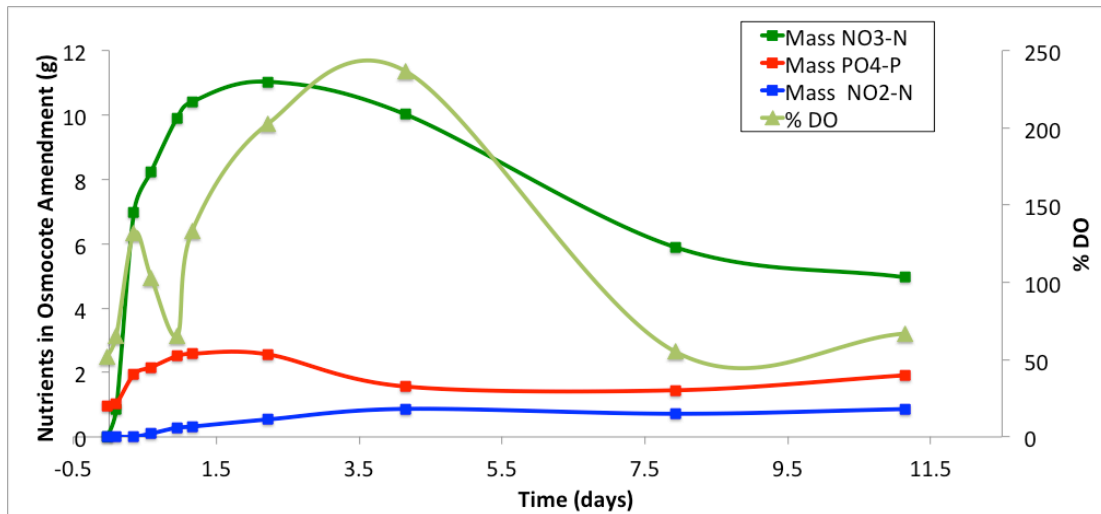
### 2.3.3.2 Mesocosm Test Results

Dissolved oxygen measurements in both mesocosms (Figure 2.16) indicated an increase in biological activity due to the nutrient amendments. The Osmocote™ mesocosm experiment (Figure 2.16a) shows a significant shift in DO in the system earlier than the 2013 fertilizer mixture. This DO shift is likely caused by eutrophication where excessive biomass production consumes the DO. A subsequent further decrease in DO coincides with the decomposition of biomass (McCormick and Laing, 2003).

Mesocosm tests revealed differences between release rates for fertilizers used in 2012 and 2013 (Figure 2.16). A rapid increase in nutrient mass in the water column was observed for NO<sub>3</sub>-N and PO<sub>4</sub>-P in both amendments. However, the sharp spike in nutrient concentrations was most prevalent in the Osmocote™ only amendment. The maximum change in NO<sub>3</sub>-N mass inside the mesocosm from the 2013 fertilizer amendments was 21% of the Osmocote™ amendment. Similarly, the change in PO<sub>4</sub>-P mass from the 2013 fertilizer amendments was only 16% of the Osmocote™ amendment.

After approximately two days, nutrient concentrations in both mesocosms decreased and NO<sub>2</sub>-N concentrations gradually increased. An increase in DO was observed in both mesocosms that correlated with the decrease in nutrients. The DO increase was more rapid in the Osmocote™ amendment but was not sustained throughout the experiment. DO was measured every 6 hours in the first 1.5 days of the experiment and shows diel cycles. All DO measurements after 1.5 days were sampled between 12 and 4 PM, with the exception of the value near day 8, which was measured at 9 AM.

a.



b.

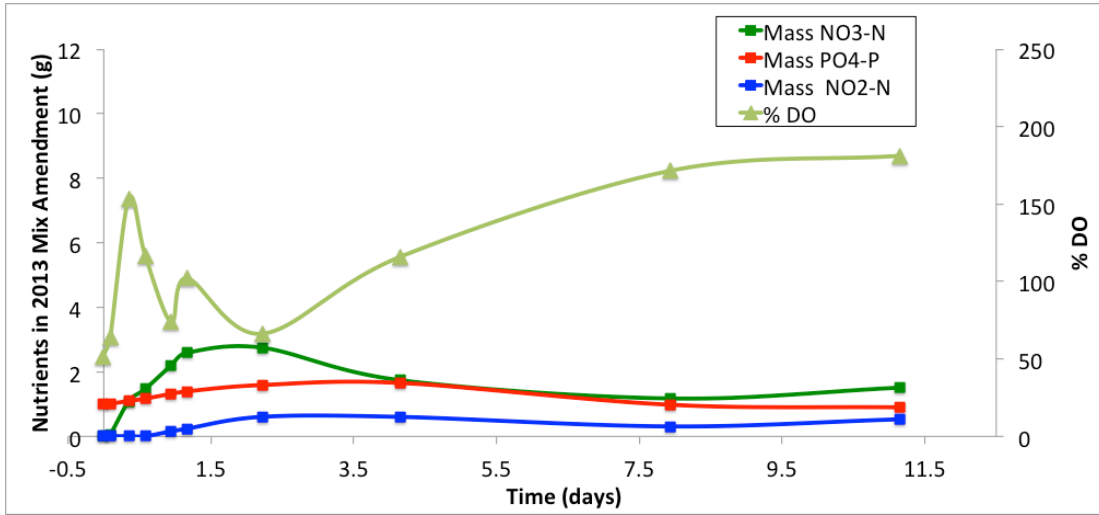


Figure 2.16. Mass of nutrients in the water column for a) the Osmocote™ amendment and b) the 2013 mix amendment.

### 2.3.3.3 Determining Nutrient Release Rate Constants from Buckets and Mesocosms

Release rate constants relate the release rate of a given nutrient (to the water column) ( $R_{nutr}$ ) to the mass of solid phase nutrient present in the system (Equation 2.1):

$$R_{nutr} = k_{release} \left( f_{fert}^{nutr} \left( M_{fert} \right) \right) \quad (2.1)$$

where  $k_{release}$  represents the release rate constant,  $f_{fert}^{nutr}$  is the mass fraction of nutrient in the fertilizer,  $M_{fert}$  is the mass of solid fertilizer in the system.

Release rate constants were determined using data from the bucket tests (Figure 2.15) and mesocosm tests (Figure 2.16) in order to obtain release rate constants as a function of temperature, time, and the composition of the fertilizer. The slope of the line of best fit for each bucket test condition (new bags inside, new bags outside, old bags inside, old bags outside) represented the release rate ( $\text{g}_{nutr}\text{-day}^{-1}$ ). The release rate was converted to a rate constant ( $\text{day}^{-1}$ ) by normalizing the release rate (or flux) to the mass of the nutrient in the solid phase fertilizer. The fertilizer composition is found in Appendix A. This provided a rate constant for the fertilizer under each of the four conditions in Figure 2.15 associated with the temperature and time submerged in water.

Bucket tests were not conducted for the 2013 mixture of nutrients. Therefore the mesocosm tests were used to compare the release rate of nutrients into the water column from the 2012 and 2013 fertilizer mixtures. Assuming that uptake was negligible at the beginning of the mesocosm experiments (i.e., DO follows a normal diel cycle; e.g., first 1.5 days) the subsequent larger increase in DO (Figure 2.16) likely reflects growth of photosynthetic organisms in response to the amendment. Under these initial conditions (e.g., first 1.5 days) nutrient release

is assumed to dominate over uptake, and the release rate is obtainable from the slope of the nutrient concentration versus time (Figure 2.16).

The NO<sub>3</sub>-N and PO<sub>4</sub>-P release rate for the 2013 mixture was 21% and 16%, respectively, of the release rate from the 2012 Osmocote™ during the early stages of the mesocosm experiment (Figure 2.16). These ratios (0.21 and 0.16) were multiplied against the release rate constants for the 2012 Osmocote mixture (bucket tests) (Figure 2.15) to estimate temperature and deployment time dependencies of release rate constants for NO<sub>3</sub>-N and PO<sub>4</sub>-P release from the 2013 mixture. Table 2.3 shows the release rate constants from bucket and mesocosm tests.

Table 2.3. Release rate constants from bucket and mesocosm tests.

		NO <sub>3</sub> -N		PO <sub>4</sub> -P	
		2012	2013	2012	2013
		rate	rate	rate	rate
Deployment		constant	constant	constant	constant
Time (days)	Temp (C)	(1/days)	(1/days)	(1/days)	(1/days)
78.00	12.8	1.1E-03	2.4E-04	2.8E-04	4.5E-05
78.86	12.8	1.1E-03	2.4E-04	2.8E-04	4.5E-05
81.90	12.8	1.1E-03	2.4E-04	2.8E-04	4.5E-05
85.12	12.8	1.1E-03	2.4E-04	2.8E-04	4.5E-05
89.97	12.8	1.1E-03	2.4E-04	2.8E-04	4.5E-05
96.23	12.8	1.1E-03	2.4E-04	2.8E-04	4.5E-05
0.00	12.8	2.8E-03	5.9E-04	2.2E-04	3.5E-05
0.86	12.8	2.8E-03	5.9E-04	2.2E-04	3.5E-05
3.90	12.8	2.8E-03	5.9E-04	2.2E-04	3.5E-05
7.12	12.8	2.8E-03	5.9E-04	2.2E-04	3.5E-05
11.97	12.8	2.8E-03	5.9E-04	2.2E-04	3.5E-05
18.23	12.8	2.8E-03	5.9E-04	2.2E-04	3.5E-05
102.41	28.3	2.5E-03	5.3E-04	9.9E-04	1.6E-04
105.24	29.4	2.5E-03	5.3E-04	9.9E-04	1.6E-04
107.22	25.6	2.5E-03	5.3E-04	9.9E-04	1.6E-04
112.05				9.9E-04	1.6E-04
24.41	28.3	8.2E-03	1.7E-03	1.7E-03	2.7E-04
27.24	29.4	4.5E-03	9.3E-04	1.5E-03	2.4E-04
29.22	25.6	3.4E-03	7.1E-04	1.4E-03	2.3E-04
34.05				1.2E-03	2.0E-04
300.00	12.8	1.1E-05	2.4E-06	2.8E-06	4.5E-07
300.00	27.6	2.5E-05	5.3E-06	9.9E-06	1.6E-06

It should be noted that the release rate constants lump multiple processes. For example, rate constants for NO<sub>3</sub>-N release subsume processes beyond release from fertilizer, specifically transformations of ammonia and urea to nitrate. This is indicated by the formation of nitrite (Figure 2.16) during the mesocosm experiment, which is an intermediate substrate in the

transformation of ammonia to nitrate. The release rates and removal rates of nitrogen from the fertilizer determined in this study are complicated by two forms of nitrogen in Osmocote™ (nitrate and ammonia) and urea found in the 2013 mixture of fertilizers. The chemical transformation of ammonia and urea to nitrate require 2 and 3 steps, respectively, and the corresponding rates of hydrolysis and nitrification contribute to the lumped release rate constant that we report.

Whereas the bucket and mesocosm tests define release rate constants dependences on temperature and deployment time, they do so for a limited range of values. To expand the range of temperature and deployment time values to match conditions in the amended plots, multivariate linear regression was used. In order to avoid negative estimated release rates, which might result from field temperatures and deployment times outside the range provided by the bucket tests, two rate constants were added to the regressed data (at 300 days at 12°C and 28°C). These rate constants better constrained the regressions at the upper end of the deployment time, and the lower and upper ends of the temperature range, experienced in the field. These estimated minimum and maximum rate constants are included in the table of rate constants (Table 2.3).

MATLAB was used to perform the multivariate linear regression. The MATLAB script file is provided in Appendix A. For both years (2012 and 2013) equations were produced for NO<sub>3</sub>-N and PO<sub>4</sub>-P release rate constants as a function of temperature and deployment time (Table 2.4). Figure 2.17 shows the results from the multivariate regression for the range of temperatures observed in the field and the regressed data.

Table 2.4. Equations describing nutrient release rates ( $k_{release}$ ) for the 2012 and 2013 fertilizer mixtures.

2012 NO <sub>3</sub> -N	$-0.0000147(\textit{deployment time})+0.000138(\textit{temperature})+0.000101$
2012 PO <sub>4</sub> -P	$-0.000000626(\textit{deployment time})+0.0000570(\textit{temperature})+-0.000335$
2013 NO <sub>3</sub> -N	$-0.00000308(\textit{deployment time})+0.0000291(\textit{temperature})+0.000212$
2013 PO <sub>4</sub> -P	$-0.000000411(\textit{deployment time})+0.0000106(\textit{temperature})+-0.0000708$

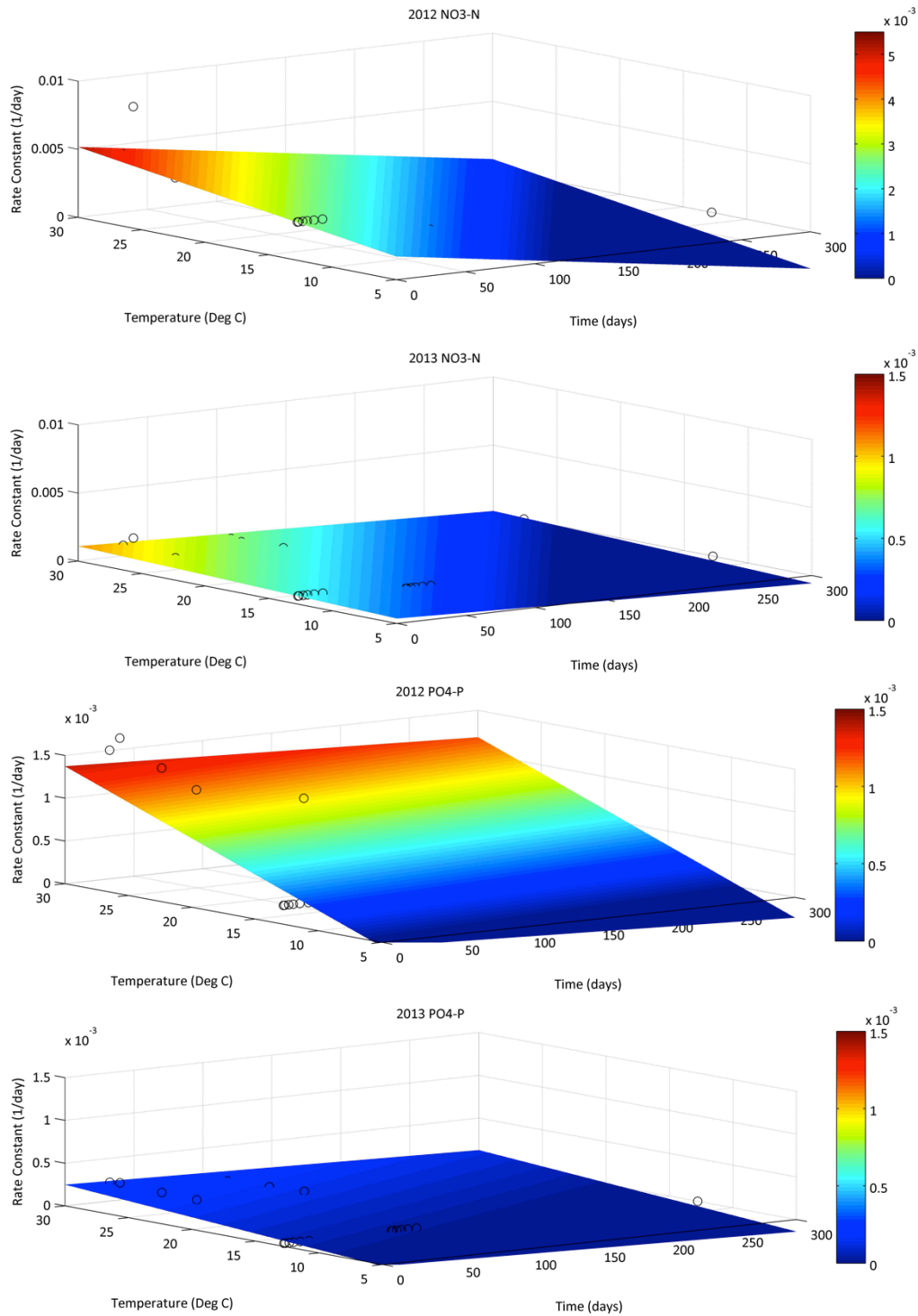


Figure 2.17. Release rate constants for  $\text{NO}_3\text{-N}$  and  $\text{PO}_4\text{-P}$  for the range of times fertilizer is submerged and water temperatures. Open circles represent discrete rate constants from the bucket and mesocosm tests. Note the different scale on the 2012  $\text{NO}_3\text{-N}$  rate constant color bar.

Figure 2.18 shows release rate constants predicted for field conditions based on the multivariate regression equations above coupled to amendment plot deployment times and Willard Spur daily temperatures recorded in the field by the Utah DWQ. For combined extreme long deployment times (e.g., >180 days) and low temperatures (e.g., 5-7 °C), the regressions led to negative  $k_{\text{release}}$  values, and in these instances the release rate constant was set to zero.

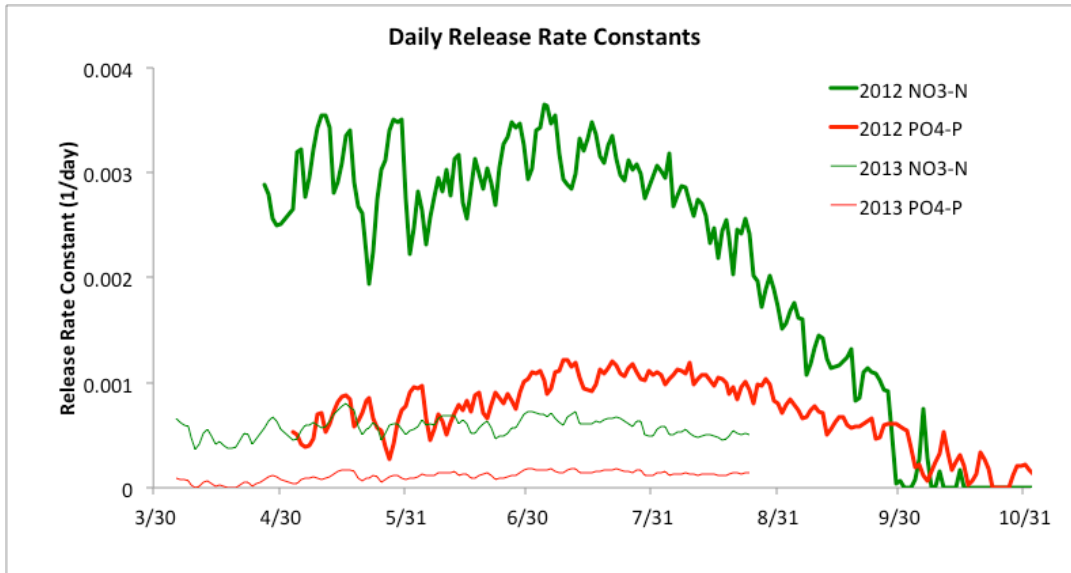
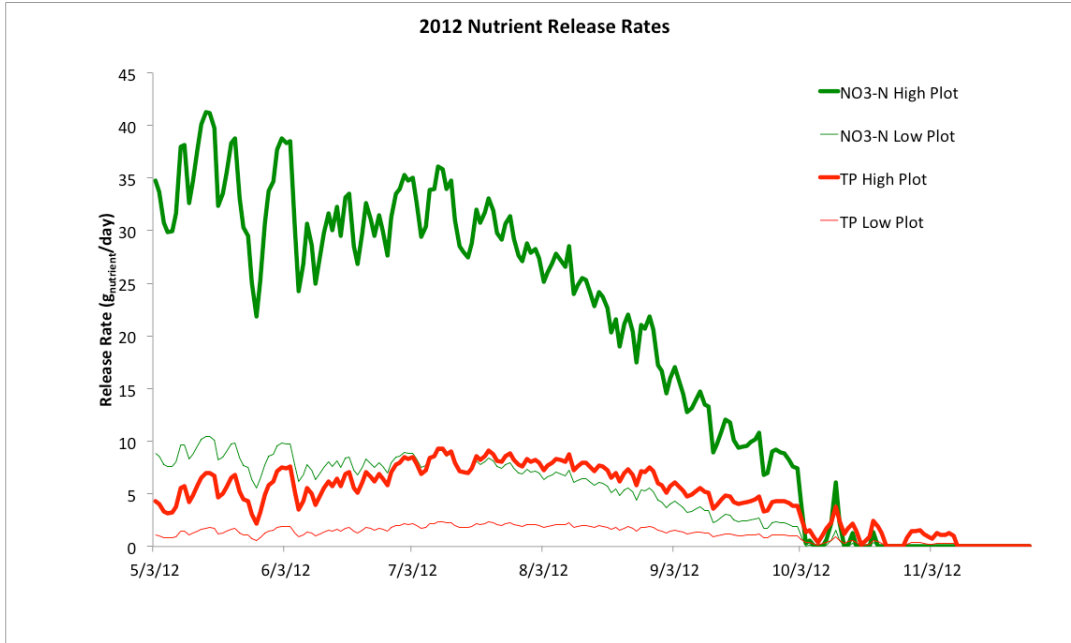


Figure 2.18. Release rate constants for  $\text{NO}_3\text{-N}$  and  $\text{PO}_4\text{-P}$  for each day during the 2012 and 2013 sampling periods.

Coupling the release rate constants to the known mass of nutrients deployed in the amended plots (Tables 2.1 and 2.2) allows estimating the daily release rate ( $\text{g}\cdot\text{day}^{-1}$ ) for each plot for both 2012 and 2013 (Figure 2.19). The daily fluxes of nutrient from the Willard Spur amendments in Figure 2.19 can be compared to other loads into Willard Spur. For the remainder of the discussion of release rate constants, it was assumed that all forms of phosphorus other than  $\text{PO}_4\text{-P}$  are negligible in the water column, and the change in  $\text{PO}_4\text{-P}$  represents the change in total phosphorus (TP).

a.



b.

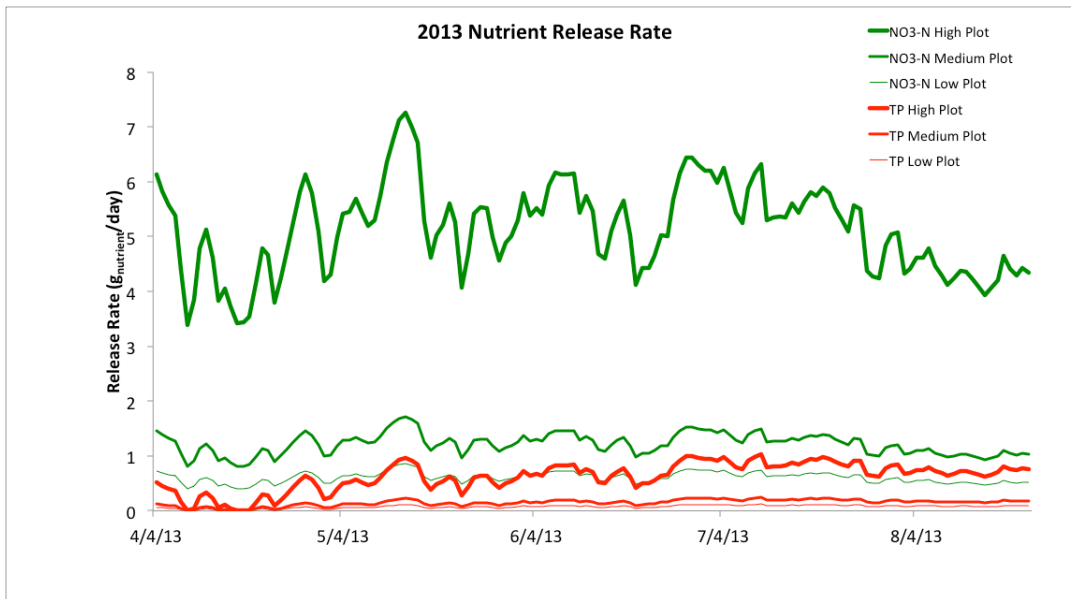


Figure 2.19. Daily release rates of NO<sub>3</sub>-N and PO<sub>4</sub>-P into the water column from the nutrient amendments during the 2012 and 2013 sampling periods.

The cumulative release from the fertilizer amendments to the water column were determined by integrating (summing) over time the mass of nutrients released each day given in Figure 2.19. The low fraction of the total nutrients released in 2013 shown in Figure 2.20 is in part due to the

variation between the difference in the change in concentration in the mesocosms for the 2012 and 2013 fertilizers. The 2013 amendments were submerged in the field fewer days than the 2012 amendments, 200 days and 140 days for 2012 and 2013, respectively.

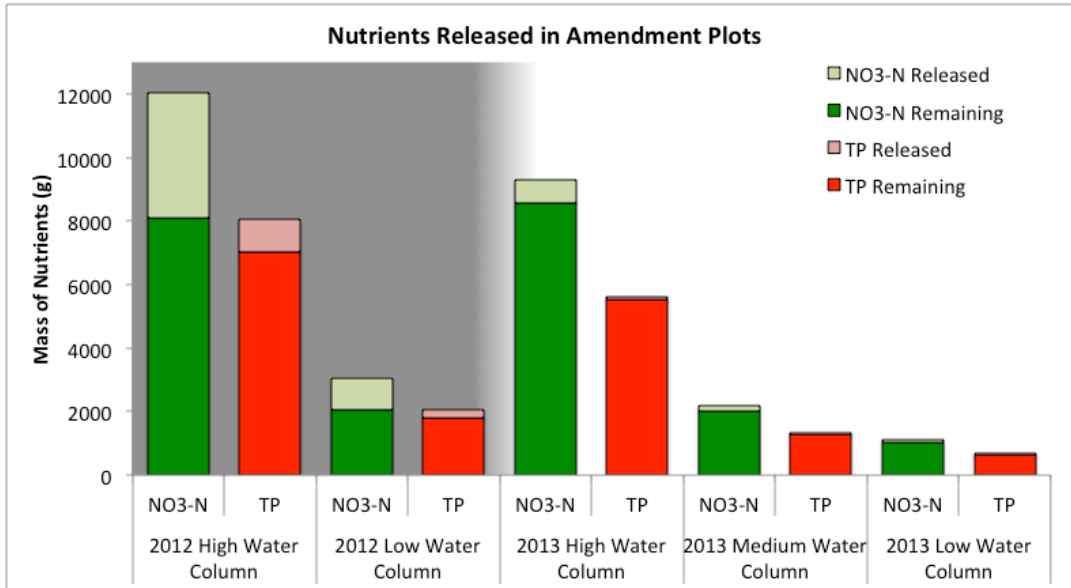


Figure 2.20. Summary of delivery of  $\text{NO}_3\text{-N}$  and TP to the water column from fertilizer amendments estimated using release rates ( $k_{\text{release}}$ ). Shaded area indicates 2012 plots.

#### 2.3.3.4 Mesocosm Nutrient Removal Rates

In this study, the term “nutrient removal” is used to describe a wide variety of processes that remove  $\text{NO}_3\text{-N}$  and TP from the water column. These processes include assimilation by SAV and algae, assimilation by microorganisms in the sediment and water column, and precipitation of nutrients onto the sediment. It does not include loss from dilution or advection because mesocosm experiments were conducted in essentially closed conditions. This term is intentionally broad because the scope of this study did not include quantifying individual physical processes related to the removal of nutrients from the water column.

The change in mass of a given nutrient in the water column, can be described using Equation 2.2:

$$\frac{\partial M_{\text{water}}^{\text{nutr}}}{\partial t} = k_{\text{release}} \left( f_{\text{fert}}^{\text{nutr}} \left( M_{\text{fert}} \right) \right) - k_{\text{removal}} \left( C_{\text{water}}^{\text{nutr}} \right) \left( V_{\text{water}} \right) \quad (2.2)$$

where  $k_{\text{removal}}$  represents the rate at which nutrients leave the water column, and  $C_{\text{water}}^{\text{nutr}}$  is the steady state concentration of the nutrient in the water, and  $V_{\text{water}}$  is the volume of water influenced by the fertilizer.

When the system reaches steady state where nutrient release is equal to uptake and the nutrient concentration in the water column reaches a steady value, the following equation applies:

$$k_{removal} = \frac{k_{release} \left( \int_{fert}^{nut} (M_{fert}) \right)}{C_{water}^{nut} V_{water}} \quad (2.3)$$

Mesocosm nutrient concentrations approached steady state during the last 4 days of the experiment (Figure 2.16), approaching values of 3.65 mg/L and 1.13 mg/L for NO<sub>3</sub>-N and PO<sub>4</sub>-P, respectively for the 2012 mixture, and values of 0.906 mg/L and 0.633 mg/L for NO<sub>3</sub>-N and PO<sub>4</sub>-P, respectively for the 2013 mixture. Table 2.5 shows the mesocosm nutrient release and nutrient uptake rate constants calculated using Equation 2.3 and the steady state nutrient concentrations.

Table 2.5. Comparison of nutrient release and removal rate constants in mesocosms.

	Mesocosm Rate Constants (d <sup>-1</sup> )		
	Nutrient	k <sub>release</sub>	k <sub>removal</sub>
Osmocote™	NO <sub>3</sub> -N	0.0743	2.02
	TP	0.0178	1.04
2013 Mix	NO <sub>3</sub> -N	0.0260	1.71
	TP	0.00486	0.305

### 2.3.3.5 Willard Spur Nutrient Removal Rates

Measured nutrient concentrations in the water column amended plots were predominantly equivalent to those in the ambient and control plots for both NO<sub>3</sub>-N and PO<sub>4</sub>-P in 2012 and 2013 (Figures 2.6 and 2.11). The exceptions to this generalization are the months of June, July, and August in 2012 for the high water column amendment. Inserting the corresponding release rate constants and measured nutrient concentrations into Equation 2.3 for this plot during these months yields a consistent set of removal rate constants ranging from 6.5 to 11.5 day<sup>-1</sup> for NO<sub>3</sub>-N, and from 1.5 to 2.75 day<sup>-1</sup> for PO<sub>4</sub>-P.

## 2.4 Water and Sediment Discussion

Water column NO<sub>2</sub>-N+NO<sub>3</sub>-N and dissolved P concentrations were significantly greater in the high and low water column amendment relative to the water column control in 2012 (Figure 2.7). However, significant differences between water column amendments and controls were not observed in 2013 (Figure 2.12). This reflects the difference in the amendment mixtures between 2012 and 2013. Specifically, the 2013 mixture contained approximately half of the nitrate and phosphorus content relative to the 2012 mixture.

Estimated nutrient release fluxes into the plots can be compared to the NO<sub>3</sub>-N and TP loads from the PWRWTP (Figure 2.21) as measured throughout 2012 (Denbleyker, 2013b). The calculated mass per day per volume of water in the amended plots assumes a water depth of

0.5 m. Loads from the PWRWTP were calculated in  $\text{kg}\cdot\text{day}^{-1}\cdot\text{m}^{-3}$  for two conditions, a relatively dry year where water storage in the Willard Spur is similar to 2012 levels (elevation of Willard Spur water is approximately 4200.5 ft) and a relatively wet year (elevation of approximately 4201.5 ft) (Denbleyker, 2013a). Nutrient loads from the 2012 low water column amendments were greater than PWRWTP loads in dry conditions (4200.5 ft) by factors of 5 and 40 throughout the months of May, June, and July, with the exception of the significant decrease observed in PWRWTP  $\text{NO}_2\text{-N} + \text{NO}_3\text{-N}$  loads in late July and early August. From September through November, nutrient loads from the PWRWTP approach and exceed loads from the 2012 low water column amendment.

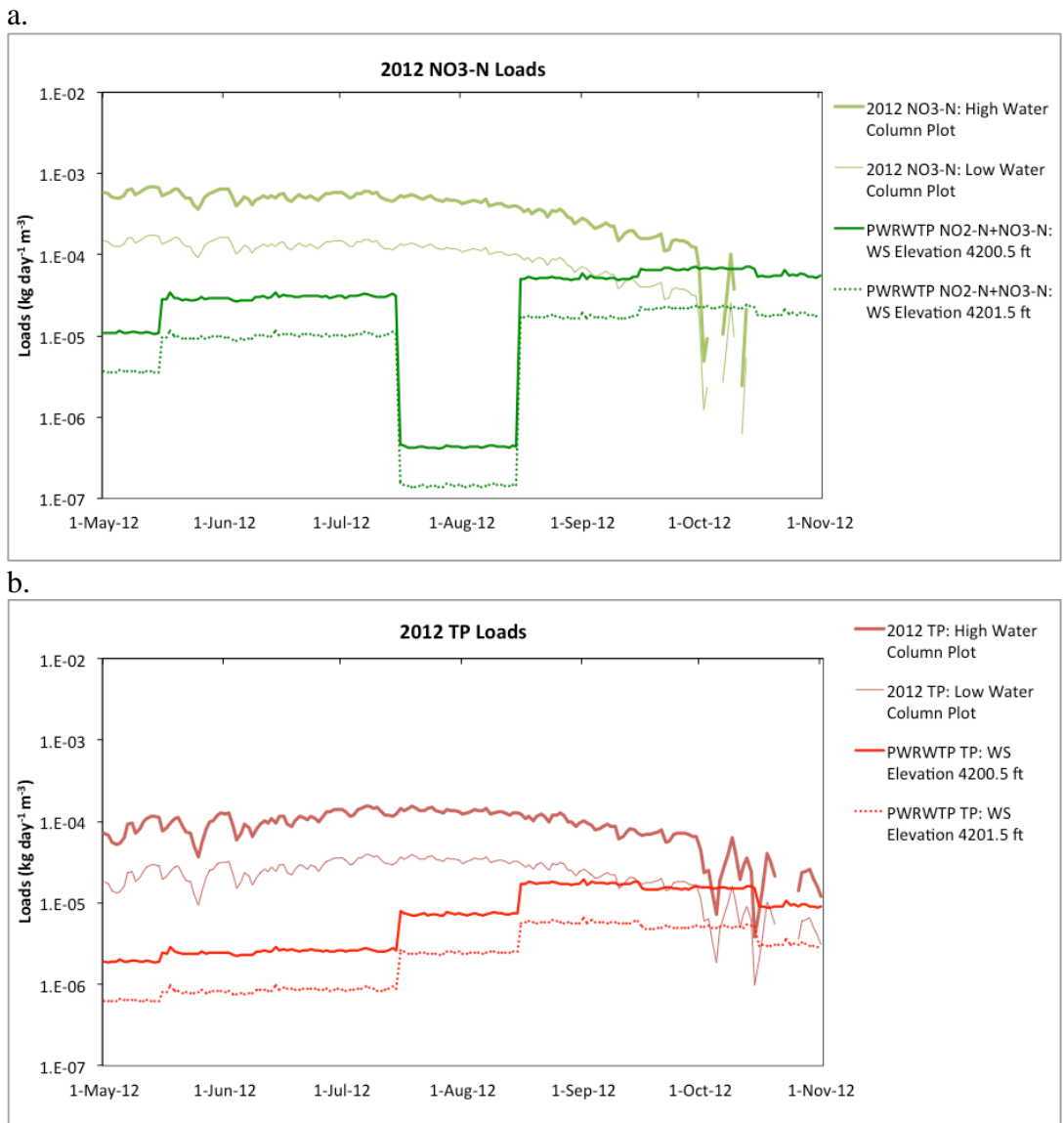


Figure 2.21. Comparison of estimated  $\text{NO}_3\text{-N}$  and TP loads from 2012 nutrient amendments and PWRWTP.

Uptake rates in the Willard Spur amended plots and the Farmington Bay mesocosms were similar (in the same order of magnitude). However, Willard Spur uptake rates were approximately a factor of 3-6 and 2-6 higher for NO<sub>3</sub>-N and PO<sub>4</sub>-P, respectively, than those from the Farmington Bay mesocosms. These differences can be attributed to the location, i.e., the mesocosm experiments were performed at a Farmington Bay impounded wetland (elevated nutrient and legacy contaminant concentrations) (Carling et al., 2013), and to the season, i.e., the Willard Spur uptake rates correspond to the active growing season (June-August) whereas the mesocosm uptake rates correspond to early fall (September).

Sediment amendments in 2012 yielded measurable increases in nutrient concentrations in sediment (Figures 2.8). Additionally, nitrogen isotope effects were also observed in the sediment-amended plots. The fertilizer δ<sup>15</sup>N was approximately 0‰, whereas the ambient sediment δ<sup>15</sup>N was approximately 7.25‰. A simple mixing of these two sources would suggest a negative Δ<sup>15</sup>N<sub>amendment-control</sub>, implying that fertilizer addition to sediment would yield δ<sup>15</sup>N values ranging from 0 to 7.25‰. Instead, amended sediment showed enriched δ<sup>15</sup>N values (e.g., 8 to 10.5‰), yielding a positive Δ<sup>15</sup>N<sub>amendment-control</sub> of 1.5‰ in the high sediment amendment (Figure 2.9). Notably, the corresponding plant leaves were depleted relative to control leaves, with a negative Δ<sup>15</sup>N<sub>amendment-control</sub> of -1.5‰ in the high sediment amendment (Hoven et al., 2013a). In fact, this isotope effect is expected in soils where excess ammonia is available (Heaton, 1986). This occurs when either labile organic nitrogen is rapidly converted into ammonium during the early stages of mineralization or when ammonium is added from an artificial source. Usually the formation of ammonia from organic nitrogen in the soil (Step 1 in Equation 2.4) is the rate-limiting step in the formation of nitrate.



Very little fractionation is observed in this reaction (ε<sub>NH<sub>4</sub><sup>+</sup>-org. N</sub> approximately 0‰). However large kinetic fractionation (ε<sub>NO<sub>3</sub><sup>-</sup>-NH<sub>4</sub><sup>+</sup></sub> of up to -35‰) is observed in the transformation of ammonia to nitrate (steps 2 and 3 in Equation 2.4). Consequently, nitrogen isotopes of the most available form of nitrogen to plants, nitrate, are significantly depleted. Therefore when the transformation of ammonia to nitrate is the rate-limiting step, plant tissue is depleted in <sup>15</sup>N and sediment is subsequently enriched in <sup>15</sup>N.

For the most part, the amendments to the water column did not yield dramatic accumulation of nutrients in the water column, presumably due to dilution and losses via plant and sediment uptake, settling of particle associated forms, and other potential factors in the Willard Spur system. The measured concentration depends on both the rate of release of the nutrients from Osmocote™ and the residence time of the nutrients within the plot, both of which are unknown. Factors such as wind, surface water flow, and plant and sediment uptake influence residence time of nutrients in the water column within the plots. The rate of nutrient release from Osmocote™ decreases below 60 °F and after 2-3 weeks of deployment (Heck et al., 2000).

Despite apparent lack of nutrient accumulation in the water column, the amendments appeared to influence plant health as indicated by plant metrics in 2012 and 2013 (Hoven et al., in preparation). In May and June of 2012 significant treatment effects were observed on percent cover of algae on SAV (attached or loosely associated macroalgal epiphytes) and branch densities (Hoven et al., 2013a). There were stronger and more lasting effects from the sediment amendments relative to the water column amendments in 2012. In 2013 gross observations include plot scale visual observations. For example, in 2013 areal coverage by plants was distinctly different within versus outside the amended area. In late July the high water column amendment showed no SAV on the surface, decreased areal coverage of SAV, and increased bleached appearance relative to the low water column amendment (Figure 2.22). Furthermore, SAV were prevalent on the surface in the low water column amended area (Figure 2.22.b) but not outside the amended area. Areal coverage and the bleached appearance decreased from the high to low amendments.

Plant responses measured in the Willard Spur test plots demonstrate that the fertilizer amendments succeeded in bracketing the range of nutrient loads below which no impacts to plant health are expected, and above which plant health is known to decline. Sensitive indicators of detrimental impacts to plant health are presented in the next section on vegetative response (Section 3).

a.



b.



c.



d.



*Figure 2.22. Surface SAV branch coverage in a) high water column plot and b) low water column plot. Areal SAV coverage and color of SAV varied significantly between c) the high water column plot and d) the low water column plot.*

## 2.5 Water and Sediment Summary

During 2012 and 2013 the Willard Spur nutrient cycling plots were exposed to a broad range of nutrient loads through the nutrient amendments. A significant difference in nutrient concentrations between plots was not measurable in the water column but plant responses varied significantly. Easy to measure parameters such as nutrient concentrations in the water column did not reflect the stress experienced by plants demonstrated in sensitive SAV plant metrics.

Beginning around July 2012 and throughout 2013 the Willard Spur water levels decreased to where it was no longer flowing into the Great Salt Lake. This impoundment could possibly have a profoundly negative effect on the Willard Spur. The storage of the Willard Spur ranged between close zero when it dried in August 2013 and over 1,400 acre-feet in 2011 when it was flowing into the Great Salt Lake.

Impounded wetlands and sheet flow wetlands have distinct differences. The hydrologic and biologic conditions are far more varied in sheet flow wetlands relative to impounded wetlands (Carling et al., 2013). During high water years when the Willard Spur is connected to the Great Salt Lake soluble and suspended constituents are transported out of the wetland. Figure 21 shows the effect of the PWRWTP effluent would have on dissolved nutrient concentrations under 2012 water levels. However, these estimates do not include estimates for the uptake capacity of the Willard Spur and the channel that connects the effluent outfall and the main body of the Willard Spur. Impounded conditions in the Willard Spur are vastly different than wet years where the area and volume of water is much greater. The increase in the area of the Willard Spur likely corresponds with an increase in its total uptake capacity as more sediment is inundated and SAV habitat expands.

Parameters indicating sheet flow wetland health are extraordinarily difficult to define and constrain. It is challenging to identify indicators of wetland health in systems with multiple “functional states” (Ostermiller, 2013). These results indicate that sediment and surface water chemistry both influence plant health in the various functional states of the Willard Spur. This is especially true in sheet flow wetlands with wide ranges of hydrologic conditions that support SAV growth. Plant health metrics such as those developed by Hoven et al. (2011) coupled with a variety of sediment and surface water parameters, possibly specific to individual water bodies, provide the most complete picture of wetland health.

## 3. 2013 VEGETATIVE RESPONSE

### 3.1. Summary of 2012 Significant Biological Indicators and 2013 Research Objectives

Results from the 2012 research in Willard Spur identified that elevated nutrient regimes imposed during a dry year, i.e., low precipitation and runoff, yielded responses in the SAV community in late April through June, following initiation of above-ground growth in mid-April. Based on this 2012 result, we condensed the 2013 research program to a more intensive window that focused on the early portion of the growing season. Sensitive metrics that were identified during 2012 (percent cover forageable SAV, branch density, percent cover associated algae, BDS) were chosen as key metrics to use during 2013. Other metrics were chosen (percent cover total SAV, percent cover surface mat, and light penetration) to help characterize natural biological trends in the Spur. Assessment of phytoplankton and macroinvertebrates was discontinued after the first year due to their late season responses that were independent of the SAV community. Using the above metrics, and SAV leaf tissue nutrient analysis, we sought to identify key biological indicators that responded to nutrient enrichment separate from the natural range of biological responses within the SAV community of Willard Spur, as well as to identify threshold concentrations of nitrogen and/or phosphorous yielding biological response among SAV.

Another key finding during 2012 was that biological responses outside the nutrient-amended research plots were significantly different relative to those inside the plots. This allowed us to additionally assess ambient conditions, lacking influence from physical plot disturbance (controls were physically disturbed to match nutrient-amended plots), in order to remove this potential bias from our interpretation (where applicable).

### 3.2 Vegetative Metric Methods

#### 3.2.1 Field Methods

Percent cover determination of SAV and algae followed protocols outlined in the State approved and published standard operating procedures (SOP) published on <http://www.willardspur.utah.gov> for monitoring and research activities in Willard Spur and other Great Salt Lake wetlands. An exception to the above is that observations were not recorded along transects; rather, the observations were recorded at five pre-assigned random locations (quadrats of 0.5m x 2m dimension) in each amendment plot. Chlorophyll *a* samples were collected at pre-assigned random quadrats within each plot, but otherwise followed published State protocol for the Willard Spur program. A draft SOP for biomass cores and benthic diatoms was submitted to the project manager May 26<sup>th</sup> 2012. This SOP includes protocol for collecting and processing branch density, tuber and drupelet biomass, which were all carried out during 2012. Only branch density was carried out during 2013.

Light penetration was determined within 3 to 5 quadrats per plot using LI-COR LI-193 underwater spherical quantum sensor as described in Hoven (2010).

SAV tissue nutrient samples for total carbon, nitrogen, and phosphorus (CNP) were collected during July (leaves) and composited from June and July (tubers and drupelets) to obtain adequate sample following

the protocol described in Hoven (2010). Only leaf samples were collected for CNP analysis twice in May and once in June during 2013. Processing CNP samples took priority and were processed quickly (within 2 days) to avoid loss of nutrients by leaching (Vymazal 1996). After removal of debris, sediment, most periphyton and epifauna, samples were sorted by tubers, shoots and leaves, and drupelets, or just leaves, for individual analysis. There were a total of 3 replicates of the plant tissue types per plot per month when adequate sample was available. Percent carbon and percent nitrogen analyses was conducted at the University of Utah.

### 3.2.2 Statistical Analyses

#### 3.2.2.1 Bioindicators

In 2012, we conducted multivariate analysis of variance (MANOVA) on several SAV metrics and nutrients vs. nutrient enrichment treatments and month on water column and sediment amendment data separately. MANOVAs are simply ANOVAs with several dependent variables. ANOVAs tests for the difference in means between two or more groups, while MANOVA tests for the difference in two or more vectors of means. We used three criteria for evaluating significance of MANOVA results: Wilks, Lawley-Hotelling, and Pillai's tests. We then conducted individual ANOVAs on each dependent response variable because MANOVA results were significant. This allowed us to determine which responses were significant. We also created 90% CI graphs to compare metric responses. Any non-overlap in 90% CIs was considered significant. For several comparisons we used simple correlations if we did not consider either variable to be a response to the other variable (i.e., if there was not a known cause and effect relationship).

In 2013, nine plant metrics were evaluated for use as bioindicators: Branch Density, % Total SAV, % Total Mat, % Forageable SAV, % BDS on SAV, % Algae on SAV, % Algae and BDS on SAV, DWQ Condition Index, and a Modified Condition Index. The plant metrics were compared using box plots (median, 25<sup>th</sup> and 75<sup>th</sup> percentiles) and separate non-parametric Kruskal-Wallis tests were performed for each of nine plant metrics by two factors, Julian weekly date and treatment. We used the Steel-Dwass-Critchlow-Fligner (1984) two-tailed test of multiple pairwise comparisons. This test is a more complex method than the Dunn (1964) or Conover and Iman (1999) tests, and is recommended by Hollander and Wolfe (1999). It requires the recalculation of the ranks for each combination of treatments. The  $W_{ij}$  test statistic was calculated for each combination and the corresponding p-values were then calculated using their asymptotic distribution. Parametric two-way ANOVAs on date and treatment were also conducted on all plant metrics to determine if there were interaction effects between Julian date and treatments because the non-parametric K-W tests did not include interaction effects. All two-way ANOVAs showed interaction effects between date and treatments, although the data were not normally distributed, even after transformations, and we considered non-parametric tests to be more appropriate. Results of the two-way ANOVA date and treatment effects for all metrics were similar to the Kruskal-Wallis tests. We therefore elected to present the non-parametric test results.

#### 3.2.2.2 Establishing an Ecological Time-frame for Statistical Comparisons

Identification of significant trends outside of those occurring naturally in a dynamic system is challenging when the system is influenced by seasonal as well as inter-annual changes in air and water temperature,

hydrology, water and sediment chemistry, as well as biota. One of the points that came to light during discussions with the Science Panel was the need for a common denominator so that all biological responses could be compared on an even scale. We considered the use of cumulative days to give the common denominator an ecological basis. However, the choice of where cumulative degree day measurement data are collected is subjective and these values likely vary spatially. Cumulative degree day data were not collected from within the experimental plots and the two closest available data sites, WS2 and WS6, had different degree day values ([Appendix E.1](#)). In addition, data from these two sites were inconsistently recorded in 2012 and 2013.

Julian weekly dates were compared with cumulative degree days for WS2, WS6, as well as the average of the two sites ([Appendix E.1](#)). Pearson's correlation tests showed that weekly Julian dates were highly correlated and interchangeable with cumulative degree days ([Table E.2](#)), therefore we elected to use Julian dates and associated calendar dates in our statistical analyses. If degree day values are preferred by managers, then values in [Appendix E.1](#) can be substituted for Julian dates.

### **3.3.2.3 Thresholds**

We conducted classification and regression tree analyses (CART) to develop models of the relationships between relevant SAV metrics and measured environmental variables using S-Plus 8.1 (TIBCO 2009). CART models provided a more powerful alternative to linear and additive regression models for our quantitative data and to linear and additive logistic models for classifications for our categorical data. CART models were fit by successively splitting the data to form homogeneous subsets. The results were hierarchical trees of decision rules that were useful for prediction or classification of plant metrics. Trees were 'pruned' using cost-complexity pruning deviance and optimal recursive shrinking methods, since regression tree analyses tend to over fit the data. Cost complexity pruning determined the nested sequence of subtrees by recursively "snipping" off the least important splits, based upon a cost-complexity measure suggested by recursive shrinking results, typically yielding trees of 4 to 5 branches. When interpreting CART models, the longest "branches" are the most important factors contributing to the regression. Ordinary least squares (OLS) multiple regressions were conducted using the variables selected in the CART models to examine how well the CART model predictors influenced the metrics linearly or additively. ([Table 3.5.1](#)).

## **3.3 2013 Vegetative Response Results**

### **3.3.1 Ambient data**

Ambient SAV metrics and H<sub>2</sub>O depth values varied within treatments and among different dates, but were mostly similar to control values. In general, ambient % algal mat and % other mat were insignificantly greater than those in the control plots, but occasionally the ambient values differed significantly from those in control plots at the end of the experiment (6/27 and 7/10, [Appendix C](#)). This suggested that the experimental setup may have had slight effects on biological responses but not enough to affect the results and conclusions of the experiment. Because the ambient data added additional variability to the metrics, they were excluded from further statistical analyses.

### 3.3.2 Vegetation Metrics

During 2013, the water depth was consistently greater than 50 cm throughout the month of May and then steadily declined due to little or no inflow and evaporation, leaving a standing pool of water in Willard Spur around the UUWS research plots (Figure 3.1).

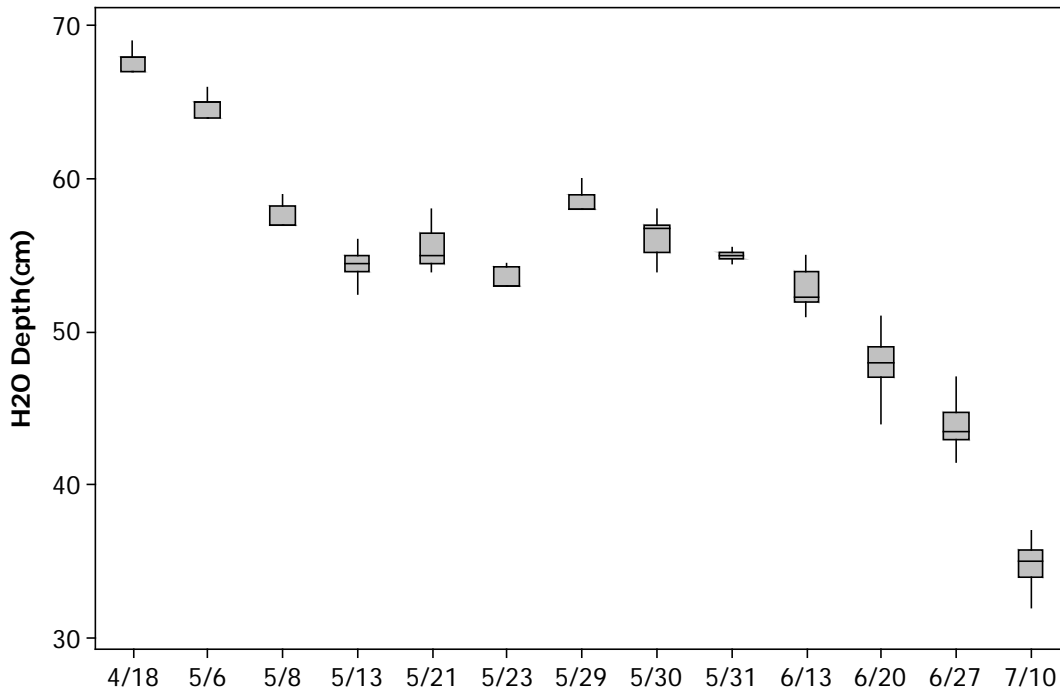


Figure 3.1. Average water depth at the UUWS research plots during 2013. Box plots include median (line) and 25<sup>th</sup> and 75<sup>th</sup> percentiles.  $n = 5$ .

Percent cover total SAV shows early establishment of SAV during April, followed by increasing growth during the first three weeks of May (Figure 3.2). Total SAV, which is the sum of forageable (e.g., *Stuckenia pectinata*, *S. filiformis*, *Ruppia cirrhosa*, *Zannichellia palustris*, *Potamogeton sp.*) and non-forageable (e.g., *Ceratophyllum demersum*), sustained high levels of cover through June, although high variability was common in the high amendment plot and occasionally in the control (not significantly different by date Tables D.1 and D.2). By the third week of June, significant declining trends in percent cover total SAV occurred with lowest percent cover in the high amendment plot ( $p$ -value < 0.01, Tables D.1 and D.3).

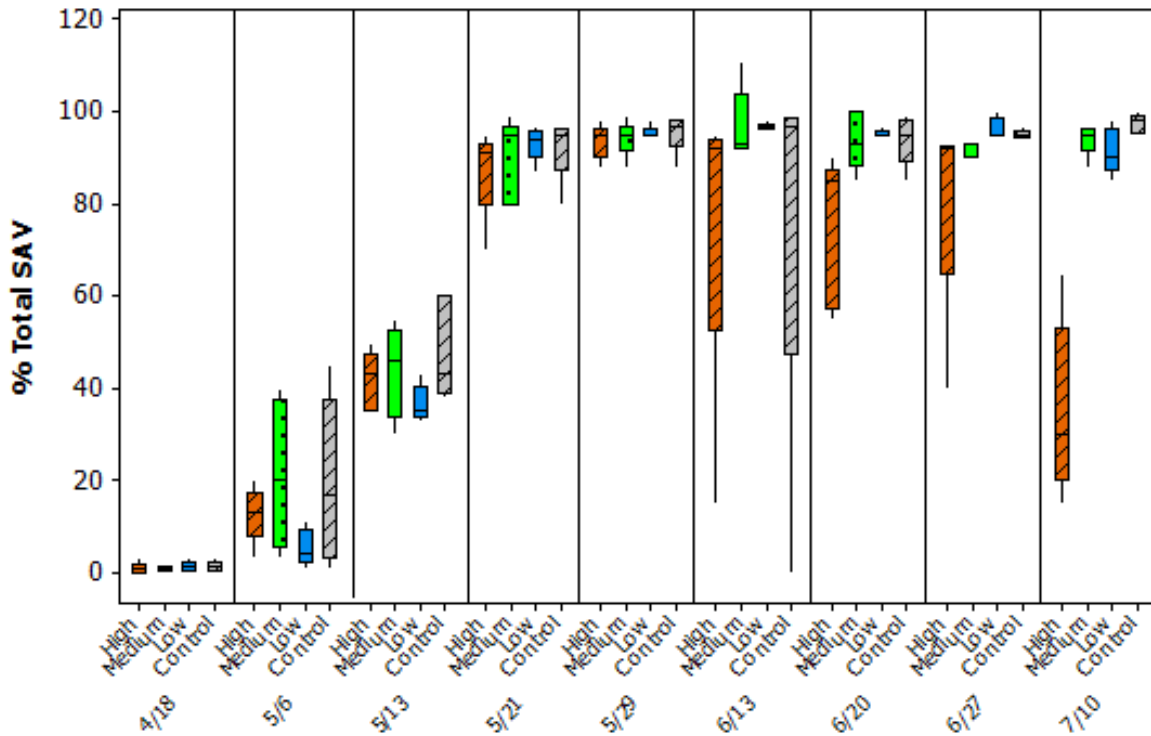


Figure 3.2. Mean percent total SAV in UUWS research plots during 2013. Box plots include median (line) and 25<sup>th</sup> and 75<sup>th</sup> percentiles. n = 5.

When the percent cover data was restricted to forageable SAV, similar trends in establishment were evident, and declining trends were again evident by the third week in July, but not significantly so (Figure 3.3, Tables D.1 and D.3). Variability among amendments and control was high by mid-June onward. Both Total % SAV and % Forageable SAV only distinctly showed SAV decline by the 2<sup>nd</sup> week in July.

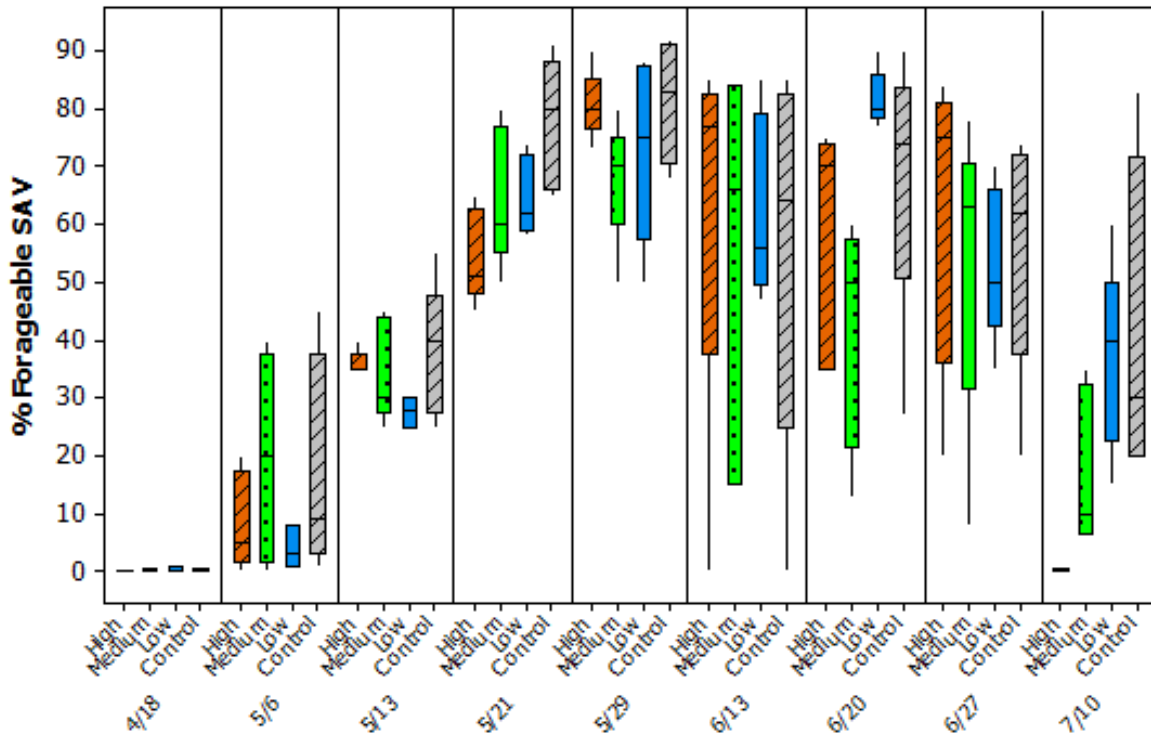


Figure 3.3. Mean percent forageable SAV in UUWS research plots during 2013. Box plots include median (line) and 25<sup>th</sup> and 75<sup>th</sup> percentiles.  $n = 5$ .

More temporal sensitivity is gained by using the branch density metric in terms of monitoring the health of the SAV (Hoven et al. 2011). This was possible due to the dominance of sheathed macrophyte species in Willard Spur. SAV in the high and medium amendments were slow to develop during May and both were consistently lower than SAV in low amendment plots during June (Figure 3.4). Declining trends in SAV branch density for all treatments and control were evident by the third week of June, and continued to decline through the second week of July ( $p$ -value < 0.01 date and treatment, Tables D.1 – D.3). By the second week in July, SAV from all treatments and controls had nearly negligible numbers of attached leaves, indicating severe die-off. Although die-off occurred in all plots (including control and ambient), earlier die-off was induced in the high nutrient amendment plot, as was the case during 2012. Interestingly, SAV growing in the low treatment plots (2013) sustained the best growth well into June, suggesting a slight nutrient enhancement above ambient levels is beneficial for SAV.

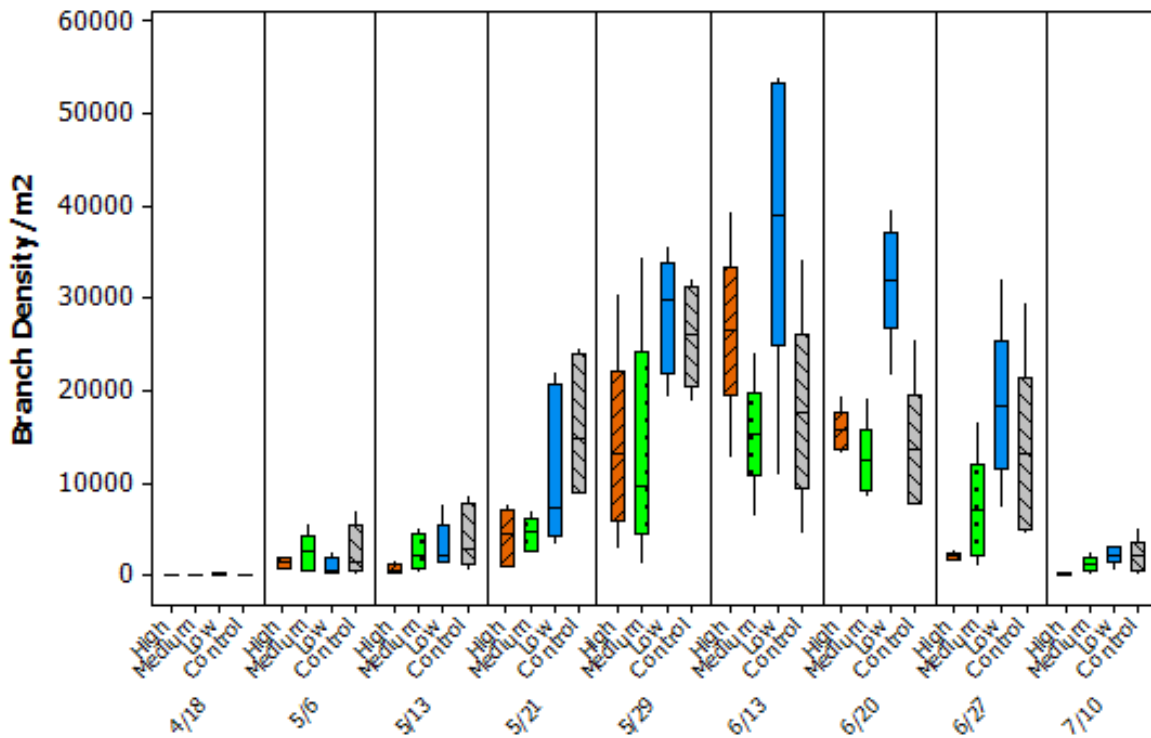


Figure 3.4. Branch density of SAV in UUWS research plots during 2013. Box plots include median (line) and 25<sup>th</sup> and 75<sup>th</sup> percentiles.  $n = 5$ .

Several metrics were used to explore possible reasons why the SAV dies off prematurely in Willard Spur. Algae sometimes grows abundantly in other open water wetlands, such as impounded Farmington Bay wetlands, with no apparent detriment to SAV. It is commonly the most salient characteristic driving SAV senescence, yet it raises the question whether the promoted link between competition for light and premature die-off of SAV is an issue in Willard Spur (Howard-Williams 1981). While some surface algae established in our research plots during 2013, it was minimal and late in the growing season after SAV growth declined and no significant differences were found among treatments or date (Figure 3.5, Table D.1). As in 2012, surface algal mat was not indicated as a stressor for SAV in Willard Spur during 2013.

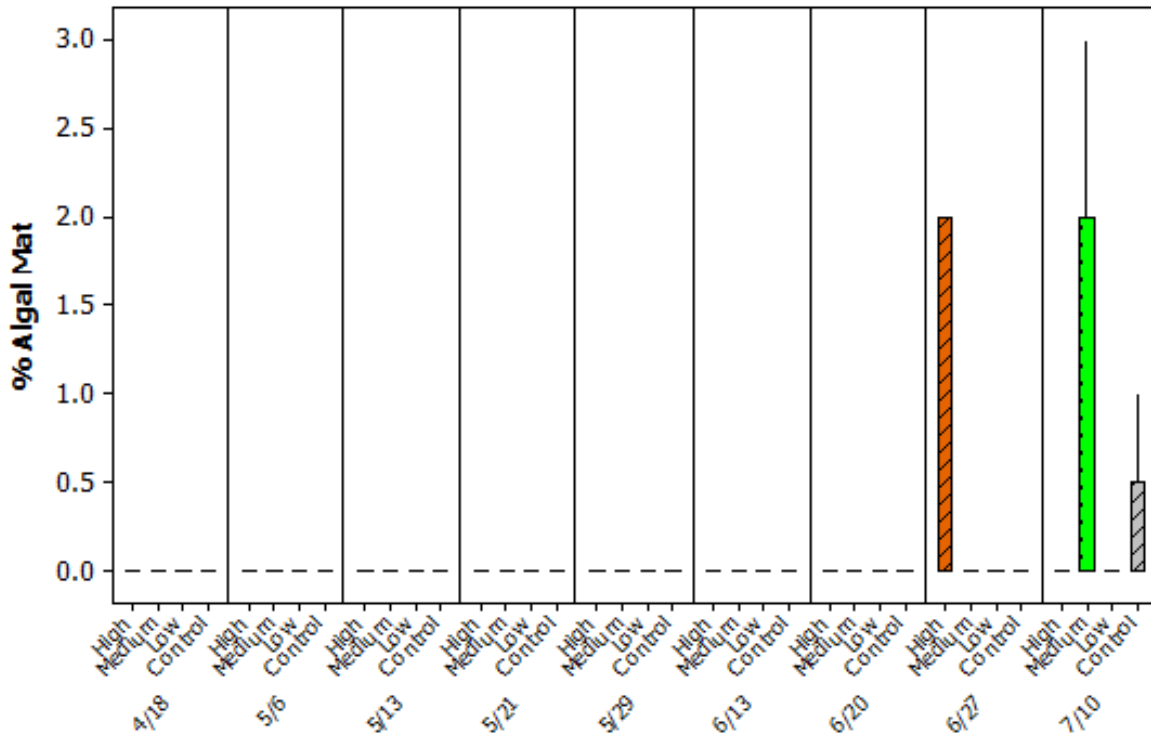


Figure 3.5. Percent algal mat in UUWS research plots during 2013. Box plots include median (line) and 25<sup>th</sup> and 75<sup>th</sup> percentiles.  $n = 5$ .

During 2012, the structure of the experimental plots included a grid of ropes on the surface of the water. Excessive amounts of plant debris (mostly drifting SAV branches) collected in the plots due to being restrained by the ropes, and created a potential artifact to the study that year. The 2013 plot design excluded surface ropes, which allowed drifting plant material to pass through the plots. There was negligible accumulation of drift, and what accumulation did occur was representative of Willard Spur overall (Figure 3.6). Further, the highest levels accumulated in the Low amendment plot, which had the best SAV growth. Thus, drifting plant debris was not considered an impediment to the SAV.

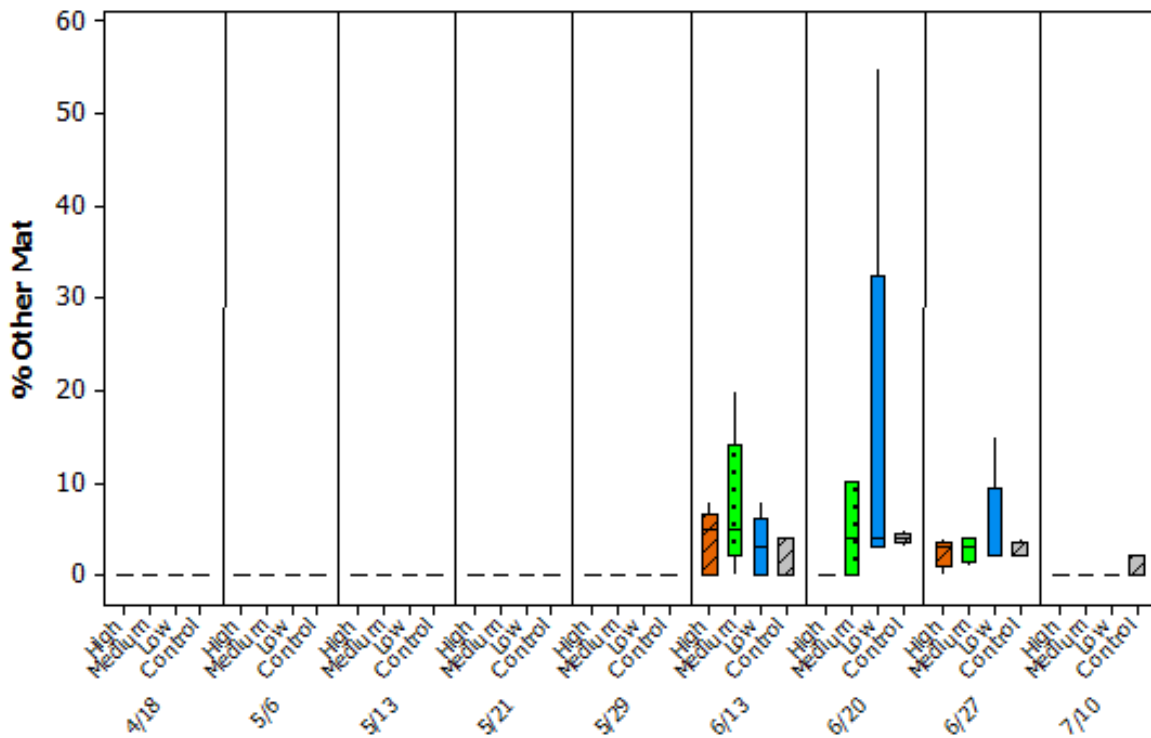


Figure 3.6. Percent cover other mat in the UUWS research plots, consisting primarily of drift SAV, during 2013. Box plots include median (line) and 25<sup>th</sup> and 75<sup>th</sup> percentiles. n = 5.

The surface of SAV leaves frequently serves as a substrate for other flora, fauna and sediment (Carpenter & Lodge 1989), occasionally to the detriment of the plants (Twilley et al. 1985). In Willard Spur, spring runoff was highly turbid during 2012 and 2013. The metric BDS, or biofilm, diatoms and sediment on SAV leaves, accounts for any coating that forms on the leaves. During 2013, sediment accumulated on all leaves as soon as SAV established. Soon thereafter, diatom and possibly biofilm communities developed on leaf surfaces, particularly on those growing in the high and medium nutrient amendments (Figure 3.7). BDS was highest on SAV leaves growing in the high nutrient amendment plot until the second week in July when BDS was high in all plots including the control (p value < 0.01 for date and treatment, Tables D.1-D.3).

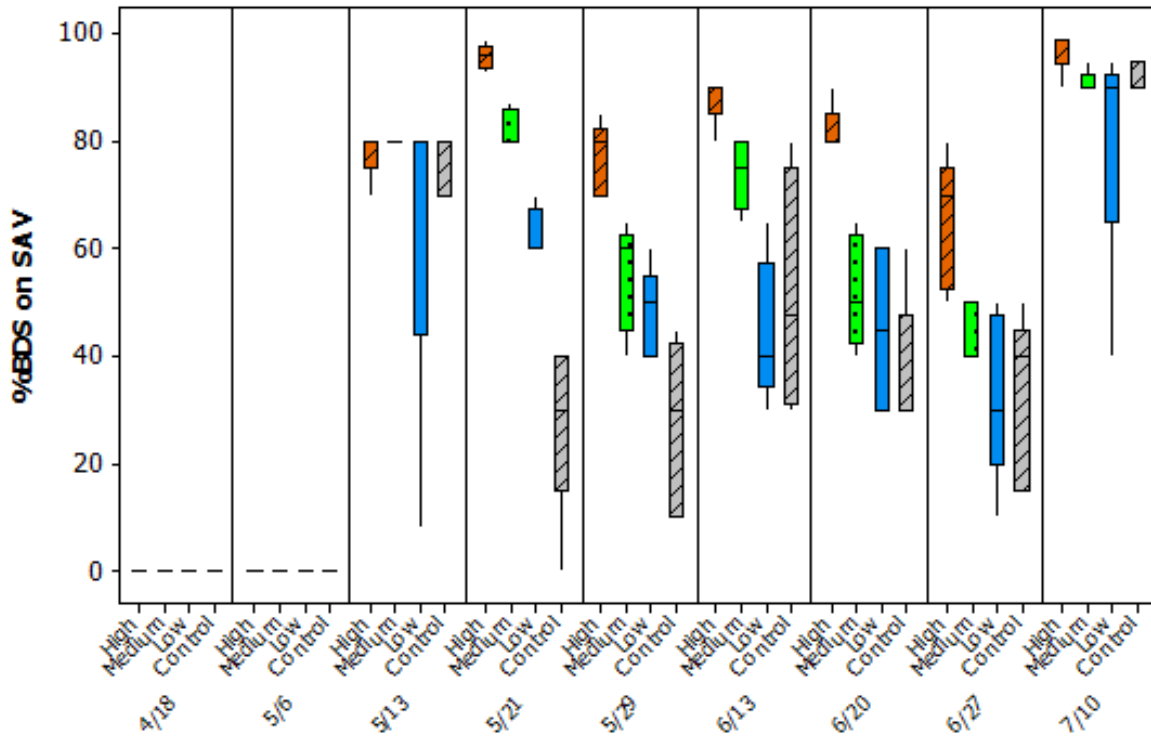


Figure 3.7. Percent cover BDS on SAV leaves in the UUWS research plots during 2013. Box plots include median (line) and 25<sup>th</sup> and 75<sup>th</sup> percentiles. n = 5.

Algae on SAV (as loosely associated macroalgae) developed approximately one month after leaves were present (Figure 3.8). By the end of May, there was slightly more algae on SAV leaves in high and medium amendments, however the levels were fairly low and certainly not excessive during June when SAV health began to decline (Table D.1 – D.3). The initial pulse of algae during the last week of May could have reflected amendment nutrient levels as decreased flow from reduced inflows from runoff was evident and less transport of amendment nutrients out of the plots likely occurred. A second pulse of macroalgae occurred during July and is discussed below in the plant tissue nutrient section (3.3.3).

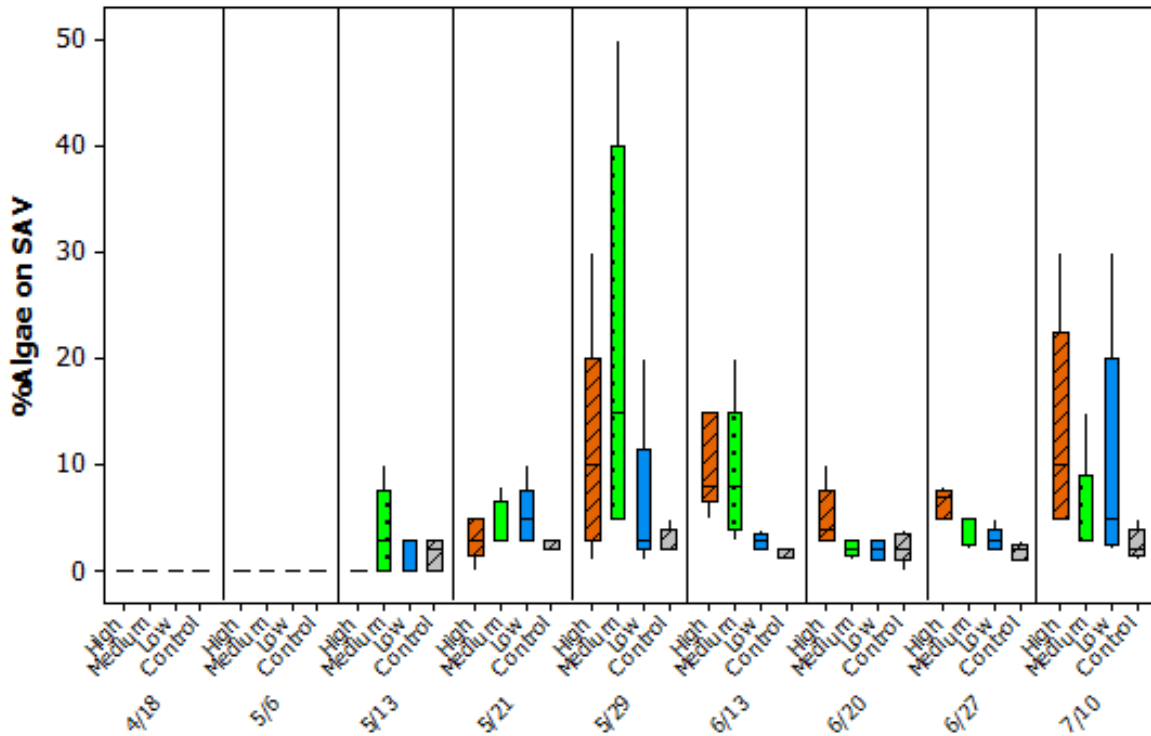


Figure 3.8. Percent algae on SAV in UUWS research plots during 2013. Box plots include median (line) and 25<sup>th</sup> and 75<sup>th</sup> percentiles.  $n = 5$ .

Condition index (CI, DWQ 2011) places whole integer values on SAV condition ranging from 1 for decomposing or senescing, to 2 for intact but stressed, to 3 for healthy. The first indication of less than ideal SAV condition was recorded in mid-June at the high amendment plots, although there was substantial variability (Figure 3.9). By the third week of June, SAV in all plots including control had a CI of 2 or higher but by the last week of June, CI of SAV in the control plots fell below 2. By the second week of July, the CI of SAV in all plots was 2 or below ( $p$ -value < 0.01 for both date and treatment, Tables 3.1 – 3.3).

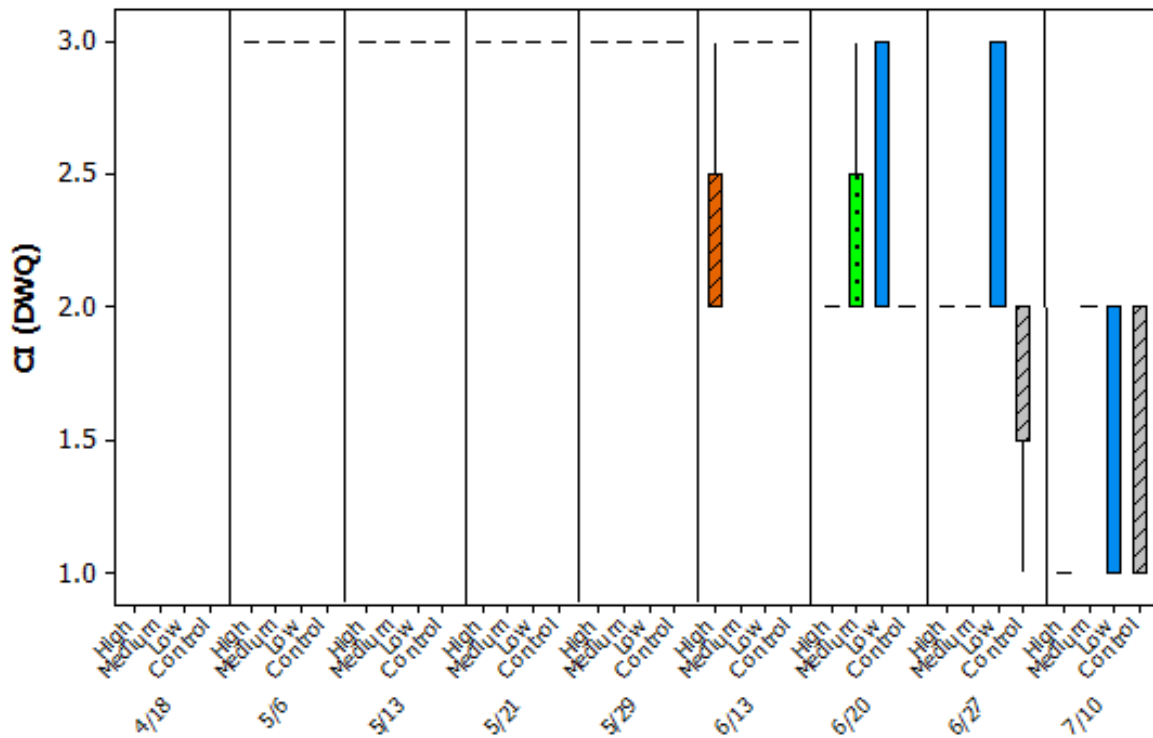


Figure 3.9. Condition index (CI) of SAV in the UUWS research plots during 2013. Box plots include median (line) and 25<sup>th</sup> and 75<sup>th</sup> percentiles. n = 5.

### 3.3.3 2013 Plant Tissue Nutrients

SAV leaf  $\delta^{15}\text{N}$  values were depleted (lower) in the high and medium amendments relative to control for all 2013 sample dates, indicating absorption of artificial fertilizer, which has  $\delta^{15}\text{N}$  values near zero (Figure 3.10).  $\delta^{15}\text{N}$  values from SAV leaves growing in the low amendment and control plots were comparable. During 2012, SAV leaf samples did not show  $\delta^{15}\text{N}$  depletion in the water column amendments. While nutrient amendments were delivered effectively both years, the 2012 samples may have been collected too late in the growing season (July) to reflect uptake of artificial N as both C and N isotopes of aquatic species vary highly between the onset of growth and senescence among other factors (Cloern et al. 2002).

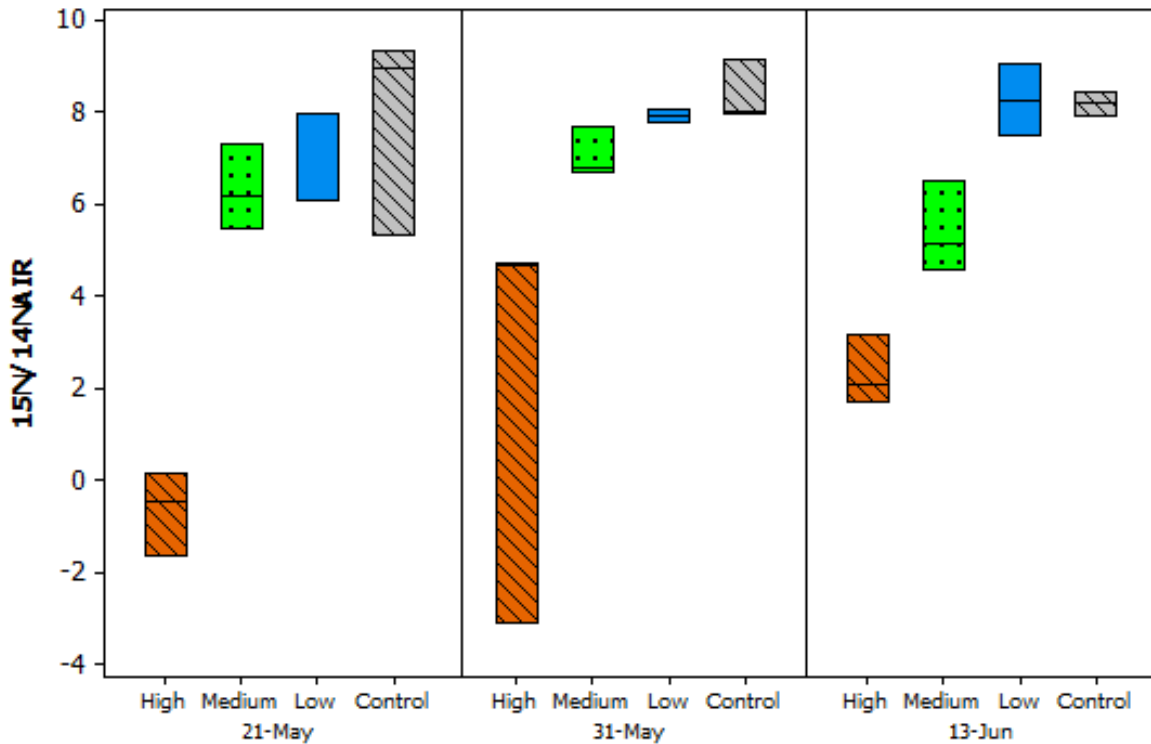


Figure 3.10. Comparison of  $\delta^{15}\text{N}$  values by three dates and four treatments, 2013. Box plots include median (line) and 25<sup>th</sup> and 75<sup>th</sup> percentiles.

Percent N by weight in *Stuckenia filiformis* leaf samples revealed lower levels of nitrogen in all amendments and control by June 13<sup>th</sup> (Figure 3.11). By June 13<sup>th</sup>, leaf N levels from SAV growing in the different amendments were significantly higher than the control at an alpha of 0.10 (p-value = 0.07). Branch densities were consistently higher in SAV growing in the low amendment plot during June than all other amendment and control plots. Additionally, it was during most of June that significant signs of die-off occurred in all but the low amendment plot. This collection of observations suggests that healthy conditions for SAV growth is reflected by the low nutrient amendment, and that perhaps SAV die-off is associated with both low nitrogen conditions (control) and nitrogen enriched conditions (medium and high amendments). Optimal nitrogen levels supporting SAV growth in Willard Spur may lie between the medium amendment and control N levels. This suggests that *S. filiformis* (and associates) may be slightly N-limited, although it is rare that sago (currently named *S. pectinata*) is limited by N (Kantrud 1990).

Apparent healthy growing conditions under low nutrient-amended levels may also indicate a trophic-level shift in nitrogen assimilation, which may contribute to the second pulse of algae on SAV during July (Fig. 3.8). As plants die off during June, nutrients released from decomposition of dead tissues are readily available and assimilated by macroalgae (Howard-Williams 1981; Carpenter & Lodge 1989), which subsequently increased in presence by mid-July. This internal cycling of nutrients and stimulation

of macroalgal growth could also explain the late-summer response in phytoplankton (documented as increased levels of chl *a*) during 2012 (Hoven et al. 2013a).

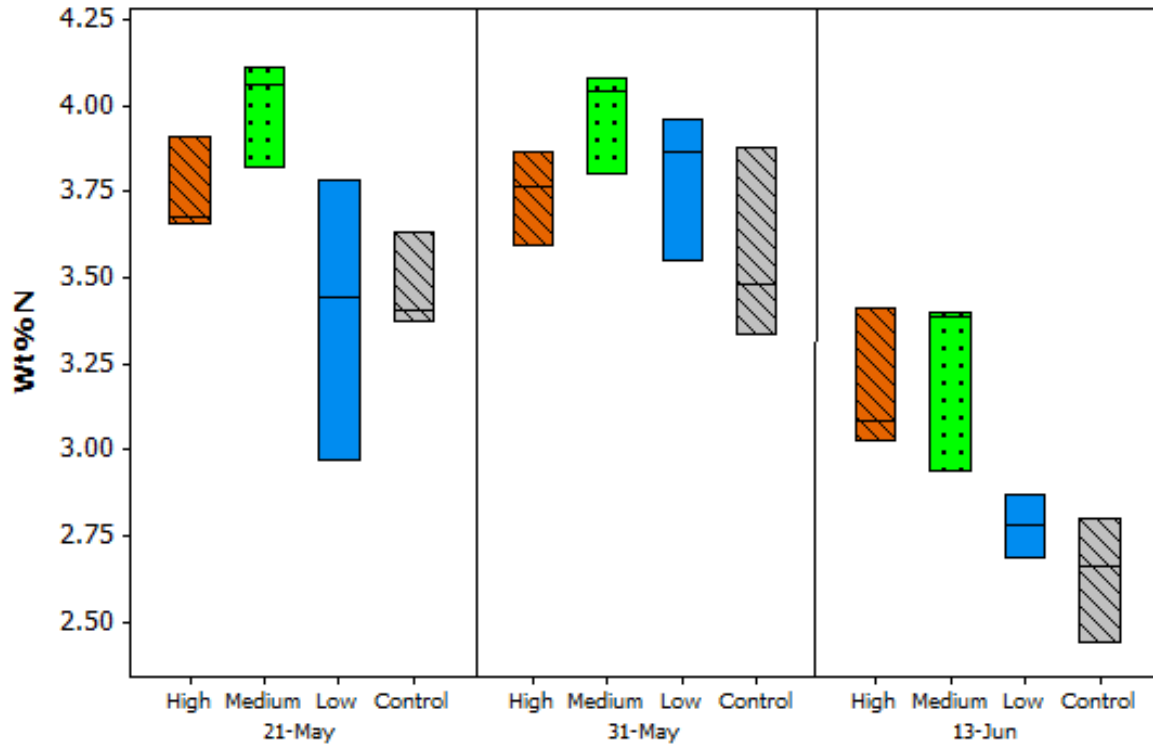


Figure 3.11. Comparison of percent weight nitrogen (Wt%N) in *Stuckenia filiformis* leaves by three dates and four treatments, 2013. Box plots include median (line) and 25<sup>th</sup> and 75<sup>th</sup> percentiles.

Macroalgae associated with SAV (primarily *Cladophora glomerata*) had increased levels of N (as percent weight) with increasing levels of nutrient amendment during the week of June 13<sup>th</sup> (Figure 3.12). Algae N levels showed a significant response to N enrichment ( $p = 0.08$ , Table D.1) and may indicate that macroalgae are limited by N availability in Willard Spur. However, there was only one sampling event making it difficult to reach conclusions without additional information.

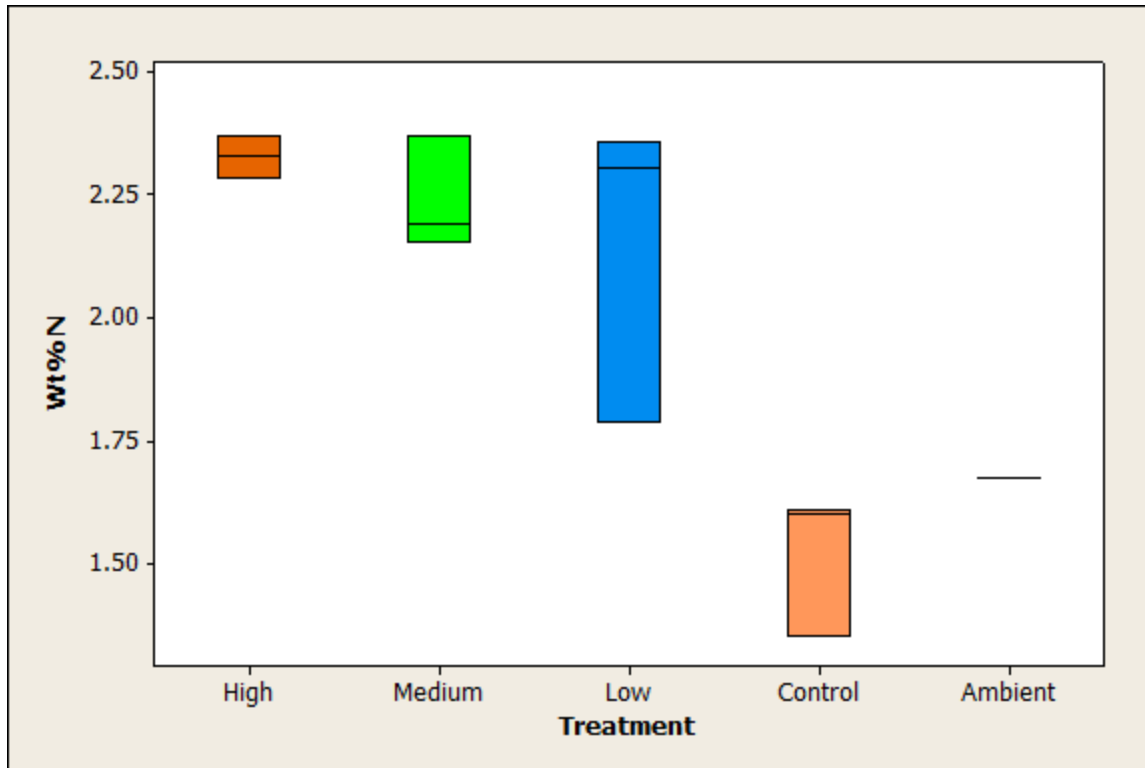


Figure 3.12. Percent N by weight in algae samples collected from SAV during the week of June 13<sup>th</sup>, 2013. Box plots include median (line) and 25<sup>th</sup> and 75<sup>th</sup> percentiles; n = 3.

*Stuckenia filiformis* leaf phosphorous levels were generally consistent across dates (p-value = 0.24, Figure 3.13, Table D.1), however there was lower P in *S. filiformis* leaf samples from the high amendment plot during the weeks of May 21<sup>st</sup> and June 13<sup>th</sup> (p-value = 0.10, Table D.2), which is the opposite of what Howard-Williams (1981) reported (elevated leaf P levels in highest enrichments of sago growing in an oligotrophic system). Sago may or may not reflect P levels of surrounding waters and can contain anywhere from 5 to 7,000 times as much P relative to that in the water column (as reviewed by Kantrud 1990). Clearly, *S. filiformis* (a very close relative of sago) is adept at accumulating P in its photosynthetic tissue in Willard Spur. Further, sago leaf periphyton P levels are difficult to separate from leaf P content and periphyton may even assist sago in obtaining P in its leaves (Howard-Williams 1981; Howard-Williams & Allanson 1981). Even though sago is generally poor at extracting P from sediments (Carpenter & Lodge 1989), sediment is a major source of P for sago when water column P (as SRP) is low and readily taken up by other organisms such as periphyton and macroalgae (Howard-Williams & Allanson 1981).

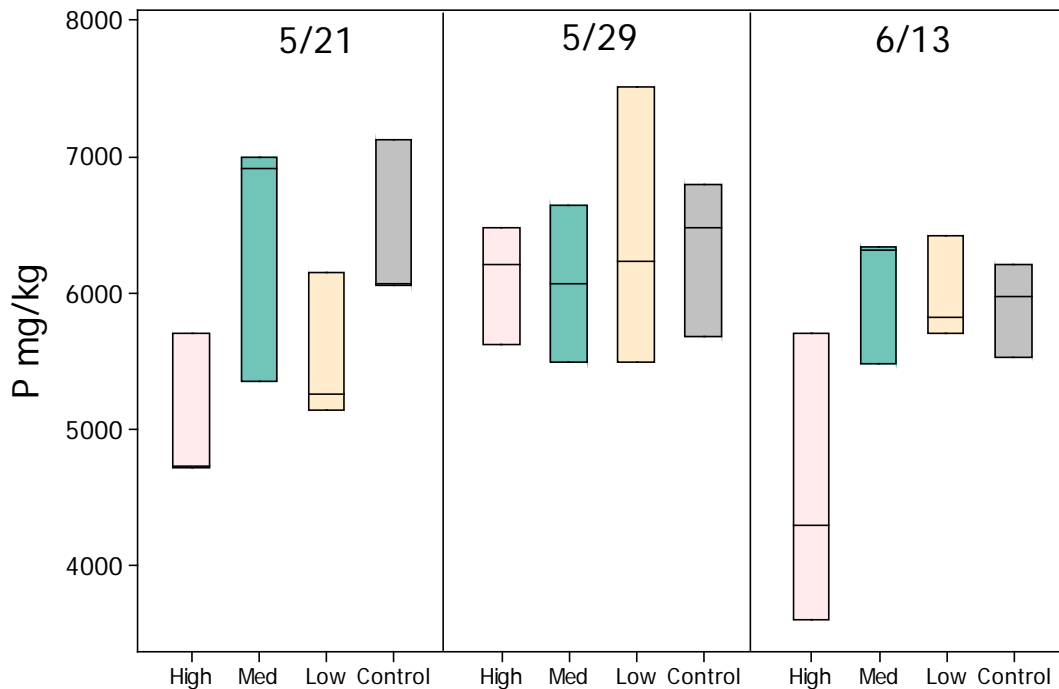


Figure 3.13. *S. filiformis* leaf phosphorous levels during 2013. Box plots include median (line) and 25<sup>th</sup> and 75<sup>th</sup> percentiles.  $n = 3$ .

When algal growth is stimulated by elevated phosphorus, e.g., significantly higher algae on SAV growing in high and medium amendments relative to the control plot (Figure 3.8, Table D.3), the phosphorous levels in algae collected from SAV growing in the medium amendments (which were similar to P levels in algae growing in high and low amendments), were significantly higher than those collected in control and ambient plots (Figure 3.14, Table D.3). The positive algal response to nutrient amendment and subsequent slight decrease in SAV leaf P suggest algae have a competitive edge in assimilating water column P, and demonstrates that *S. filiformis* is somewhat dependent upon water column derived P in addition to sediment P. Note that both *S. filiformis* and *S. pectinata* were the dominant species in the UU research plots.

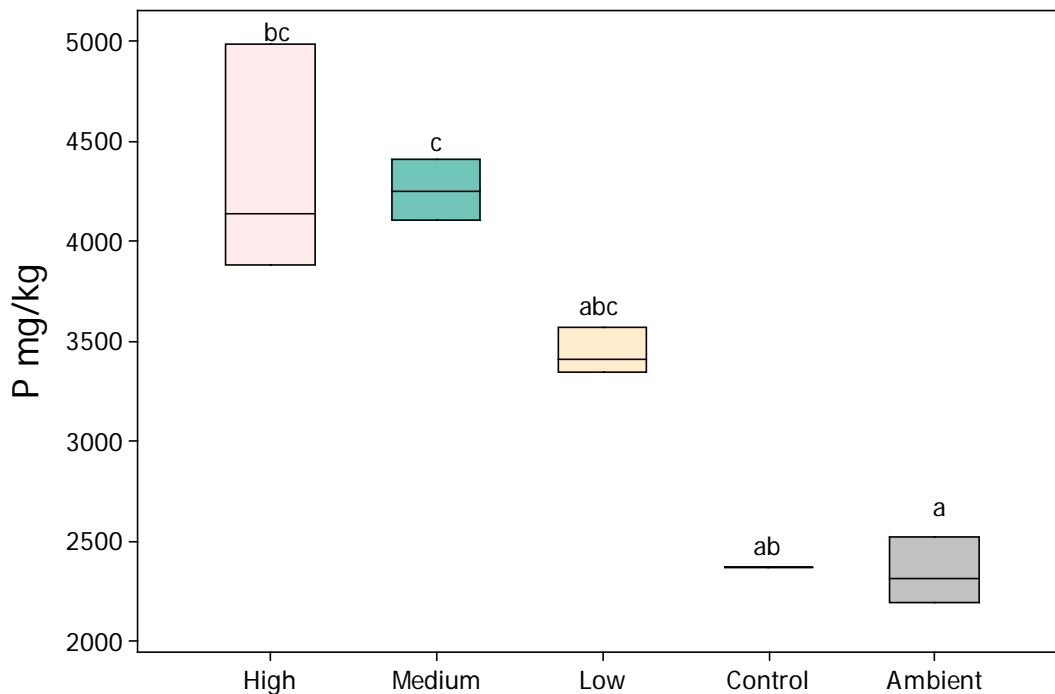


Figure 3.14. Phosphorous levels of algae collected from SAV in UUWS research plots, during the week of June 13<sup>th</sup>, 2013. Box plots include median (line) and 25<sup>th</sup> and 75<sup>th</sup> percentiles.  $n = 3$ . If the letters are different then there was a significant difference. If there are two letters together then there were ties.

Algae (specifically the macroalga *Cladophora glomerata* and related filamentous species), may be P-limited in Willard Spur once other conditions support algal growth (temperature, alkalinity, TDS, etc.). While SAV (*S. filiformis*) may be outcompeted for the nutrient, flora and fauna building up on the surface of the leaves may also impede gas exchange between the boundary layer of water around the leaves, thus limiting availability of P from the water column for SAV (BDS is always high on SAV growing in high amendments, Fig. 3.7) and further supporting its major dependence on sediment as a P source. Additionally, decomposing *S. filiformis* leaves could have released P as senescence initiated during the week of June 13<sup>th</sup> in the high amendment plots providing an additional source of P for the algae (Figure 3.9).

Algal samples were collected after algal levels reached a maximum in the research plots (June 13<sup>th</sup> versus May 29<sup>th</sup> Fig. 3.8). Budget allowed for one nutrient analysis of algae during 2013 so there was a 50:50 chance that algal growth would continue to increase from moderate levels observed during the last week of May. Since algal growth began to wane after the end of May, sample sizes were minimal (e.g., samples from the control plot needed to be composited into one sample because they were so small and ambient samples were included as a supplement to the control sample to allow statistical comparison between treatments and control). If, however, algal P-uptake tracked similarly to that of *S. filiformis* leaves when greater differences were apparent by the week of June 13<sup>th</sup>, the timing of algal

sampling was fortuitous. That said, additional research with more replication should be completed before definitively reaching any conclusions about P-limitation on algal growth in Willard Spur.

*S. filiformis* leaf carbon (as percent weight) illustrated a treatment affect during 2013 such that leaf carbon was significantly lower in *S. filiformis* growing in the high amendment plot than the other amendment and control plots (p-value < 0.01, [Tables D.1 and D.3](#), [Figure 3.15](#)). Such a dilution effect of C is considered common when there is high assimilation of N and P as discussed in Li et al. (2013). Additionally, leaf carbon declined (all amendments and control) as the spring progressed (p-value < 0.01, [Tables D.1 and D.2](#)). The declining trend may be indicative of decreased availability of inorganic carbon as pH levels in Willard Spur consistently exceeded pH of 10.0 during daytime measurements taken from mid-May through June, with pH of 10.5 or higher during the last week of May in all amendments and control plots ([Figure 3.16](#)). Continuous recordings taken from June 22<sup>nd</sup> through mid-July at the State's nearby monitoring site, W3, had daytime maxima exceeding pH of 10.4 between June 22<sup>nd</sup> and 25<sup>th</sup> and remained above pH of 10.0 through July 14<sup>th</sup>. Values of pH were consistently above 8.7 during nighttime recordings, with the lowest occurring after July 10<sup>th</sup> (data not presented), indicating potential diurnal shifts from bicarbonate ( $\text{HCO}_3^-$ ) during the nighttime, lower pH, to increased presence of carbonate ( $\text{CO}_3^{-2}$ ) systems during higher pH in the daytime. Although atmospheric  $\text{CO}_2$  is a constant supply to the total carbon pool in an open system, "the diffusion coefficient of  $\text{CO}_2$  in water is about 10000 times smaller than in air so that diffusion through the unstirred boundary layer around the leaves of aquatic plants is an important rate limiting step in photosynthesis" (Keeley and Sandquist 1992). *S. pectinata* is not a CAM plant (when the first step of carboxylation occurs during the night; Winter 1978; Keeley 1989; Keeley and Sandquist 1992) and must use an alternative mechanism to C3 pathway to utilize  $\text{HCO}_3^-$  when pH is above 8.0 (Winter 1978; Keeley 1989). Further, when pH is at or exceeding 10.5 and  $\text{CO}_3^{-2}$  is the dominant carbon form, growth and photosynthesis are completely inhibited in *S. pectinata* because the  $\text{HCO}_3^-$  compensation point for *S. pectinata* is surpassed and most plants cannot assimilate  $\text{CO}_3^{-2}$  (Lucas 1983; James 2007).

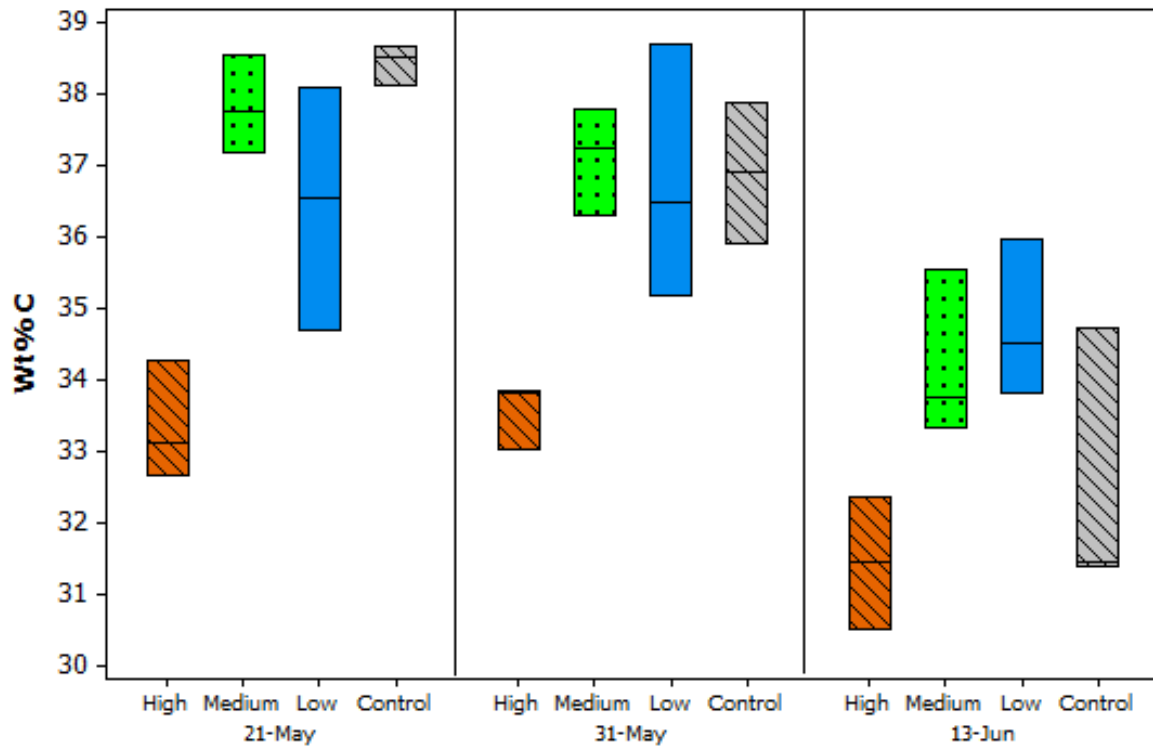


Figure 3.15. Comparison of percent weight carbon (Wt%C) in *S. filiformis* leaves by three dates and four treatments, 2013. Box plots include median (line) and 25<sup>th</sup> and 75<sup>th</sup> percentiles.

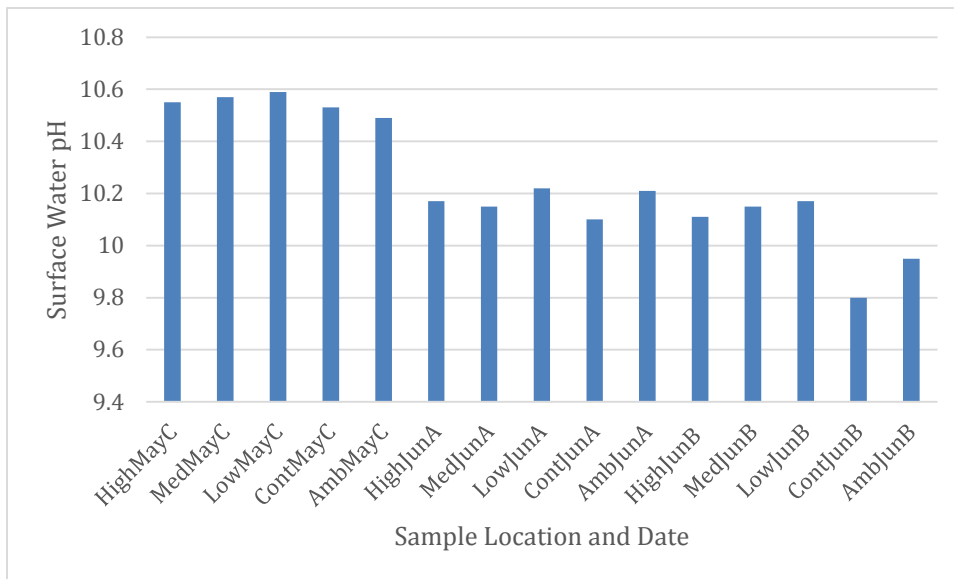


Figure 3.16. Surface water pH during late morning to early afternoon, May 30 (May C), June 13 (June A), and June 27 (June B), in high, medium, low, control and ambient plots, 2013.

Dependence on  $\text{HCO}_3^-$  carboxylation may limit the productivity of sago (Sand-Jensen 1982; Kantrud 1990; Keeley and Sandquist 1991) and perhaps its close relative, *S. filiformis* as well. Photosynthetic rates are much reduced in sago growing in waters that are high in pH due to  $\text{CO}_3^{2-}$  inhibition of  $\text{HCO}_3^-$  uptake or by increasing capacity to buffer  $\text{H}^+$  efflux from the plant (Sand-Jensen 1982). Huebert & Gorham (1983) suggest that sago needs at least  $30 \text{ mg}\cdot\text{L}^{-1}$   $\text{HCO}_3^-$  in the aqueous phase to support survival and growth. Our data indicate that during June 2012, bicarbonate in the high water column amendment was  $36.75 \pm 3.0 \text{ mg}\cdot\text{L}^{-1}$ , low water column amendment was  $45.5 \pm 6.0 \text{ mg}\cdot\text{L}^{-1}$ , and the control was  $48.3 \pm 0.58 \text{ mg}\cdot\text{L}^{-1}$ . In 2013, when we had the opportunity to sample earlier in the year,  $\text{HCO}_3^-$  was even lower (Figure 3.17). Bicarbonates were near or frequently below the  $30.0 \text{ mg}\cdot\text{L}^{-1}$  compensation point from the last week of May through the end of June of 2013 suggesting that carbon limitation may be associated with premature SAV die-off in Willard Spur. Note that  $\text{HCO}_3^-$  levels in low amendment plots are very nearly  $30.0 \text{ mg}\cdot\text{L}^{-1}$  or higher during every measurement and that it was SAV in the low amendment that grew best among all amendments and control. When  $\text{HCO}_3^-$  is the dominant carbon form (pH between 8.5 – 10.3), the boundary layer of water around SAV leaves plays a significant role in availability of carbon for uptake among other issues, and this is discussed below in more detail.

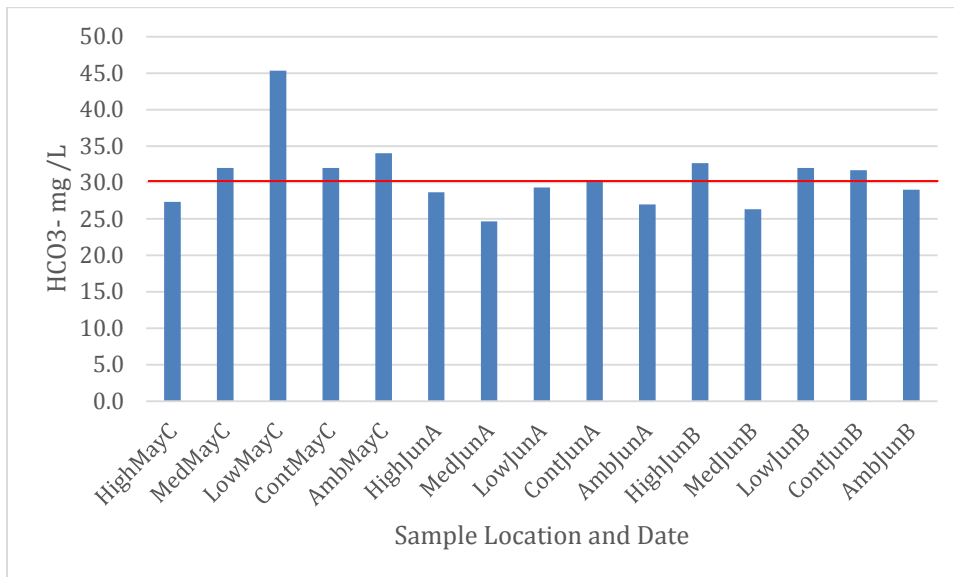


Figure 3.17. Total bicarbonate, aqueous phase from UUWS research plots during 2013. Red line indicates  $30 \text{ mg}\cdot\text{L}^{-1}$   $\text{HCO}_3^-$  compensation point for *S. pectinatus* (Huebert & Gorham 1983).

Stable carbon isotopes ( $\delta^{13}\text{C}$  compared to Pee Dee Belemnite standard) were consistent across treatments all dates during 2013 (Figure 3.18), with a decreasing trend by date (becoming more negative) in all treatments approaching  $-15 \delta^{13}\text{C}$  values by mid-June ( $p$ -value  $< 0.01$ , Tables D.1 and D.2). During 2012,  $\delta^{13}\text{C}$  *S. filiformis* leaf values collected at the end of July, were  $-15.01, \pm 0.2 \text{ sd}$ , in the control plot, (Hoven et al. 2013). It should be noted here that  $\delta^{13}\text{C}$  values are generally not indicative of photosynthetic pathways in aquatic plants (Keeley et al. 1986; Farquhar et al. 1989; Keeley and Sandquist 1992). While *S. pectinata* preferentially uses C3 carboxylation pathways at pH of 8.0 (Winters

1981), C4 pathways have not been indicated as pH rises above 8.0 and thus some other mechanisms are at play when the bicarbonate form of carbon is dominant in aquatic systems (Keeley 1991).

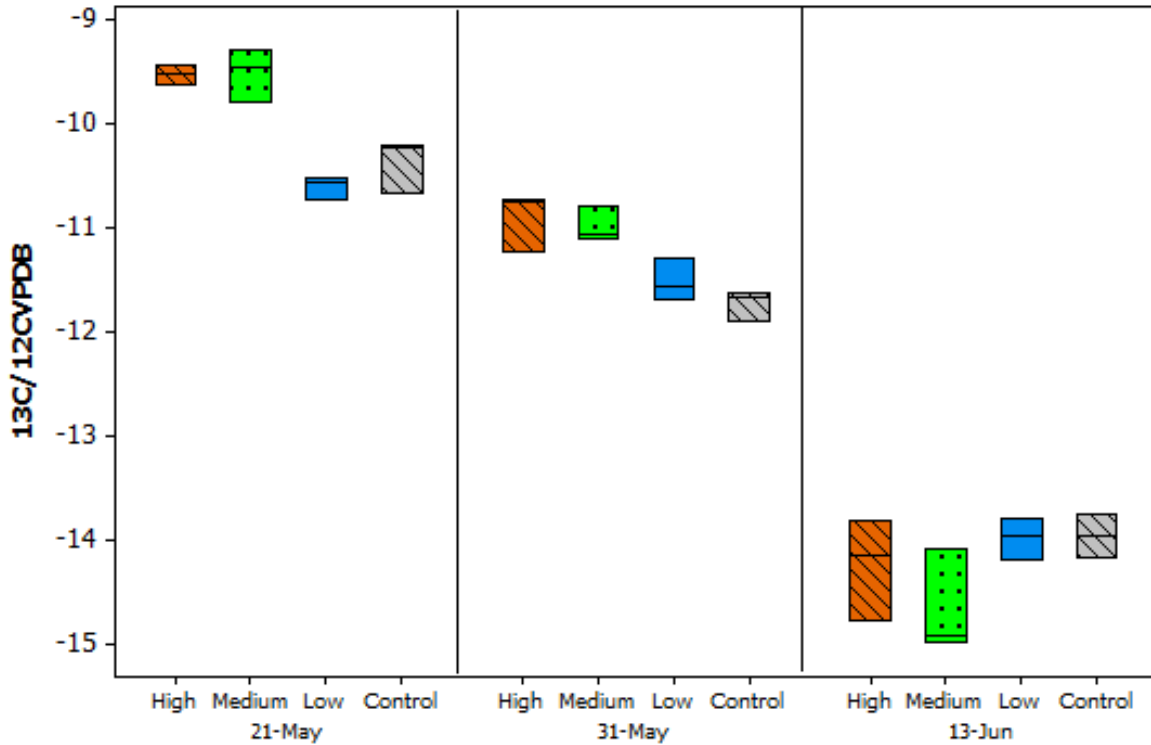


Figure 3.18. Comparison of  $\delta^{13}\text{C}$  ratios ( $^{13}\text{C}/^{12}\text{C}$  VPDB) by three dates and four treatments, 2013. Box plots include median (line) and 25<sup>th</sup> and 75<sup>th</sup> percentiles.

Although  $\delta^{13}\text{C}$  values are typically not indicative of photosynthetic pathways in aquatic species, there are other meaningful implications. More negative  $\delta^{13}\text{C}$  values means less  $^{13}\text{C}$  has assimilated in the leaf tissue yet  $^{13}\text{C}$  can be assimilated from either  $\text{CO}_2$  or  $\text{HCO}_3^-$  (Keeley 1989). The proportion of these 2 carbon species that is assimilated depends upon species-specific differences in the capacity for active transport of the  $\text{HCO}_3^-$  and on the proportion of  $\text{CO}_2$  and  $\text{HCO}_3^-$  in the boundary layer of the leaf. Normally, the  $\delta^{13}\text{C}$  ratio varies diurnally and seasonally, which makes it difficult to discern the effect of  $\text{CO}_2$  vs  $\text{HCO}_3^-$  assimilation of the total plant (Keeley and Sandquist 1992). Nonetheless, C3 plants that have the capacity to assimilate  $\text{HCO}_3^-$ , such as *S. pectinata*, become less discriminating toward  $^{13}\text{C}$  in stagnant water where carbon sources within the boundary layers are considered finite (Keeley and Sandquist 1992). Keeley (1989) also suggests that in stagnant aquatic environments, fractionation events including diffusion resistances of  $^{13}\text{C}$  uptake by C3 plants, simply due to heavier mass of the isotopes, and  $^{13}\text{C}$  discrimination by the RUBISCO enzyme in the carboxylation step of photosynthesis ( $K_m$  for  $\text{HCO}_3^-$  uptake is much higher than  $K_m$  for  $\text{CO}_2$  uptake, described also by Farquhar et al. (1989); and Keeley and Sandquist (1992)) have significant impact on photosynthetic rates and are indicated by more negative  $\delta^{13}\text{C}$  values. Thus, diffusion of  $\text{HCO}_3^-$  across the boundary layer and assimilation are rate limiting

steps in photosynthesis (Keeley and Sandquist 1992) and may contribute to premature die-off of SAV observed in all amended and control plots in Willard Spur. In Willard Spur, sustained high daytime pH likely presented limitations on photosynthetic rates due to diffusional resistance of  $\text{HCO}_3^-$ , energy costs of active transport of  $\text{HCO}_3^-$ , and potentially increased presence of carbonate, limiting available DIC altogether.

$\delta^{13}\text{C}$  values commonly become progressively more negative as the spring and summer progress in shallow ponds and in vernal pools that dry up (Keeley 1989). Bicarbonates have much lower (less negative) delta  $\delta^{13}\text{C}$  values than those of  $\text{CO}_2$  and would effectively make the  $\delta^{13}\text{C}$  value of leaf tissue less negative once assimilated. The fact that  $\delta^{13}\text{C}$  leaf values become increasingly negative as the season progressed is contradictory to the norm since high pH in the water column forced *S. pectinata* (and associates) to depend on  $\text{HCO}_3^-$  as the primary source of C. To this, Keeley and Sandquist (1992) suggest that other fractionation events play a role that lead to increasingly more negative  $\delta^{13}\text{C}$  values in systems that have predominantly bicarbonate as the free form of carbon. They explain that increasingly more negative  $\delta^{13}\text{C}$  values are due to fractionation events from photosynthetic depletion and  $\text{CO}_2$  input from decomposition of organic material and respiration, which result in a cyclic enrichment of  $^{12}\text{C}$  through the season (Keeley and Sandquist 1992). The cyclic enrichment of  $^{12}\text{C}$  is indicative of a stagnant system, which implies that diffusive resistances associated with the boundary layer of the macrophyte leaves in stagnant systems could be very important as Willard Spur becomes impounded during dry years.

No clear associations between macrophyte nutrient reserves and water column nutrients have been established for sago (Carpenter & Lodge 1986; Demars & Edwards 2007; Esteves & Suzuki 2010). However, carbon to nitrogen ratios in *S. filiformis* leaves showed different responses between high amendment and control samples (Figure 3.19, Tables 3.1-3). Control samples always had higher C:N ratios than high amendment samples, markedly so by June 13<sup>th</sup>. Samples from low nutrient amendments had similar values as control samples. Low C:N ratios are a result of higher N and P nutrient availability and assimilation in the high amendment plot, which occurs when growth limitation is related to parameters other than N and P availability (Li et al. 2013). Nonetheless, die-off of SAV in the high nutrient amended plots was significantly earlier than that in the low and control plots based primarily on branch density and condition index (Fig's. 3.4 and 3.9), indicating that nutrient enrichment (above the low 2013 level) had a negative and detrimental effect on the SAV. The low ratios in the plants growing in high nutrient amendments could be related to earlier die-off in high amendment plots that preceded die-off in low amendment and control plots, and may be related to limited gas exchange influenced by the buildup of BDS on macrophytes in the high nutrient amendment plot (Figure 3.7).

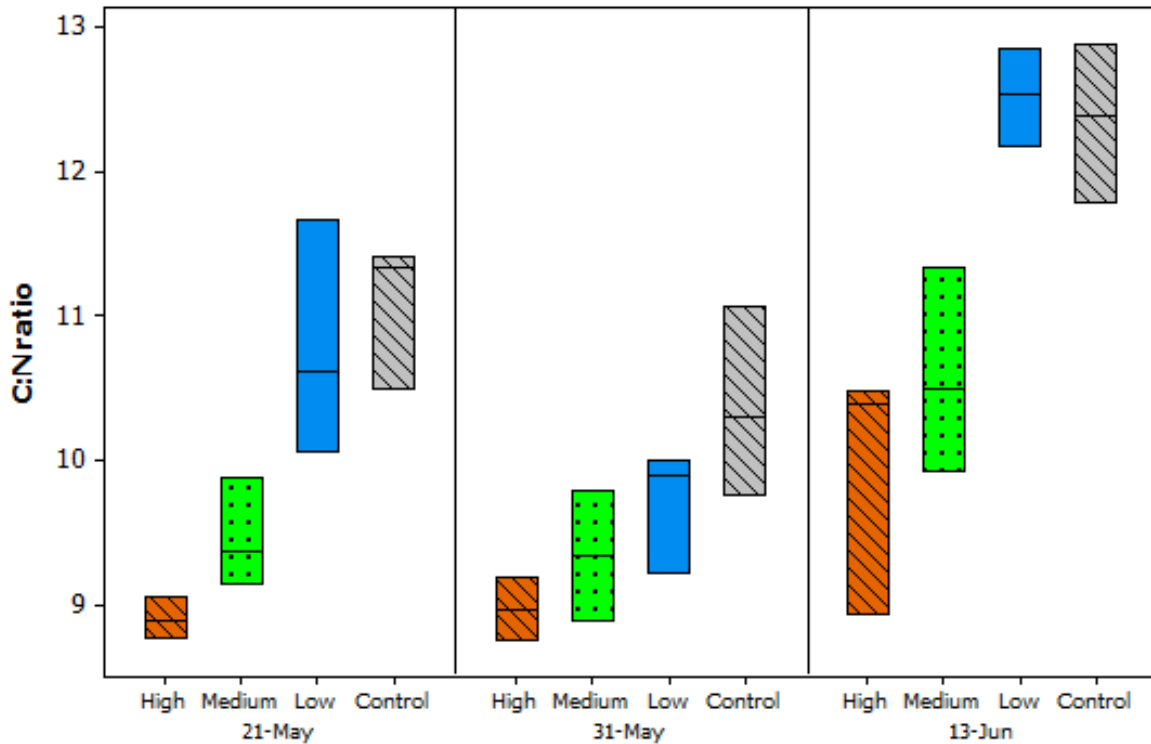


Figure 3.19. C:N ratios by three dates and four treatments, 2013. Box plots include median (line) and 25<sup>th</sup> and 75<sup>th</sup> percentiles.

### 3.4 2013 Metric Analysis and Bioindicator Selection

#### 3.4.1 Metric Selection

Five metrics indicated biological response to nutrient amendments and were selected as the most appropriate indicators for Willard Spur (Table 3.4.1), based on Kruskal-Wallis tests (Appendix D.1) and examination of box plots (Figures 3.2-3.9): branch density (log +1), % total SAV, % BDS on SAV, % algae on SAV and DWQ condition index. Response direction, seasonality and sensitivity were characterized and demonstrate the strengths of the metrics as bioindicators and the time of year when they are most useful (Table 3.4.1). Sensitivities were rated according to the span of nutrient amendment levels across which significant biological responses occurred (e.g high, medium and low). Based on sensitivity first, we recommend pairing at least two metrics: % BDS on SAV and Branch Density (log+1) due to their sensitivity to high and medium nutrient amendments, respectively, and because their seasonality is early in the growing season (mid-May). Depending on assessment objectives, a third metric could be added as a follow-up during mid-June to verify the general condition of the SAV community, using either % Total SAV or Condition Index. Alternatively, if assessment objectives only require determination of the general condition of the SAV community, either or both % Total SAV and Condition Index could be assessed mid-June.

Table 3.4.1 Response direction, seasonality and sensitivity of five bioindicators of nutrient enrichment based on on Kruskal-Wallace tests and box plot examination.

Bioindicator	Response Direction	Seasonality	Sensitivity
Branch Density (log+1)	<i>Decrease</i> at medium and high treatment levels; Slight increase at low treatment levels	Mid May	Medium
% Total SAV	<i>Decrease</i> at high treatment levels	Mid June	Low
% BDS on SAV	<i>Increase</i> at all treatment levels	Mid May	High
% Algae on SAV	<i>Increase</i> at high treatment levels	Mid May	Low
Condition Index	<i>Decrease</i> at high treatment levels	Mid June	Low

### 3.4.4 Metric Response Thresholds

#### 3.4.4.1 % Algae on SAV

Percent algae on SAV was strongly associated with TDS greater than 2300 mg·L<sup>-1</sup> and somewhat affected by total alkalinity greater than 160 mg·L<sup>-1</sup> (Figure 3.20). SAV with 81% (considerable) coverage of macroalgae were typically found in higher alkaline water with high TDS, suggesting a stronger association with water chemistry than nutrient enrichment in particular. Algae blooms coincided with high pH in other enrichment studies (Bakker et al. 2010) and have been suggested to influence the availability of carbon species by raising pH of water closely associated with the macrophyte leaves (Westlake 1967; Søndergaard 1988; Wurts and Durburow 1992). Algae on SAV were also somewhat associated (for 46% cover algae) with increased levels of NO<sub>3</sub>-N-Flux when greater than 7.7 g·d<sup>-1</sup> when TDS was less than, 2300 mg·L<sup>-1</sup>; thus nitrates are also somewhat important for the establishment of algae on SAV.

## %Algae on SAV

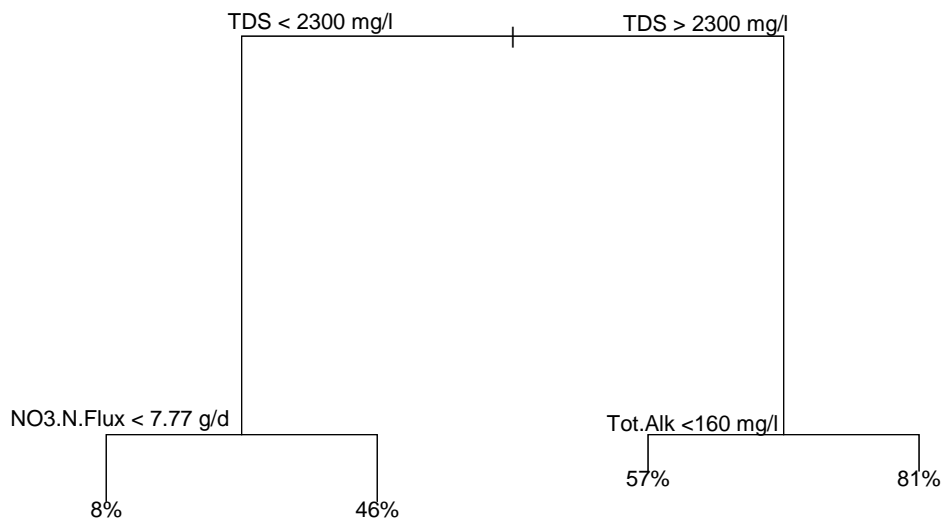


Figure 3.20. CART model of percent macroalgae associated with SAV (as % Algae on SAV) at UU Willard Spur research plots, 2012 – 2013.

### 3.4.4.2 %BDS on SAV

The most important contributor to % BDS on SAV was the year that the experiment was conducted. Approximately 80% coverage of BDS on SAV was estimated to occur when TDS was  $> 1900 \text{ mg}\cdot\text{L}^{-1}$  during 2013 (Figure 3.21) as compared to 50% BDS when TDS was  $< 1900 \text{ mg}\cdot\text{L}^{-1}$ . Although as much as 50% BDS can occur in lower levels of TDS, it is likely the cumulative effect of 80% BDS cover on a shoot that imparts the most stress on SAV by minimizing gas exchange, outcompeting the SAV for light and nutrients, and possibly allelopathic activity (Howard-Williams 1981; Twiley et al. 1986; and Gross et al. 2003). Additionally, because periphyton can raise the pH of boundary water layer, availability of free forms of carbon is affected, which may be rate limiting on photosynthesis for the SAV and, if pH is high enough, may limit the SAV completely from available carbon (Søndergaard 1988; Keeley 1991; James 2007).

## %BDS on SAV

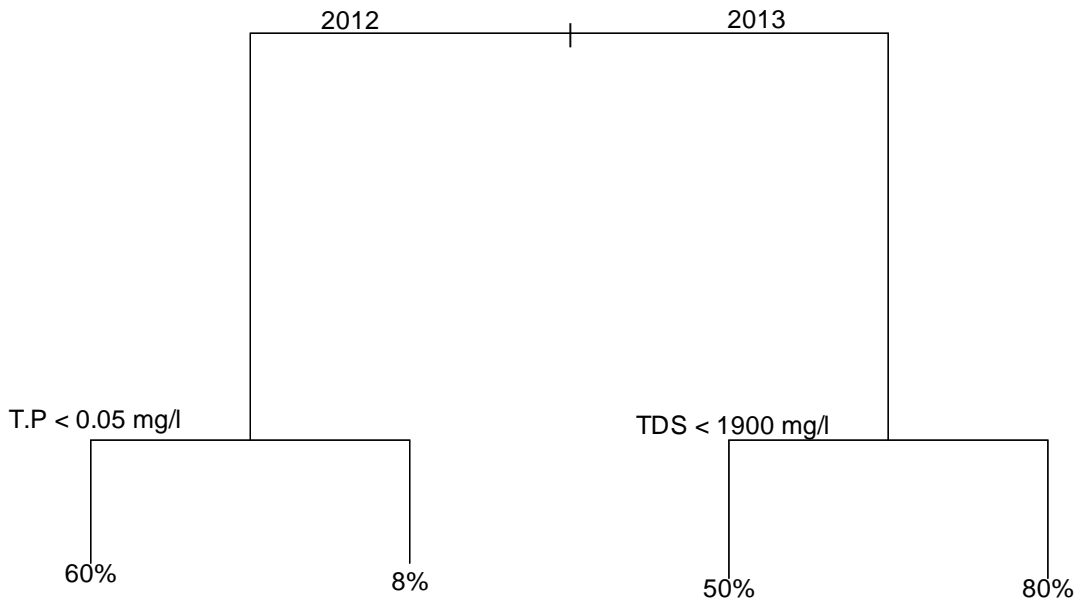


Figure 3.21. CART model of percent BDS (biofilm, diatoms, and / or sediment) associated with SAV (as % Algae on SAV) at UU Willard Spur research plots, 2012 – 2013.

During 2012, total phosphorus was a determinant for the development of BDS when levels were below  $0.05 \text{ mg}\cdot\text{L}^{-1}$  TP, perhaps indicating high rates of assimilation of P by any periphyton associated with SAV (diatoms) that may have developed a covering on the SAV. Howard-Williams (1981) demonstrated rapid uptake of  $^{32}\text{P}$  by epiphytes including associated filamentous algae and adnate periphyton and much less so by *P. pectinatus* leaves when enriched in enclosure experiments. Of particular relevance to our study, Howard-Williams found that all nutrient amendments in his study were assimilated by the macrophyte community (macrophytes, filamentous algae, periphyton, fauna, and sediments) within 24hrs of administration. In our study, detection of nutrient enrichment in the water column was minimal throughout the study both years, yet BDS and algae associated with SAV responded both years. Regardless of its trigger point for establishment of BDS on SAV, negative effects from biotic stresses are likely to be important to the health and condition of SAV.

### 3.4.4.3 Total Alkalinity

Alkalinity is a critically important factor associated with distribution of SAV in Willard Spur (Figure 3.22). Greater than 10 times the percent cover levels of SAV (85%) were estimated to occur when total alkalinity was approximately  $< 150 \text{ mg}\cdot\text{L}^{-1}$  versus when total alkalinity was approximately  $> 150 \text{ mg}\cdot\text{L}^{-1}$  (6% cover total SAV). Interestingly, lowest total alkalinity occurred during June in 2012 and during June and July in 2013, and was bracketed by much higher levels in the spring (measured only during 2013)

and rising levels during August and later months. Indications of premature SAV die-off co-occurred during June both years when lowest levels of bicarbonates were recorded, often below the bicarbonate compensation point (Huebert & Gorham 1983; Fig's. 3.4, 3.17), illustrating the overall importance of rate limiting relationships between aqueous phase of free carbon and photosynthesis in still or stagnant environments and interrelations with high pH (Keeley 1991; Wurts and Durburow 1992; James 2007).

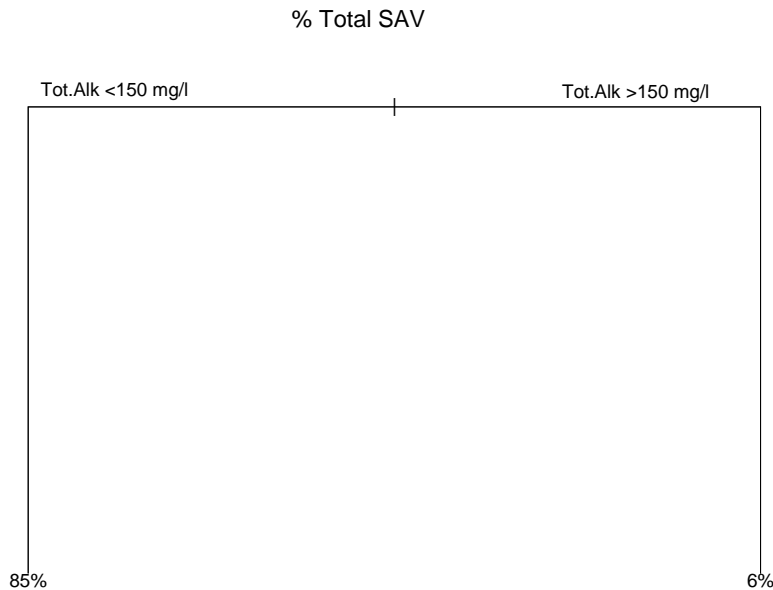


Figure 3.22. CART model of percent total SAV, at UU Willard Spur research plots, 2012 – 2013.

#### 3.4.4.4 Branch Density

Higher branch densities were mostly associated with total alkalinity  $< 150 \text{ mg}\cdot\text{L}^{-1}$ , and the highest branch densities (approximately  $13,000 \text{ attached leaves}\cdot\text{m}^2$ ) occurred when dissolved total nitrogen was  $< 1.1 \text{ mg}\cdot\text{L}^{-1}$  (Figure 3.23). Lower water column nutrients are to be expected when macrophytes and associated algae are actively growing. For example, Howard-William (1982) documented complete assimilation of nutrient additions by a sago community after 24h.

When total alkalinity was approximately  $>150 \text{ mg}\cdot\text{L}^{-1}$ ; branch densities were well below the critical threshold currently defined as  $5000 \text{ attached leaves m}^2$  in Hoven et al. (2013b). This reflected early season branch densities as well as post die-off phase. When TDS was approximately  $> 3300 \text{ mg}\cdot\text{L}^{-1}$ , branch densities were diminished even further and the macrophytes were not likely to recover. The branch density CART model implies that physico-chemical stressors in addition to stress related to excessive N or P may be related to SAV die-off.

## Branch Density/m2 (log+1)

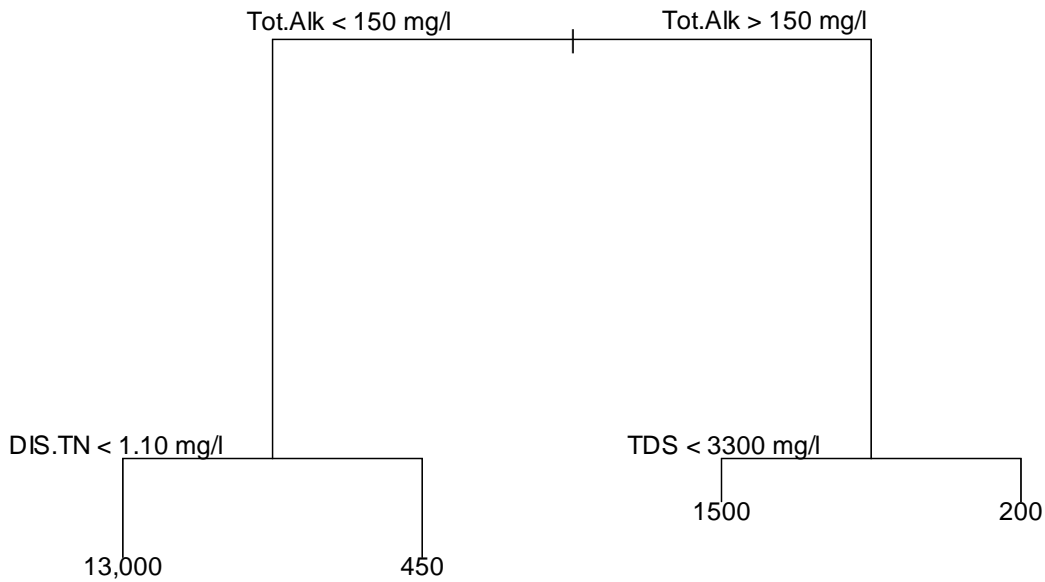


Figure 3.23. CART model of branch density, at UU Willard Spur research plots, 2012 – 2013. (Note: Estimated branch density results in figure are back transformed log +1 values).

### 3.4.4.5 Condition Index

Total phosphorous (TP) was the primary driver in the Condition Index (CI) CART model (scale being whole integers, 1 to 3, Figure 3.24). The highest estimated condition index value (CI = 3) occurred when TP was approximately  $< 0.06 \text{ mg}\cdot\text{L}^{-1}$ , TDS approximately  $< 1500 \text{ mg}\cdot\text{L}^{-1}$ , and  $\text{PO}_4\text{P-Flux}$  was approximately  $< 1.20 \text{ g}\cdot\text{d}^{-1}$ . Moderate conditions (CI = 1.9) were estimated when TDS and  $\text{PO}_4\text{P-Flux}$  were approximately  $> 1500 \text{ mg}\cdot\text{L}^{-1}$  and  $1.20 \text{ g}\cdot\text{d}^{-1}$ , respectively, and TP of less than  $0.06 \text{ mg}\cdot\text{L}^{-1}$ . The poorest SAV condition (CI = 1.0) was estimated when TP was approximately  $> 0.06 \text{ mg}\cdot\text{L}^{-1}$  and total dissolve nitrogen was  $> 1.0 \text{ mg}\cdot\text{L}^{-1}$ .

## Condition Index

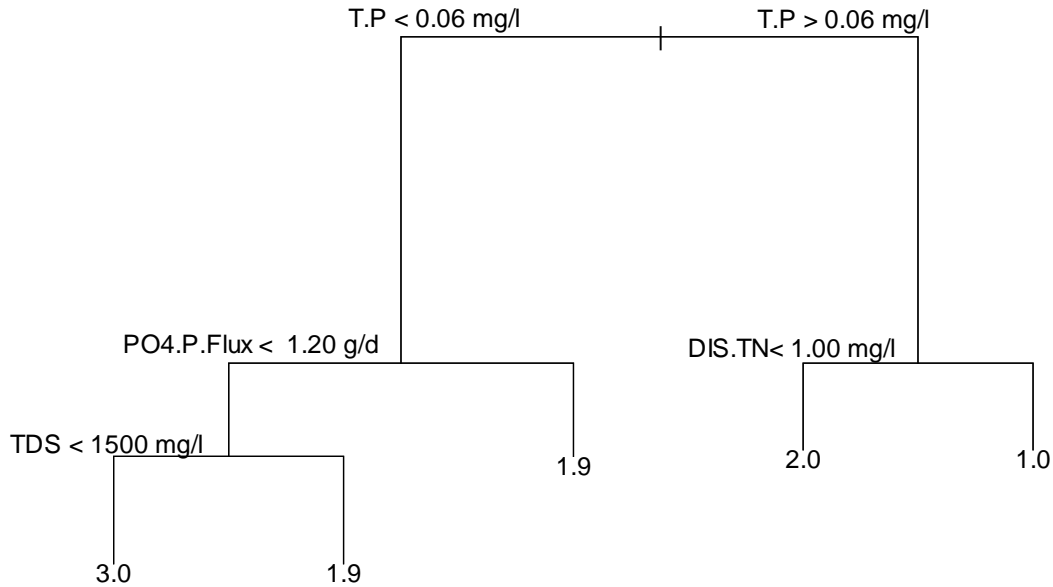


Figure 3.24. CART model of condition index (CI), at UU Willard Spur research plots, 2012 – 2013.

### 3.5 CART vs. Multiple Regression

In general, ordinary least squares (OLS) regressions models provided moderate predictive value, suggesting that the CART models were appropriate, and that as expected, the relationships between the plant metrics and the predictors may not necessarily have been linear or additive. In addition, the amount of variability not explained in OLS regression models could have resulted from predictors that were not measured or experimental error.

Table 3.5.1 OLS multiple regressions on variables used in CART

Metric	Number of predictors	R <sup>2</sup>
% Forageable SAV	3	0.34
% BDS on SAV	3	0.40
% Algae on SAV	3	0.42
% Total SAV	1	0.45
Branch Density/m <sup>2</sup> (log+1)	3	0.47
Condition Index	4	0.68

### 3.5.1 Relationships between metric predictors

Pearson’s correlations of the physical and chemical characteristics of the surface water, including explanatory variables used in CART, are presented in [Appendix F](#). Most of the predictors were significantly correlated (co-varied), which demonstrates the difficulty in separating out single factors affecting health and survival of macrophytes in Willard Spur. However these correlations also provide some direction for selection of predictor variables that could be used interchangeably if there are sampling limitations or to improve efficiency.

Notably, there were many negative correlations between chemistry and water depth and all were positively correlated with weekly Julian date. Water depth was negatively correlated with weekly Julian date. These simple correlations clearly describe the hydrological tendency of Willard Spur to become a standing pool most years and demonstrates the evaporation effects on seasonal changes in water quality.

### 3.6 Bioindicator Metric Thresholds

Predictor variables that related the most to responses detected by each bioindicator are given in order of importance (1 being most important, highlighted in blue) as identified by CART ([Table 3.6.1](#)). It is important to note that the selected indicators apply only to Willard Spur and are not recommended lake-wide for all submersed aquatic wetlands of Great Salt Lake, as seasonality of biological responses and site specific conditions vary significantly ([Hoven et al. 2011, 2013b](#)). Notice that the same variables do not always impart the same (approximate) threshold levels for biological response among metrics. For example, total alkalinity above 150 mg·L<sup>-1</sup> is the primary factor affecting branch density and % Total SAV in the negative direction, but total alkalinity above 160 mg·L<sup>-1</sup> (as third-most important factor) affects % algae on SAV in a positive direction. Total dissolved solids was identified a number of times, having several (approximate) thresholds for the various responses.

*Table 3.6.1. Five proposed bioindicators; environmental variables most related to changes in each; approximate threshold levels; and the direction of change (based on CART)*

Bioindicator	Environmental Variables	Approximate Threshold Level	Direction
Branch Density (log+1)	1. Total Alkalinity	> 150 mg·L <sup>-1</sup>	Decrease
	2. Dissolved Total Nitrate	> 1.10 mg·L <sup>-1</sup>	Decrease
	3. Total Dissolved Solids	> 3300 mg·L <sup>-1</sup>	Decrease
% Total SAV	1. Total Alkalinity	> 150 mg·L <sup>-1</sup>	Decrease
% BDS on SAV	1. Year	2013	Increase
	2. Total Phosphorus	> 0.05 mg·L <sup>-1</sup>	Decrease
	3. Total Dissolved Solids	> 1900 mg·L <sup>-1</sup>	Increase

% Algae on SAV	1. Total Dissolved Solids	> 2300 mg·L <sup>-1</sup>	Increase
	2. NO <sub>3</sub> -N Flux	> 7.77 g·d <sup>-1</sup>	Increase
	3. Total Alkalinity	> 160 mg·L <sup>-1</sup>	Increase
Condition Index	1. Total Phosphorus	> 0.06 mg·L <sup>-1</sup>	Decrease
	2. PO <sub>4</sub> -P Flux	> 1.20 g·d <sup>-1</sup>	Decrease
	3 Total Dissolved Solids	> 1500 mg·L <sup>-1</sup>	Decrease
	4. Dissolved Total Nitrogen	> 1.00 mg·L <sup>-1</sup>	Decrease

Although CART model-generated threshold values are presented above; we warn that limited data were used in these analyses (i.e. few replicate samples; two to three treatment levels), and that ‘non-demonic intrusion’ (Hurlbert 1984) likely occurred; both of which could have affected results. In essence, these thresholds represent a ballpark value accurately assessed from the data, but do not indicate a precise benchmark above or below which to determine water quality criteria, as discussed below. Nonetheless, CART results help illustrate how the most important biondicators respond to the dynamic characteristics of Willard Spur.

One should keep in mind that the approximate thresholds are not indicative of *precise* break points above or below which biological response will occur, but rather they are implicit of a threshold ranging *somewhere near* the identified break point without defining magnitude. This is because values were determined from relatively limited data for each parameter, potentially introducing experimental error and there may well be factors not yet studied or included that may have significant influence of the health and condition of the SAV community. Thus, thresholds are indicated as approximate because they can only be considered as rough in that there may be a range of values outside of the estimate values that may be closer to the true value. In addition, these threshold values may be inaccurate for other locations in Willard Spur if environmental physical-chemical conditions within the Spur vary spatially.

### 3.7 Discussion

When water chemistry is suitable for macrophyte growth, e.g., low in TP, TDS and low PO<sub>4</sub>-P-flux, a healthy macrophyte community may contribute positive feedback to water quality by providing good filtration and removal of particulates, removal of water column P that binds with particulates, and absorption of dissolved solids and other nutrients, resulting in improved water clarity and quality (Ozimek et al. 1990; Horppila & Nurminen 2003; Buhan et al. 2013). In dense, healthy sago communities in oligotrophic, unpolluted settings, P cycling is considered closed and any release of P from decaying macrophytes is readily absorbed by associated periphyton and macroalgae. As long as the macrophyte community remains healthy, the loss of P to open water would be unlikely (Howard-Williams & Allanson 1981). In the Willard Spur setting, this could be true as well, until die-off occurs, releasing nutrients to

the open water and stimulating phytoplankton growth. This could at least partially explain the greening of water during late July and August in both years (2012 and 2013) as macrophyte communities have been shown to control phytoplankton blooms during the spring by assimilating the majority of available nutrients or providing refugia from fish for grazers such as daphnids that control phytoplankton levels (Horppila & Nurminen 2003; Bakker et al. 2010). However, phytoplankton blooms were considered benign with respect to the growth and persistence of SAV in Willard Spur as it occurred well after the macrophytes declined.

In Willard Spur, there is luxuriant macrophyte growth from late spring through early summer followed by a premature die-off between June and July during both years of our study in both nutrient enriched plots and in un-amended plots. The time-frame of SAV senescence was considered premature compared to that documented in impounded wetland systems around the Lake (Hoven et al. 2011). Although premature die-off in Willard Spur may be chiefly driven by natural processes, we induced an accelerated die-off in the high nutrient-amended plots during both years. It is quite possible that the growing season of SAV in Willard Spur is shortened by conditions associated with high alkalinity and pH. As the summer progresses during dry years, Willard Spur becomes impounded due to reduced inflows during the irrigation season, low precipitation, and high evaporation rates. Stagnant conditions of a standing pool exacerbate rate limiting steps in carbon fixation due to diffusive resistance of available carbon resultant of unstirred boundary layers near the surface of macrophyte leaves (Westlake 1967; Keeley 1989; Keeley and Sandquist 1992) and elevated pH leads to dependence on  $\text{HCO}_3^-$  by macrophytes for photosynthesis, believed to be inefficiently used by *P. pectinatus* (Sand-Jensen 1982). However, at higher nutrient levels, the plants are less successful at competing for nutrients (N, P and C) with the increased presence of periphyton (both adnate flora and loosely associated filamentous algae) and die-off occurred up to one month earlier in the high nutrient amended plots than in control plots.

Although condition index aligned as a good metric associated with nutrients (most importantly, TP), changes in the condition of SAV were not detected as early as those detected by branch density, which requires much closer inspection, perhaps because one of the dominant macrophyte species in Willard Spur, *S. pectinata* (and presumably *S. filiformis*), is tolerant of conditions that are frequently limiting to other species (Sand-Jensen et al. 2000; Keeley 1991). Both condition index and branch density were identified as good bioindicators of negative responses related to nutrient enrichment in Willard Spur.

Certainly, there is complexity in the environmental variables and related biological responses, yet it is clear that increases in nutrients (as dissolved total nitrogen, total phosphorus,  $\text{NO}_3\text{-N}$ -Flux and  $\text{PO}_4\text{-P}$ -Flux, and those inclusive of total dissolved solids) have subsequent negative effects on SAV condition. Although increased levels of nutrients influence the biological responses, it is important to consider that other physico-chemical relationships in the Willard Spur SAV community impart negative effects on SAV condition and longevity as well and should not be dismissed as irrelevant when they are part of the natural dynamics of the Spur. This is particularly true when forageable SAV from high amendment plots died within two to four weeks of those in control plots, and SAV in all amendment and control plots showed no significant sign of recovery after die-off both years. Differentiating the overall condition of Willard Spur should therefore rely on more than one bioindicator as some are more closely related to nutrients than others.

Our results must be weighed with other lines of evidence before management decisions are made. The approximate threshold values derived by CART are likely accurate but not precise for WS and are a good starting point for further refinement and additional studies.

### 3.8 Summary of Project DQO's

Our study describes the natural, temporal changes that occur in Willard Spur submergent wetlands through inclusion of control plot and ambient plots in our study. We presented factors that appear to drive changes, both from natural processes and nutrient enrichment. There is some evidence that filamentous algae associated with SAV may be both N-limited and P-limited as demonstrated by a significant, positive response to both nutrients. However more robust investigation would be necessary to state this conclusively. Although availability of water column P may have been affected by increased levels of periphyton on SAV in high amendment plots, it is not convincing that *S. filiformis* (and probably *S. pectinata*) are P-limited since leaf level P was only slightly lower in the high nutrient amended plot than leaf levels in the other nutrient amendments and control. On the other hand, *S. filiformis* (and possibly *S. pectinata*) may be slightly N-limited in Willard Spur as optimal levels of growth occurred in the low nutrient amendment and N leaf levels in the nutrient amended plots were significantly higher than those in the control. The uptake of N and P by processes operating in the water column and sediment (lacking SAV) was also demonstrated in flux chambers.

The DQO's for this project outline a need to identify what constitutes a negative / unacceptable response to nutrients by the SAV, macroinvertebrate community, phytoplankton, macroalgae. As indicated previously, macroinvertebrate assemblage response occurred after the establishment and decline of forageable SAV and relied on *Ceratophyllum demersum* in the later part of the summer and early fall for habitat and foraging resources. *Ceratophyllum demersum* was the dominant macrophyte species that persisted, mostly outside of the research area. If phytoplankton were superior nutrient competitors to macrophytes and were excessive earlier in the year and linked with SAV die-off perhaps by shading, that would be an undesirable state. However, phytoplankton seem to benefit from the early senescence of the SAV in Willard Spur by flourishing from nutrients released from the SAV later in the summer and are seemingly benign. It was not clear why macroalgae were more of a presence during 2012 versus 2013 within and outside the treatment plots. Copious amounts of macroalgal surface mats preventing the establishment of SAV would not be acceptable, however, we were not able to stimulate such a scenario. We did successfully induce premature die-off of SAV up to one month earlier than what occurred naturally, suggesting a negative and unacceptable response. This response was primarily in the high amendment plots and was associated with the stimulation of algae and other flora associated with SAV leaves.

Willard Spur is a highly dynamic and productive system that shifts from high volume flow during spring runoff that undoubtedly flushes and scours bottom sediments, to deposition and assimilation of sediment and nutrients when flows subside. It is then that macrophyte communities become established and while waters subside to the point of impoundment and even complete draw down, it comes alive again the following year, however briefly. Former bird surveys show usage of the Spur and its resources as one of the most important areas around the Lake (Paul & Manning 2002) and although we didn't quantitatively survey birds during our study, it was clear that Willard Spur offered many

ecosystem services for them. As the system changes with changing hydrology and water chemistry, so do its functions as an ecosystem. Although natural processes may influence the SAV community toward premature senescence, nutrient enrichment at high amendment levels accelerated this response, which could have costly effects on the wildlife that depend on the Spur for sustenance.

## APPENDIX A. Water and Sediment Chemistry

### A.1 Methods

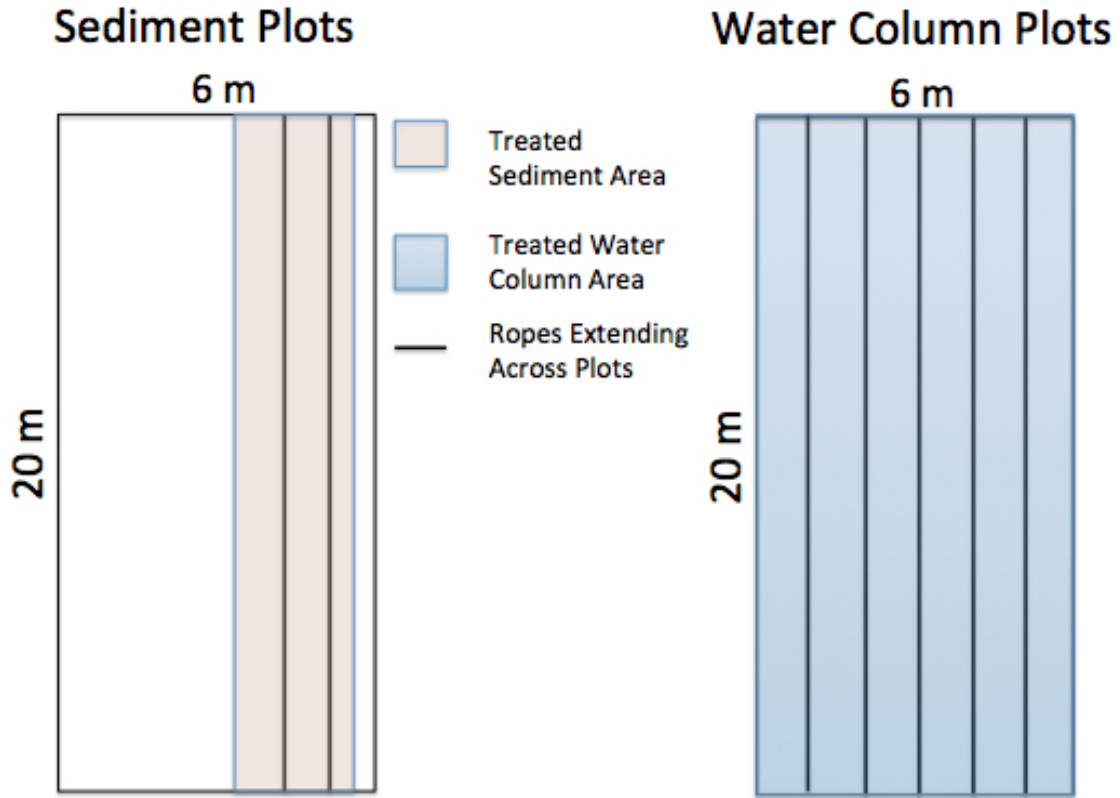


Figure A.1. The area of plots where sediment and water column was amended with Osmocote Smart Release™ fertilizer.

Osmocote™ was the only fertilizer used in the 2012 amendments ([Table A.1](#)). Osmocote™ has mass ratio of 19-6-12 for nitrogen-phosphorus-potassium (NPK ratio) with 9% of the nitrogen in the form of nitrate and 10% in the form of ammonia. The same target concentration for dissolved phosphorus in the 2012 high and low water column plots, 0.4 and 0.1 mg/L respectively, was used for the 2013 high and medium water column plots ([Table A.2](#)). The low water column plot dissolved phosphorus target concentration was set at 0.5 mg/L.

About 4% (by mass) of the fertilizer mixture was uncoated urea (46-0-0 NPK ratio). Uncoated urea is soluble and dissolved within 2 days during dissolution tests. This fraction of the mixture was intended to be a short-term source of nutrients early in the growing season. About 36% of the fertilizer mixture was polymer-coated urea fertilizer (39-0-0 NPK ratio) designed to release nitrogen for about 45 days. Release of coated urea was dependent on the breakdown of the polymer coating over time. This fraction was intended to couple the initial burst provided by the uncoated urea and provide nutrients throughout the cooler months of May and June.

The remaining 60% of the mixture was coated Osmocote Smart Release™ fertilizer (19-6-12 NPK ratio), the same fertilizer that was used in 2012. As mentioned, that is designed to release nutrients for 3-4 months, depending on the temperature. This fraction was intended to release nutrients throughout the warmer months. Temperatures during sample events did not begin to consistently reach above 60 °F until early to mid June 2013.

Table A.1. Mass of fertilizer in 2012 sediment and water column plots.

Mass of Fertilizer Added		
	Osmocote Smart Release™ per plot (kg)	Total Mass of Fertilizer per plot (kg)
High Sediment	160	160
Low Sediment	80	80
High Water Column	134	134
Low Water Column	34	34

Table A.2. Mass of fertilizer in 2013 water column amendment plots.

Mass of Fertilizer Added			
	Osmocote Smart Release™ (kg)	Urea (coated and uncoated) (kg)	Total Mass of Fertilizer (kg)
High Water Column	91.2	60.8	152
Medium Water Column	21.6	14.4	36
Low Water Column	10.8	7.2	18

Table A.3. 2012 water and sediment chemistry and number of samples per metric, per treatment plot by month and total sample number for all 6 plots. The number of samples collected each month per plot is provided for each metric. ‡ = up to six plots.

Surface Water	Method	June	July	Aug	Sept	Oct	2012 Total
<b>U of U: Johnson Lab</b>							
Field Parameters		3-4	1	1	1	1	47
Filtered Trace Elements <sup>1</sup>	EPA 200.8-Metals	3-4					23
Total and Methyl Mercury	EPA 1631E-THg; EPA 1630-MeHg	1	1	1		1	24
Dissolved NO <sub>3</sub> -N and PO <sub>4</sub> -P	EPA 300.0-DISS	3-4	4	3	3	3	101
<b>Utah State Health Lab</b>							
Filtered Trace Metals <sup>2</sup>	EPA 200.8-DISS	3-4					23
Carbonaceous BOD	EPA 405.1	3-4	1	1	1	1	47
Unfiltered Nutrients							
Ammonia, NO <sub>3</sub> -N+NO <sub>2</sub> -N, TP, TKN	EPA 350.3, 353.2, 365.1, 351.4	3-4	3	3	3	3	95
Filtered Nutrients							
NO <sub>3</sub> -N+NO <sub>2</sub> -N, TP, TN	EPA 353.2-DISS, 365.1-DISS, 4500N-DISS	3-4	3	3	3	3	95
General Chemistry							
TSS, TVS, Turbidity, Alkalinity, TDS, Sulfate	EPA 160.2, 160.4, 180.1, 2320B, 2540C, 375.2	3-4	3	3	3	3	95
<b>Sediment</b>							
<b>U of U: SIRFER Lab</b>							
N, C Content: Total/organic, isotopes		3	1	1	1	1	42
<b>U of U: Johnson Lab</b>							
Trace elements	EPA 200.8-Metals	3					18
Total and methyl mercury	EPA 1631E-THg; EPA 1630-MeHg	3	1	1	1	1	42
<b>Utah State University Analytical Laboratories</b>							
Nutrients (NO <sub>3</sub> -N, P, K)		3	1	1	1	1	42
pH/Salinity		3	1	1	1	1	42
Metals (Zn, Fe, Cu, Mn, S)		3	1	1	1	1	42
Organic Matter		3	1	1	1	1	42
<b>Nutrient Flux</b>		Up to 3			Up to 3		Up to 36 ‡

1. Li, Be, Na, Mg, Al, P, K, Ca, Sc, Ti, V, Cr, Mn, Fe, Co, Ni, Cu, Zn, As, Se, Rb, Sr, Y, Mo, Ag, Cd, Sb, Cs, Ba, La, Ce, Nd, Sm, Gd, Tb, Dy, Ho, Lu, Tl, Pb, U.

2. B, Ca, Fe, Mg, K, As, Ba, Cd, Cr, Cu, Pb, Mn, Ni, Al.

Table A.4. 2013 water and sediment chemistry and number of samples per metric, per treatment plot and total sample number for the four plots. The number of samples collected each month is provided for each metric. Three samples were collected per plot one sample was collected at the ambient site.

Surface Water	Method	Samples Per Event	Sample Events Collected	2013 Total
<b>U of U: Johnson Lab</b>				
Field Parameters		5	8	40
Total and Methyl Mercury	EPA 1631E-THg; EPA 1630-MeHg	5	3	15
Dissolved NO <sub>3</sub> -N and PO <sub>4</sub> -P	EPA 300.0-DISS	13	8	104
<b>Utah State Health Lab</b>				
Carbonaceous BOD	EPA 405.1	5	8	40
Ammonia, NO <sub>3</sub> -N+NO <sub>2</sub> -N, TP, TKN	EPA 350.3, 353.2, 365.1, 351.4	13	8	104
NO <sub>3</sub> -N+NO <sub>2</sub> -N, TP, TN	EPA 353.2-DISS, 365.1-DISS, 4500N-DISS	13	8	104
TSS, TVS, Turbidity, Alkalinity, TDS, Sulfate	EPA 160.2, 160.4, 180.1, 2320B, 2540C, 375.2	13	8	104
Sediment	Method	Samples Per Event	Sample Events Collected	2013 Total
<b>U of U: SIRFER Lab</b>				
Total/organic: N/C Content, isotopes		12	4	48
<b>Utah State University Analytical Laboratories</b>				
Nutrients (NO <sub>3</sub> -N, ammonia, available P)		12	4	48
Organic Matter		12	4	48

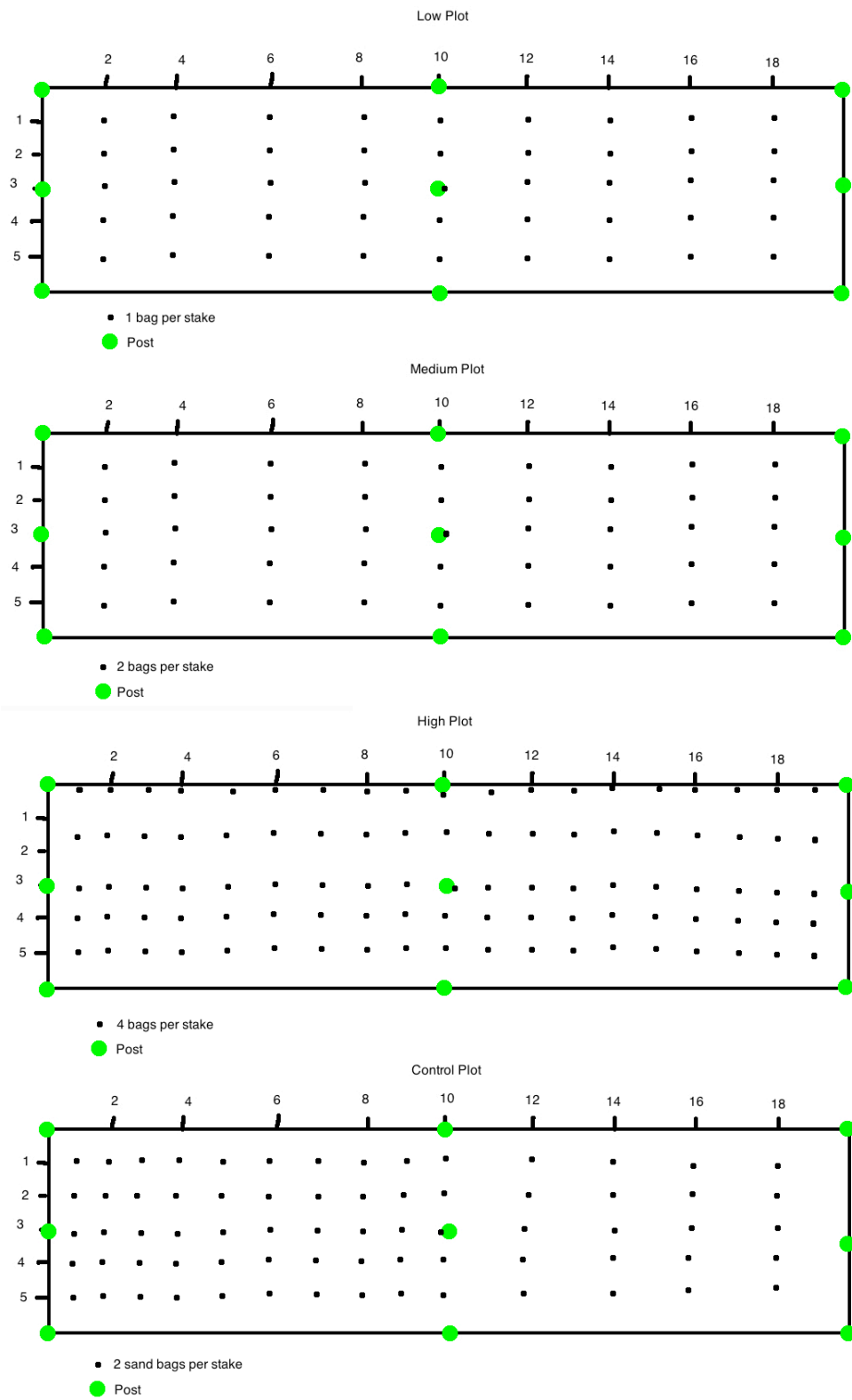


Figure A.2: Distribution of stakes and fertilizer in 2013 water column plots

## A.2 Rate Constant Regression

Contents of text files for the MATLAB script below include data from bucket tests.

Column 1 – number of days fertilizer has been submerged

Column 2 – temperature of water when sample was collected

Column 3 – rate constant according to derivative of the line of best fit

Column 4 – rate constant calculated by resulting equation from regressed data (not used in MATLAB script)

### N2012.txt

```
78.00416667 12.77777778 0.001138889 0.001631569
78.86180556 12.77777778 0.001138889 0.001618974
81.90138889 12.77777778 0.001138889 0.001574335
85.11875 12.77777778 0.001138889 0.001527086
89.96597222 12.77777778 0.001138889 0.001455901
96.23333333 12.77777778 0.001138889 0.00136386
0.004166667 12.77777778 0.002813889 0.002777058
0.861805556 12.77777778 0.002813889 0.002764463
3.901388889 12.77777778 0.002813889 0.002719824
7.11875 12.77777778 0.002813889 0.002672575
11.96597222 12.77777778 0.002813889 0.00260139
18.23333333 12.77777778 0.002813889 0.002509349
102.4069444 28.33333333 0.002530556 0.003427409
105.2402778 29.44444444 0.002530556 0.003539672
107.2194444 25.55555556 0.002530556 0.002972053
24.40694444 28.33333333 0.008153282 0.004572898
27.24027778 29.44444444 0.004451369 0.004685161
29.21944444 25.55555556 0.00337952 0.004117542
300 12.77777778 1.13889E-05 -0.001628608
300 27.61904762 2.53056E-05 0.000426688
```

### N2013.txt

```
78.00416667 12.77777778 0.000239167 0.000342629
78.86180556 12.77777778 0.000239167 0.000339985
81.90138889 12.77777778 0.000239167 0.00033061
85.11875 12.77777778 0.000239167 0.000320688
89.96597222 12.77777778 0.000239167 0.000305739
96.23333333 12.77777778 0.000239167 0.000286411
0.004166667 12.77777778 0.000590917 0.000583182
0.861805556 12.77777778 0.000590917 0.000580537
3.901388889 12.77777778 0.000590917 0.000571163
7.11875 12.77777778 0.000590917 0.000561241
11.96597222 12.77777778 0.000590917 0.000546292
18.23333333 12.77777778 0.000590917 0.000526963
102.4069444 28.33333333 0.000531417 0.000719756
105.2402778 29.44444444 0.000531417 0.000743331
107.2194444 25.55555556 0.000531417 0.000624131
24.40694444 28.33333333 0.001712189 0.000960309
27.24027778 29.44444444 0.000934787 0.000983884
29.21944444 25.55555556 0.000709699 0.000864684
300 12.77777778 2.39167E-06 -0.000342008
300 27.61904762 5.31417E-06 8.96044E-05
```

## P2012.txt

```
78.00416667 12.77777778 0.000279167 0.00034422
78.86180556 12.77777778 0.000279167 0.000343683
81.90138889 12.77777778 0.000279167 0.000341781
85.11875 12.77777778 0.000279167 0.000339768
89.96597222 12.77777778 0.000279167 0.000336735
96.23333333 12.77777778 0.000279167 0.000332814
0.004166667 12.77777778 0.000220833 0.000393025
0.861805556 12.77777778 0.000220833 0.000392489
3.901388889 12.77777778 0.000220833 0.000390587
7.11875 12.77777778 0.000220833 0.000388574
11.96597222 12.77777778 0.000220833 0.000385541
18.23333333 12.77777778 0.000220833 0.000381619
102.4069444 28.33333333 0.0009875 0.001215224
105.2402778 29.44444444 0.0009875 0.001276756
107.2194444 25.55555556 0.0009875 0.00105395
112.0458333 23.33333333 0.0009875 0.000924319
24.40694444 28.33333333 0.001707164 0.00126403
27.24027778 29.44444444 0.001529598 0.001325562
29.21944444 25.55555556 0.001425991 0.001102755
34.04583333 23.33333333 0.00122384 0.000973125
300 12.77777778 2.79167E-06 0.000205314
300 25.81196581 0.000009875 0.000947933
```

## P2013.txt

```
78.00416667 12.77777778 4.46667E-05 3.3025E-05
78.86180556 12.77777778 4.46667E-05 3.26726E-05
81.90138889 12.77777778 4.46667E-05 3.14236E-05
85.11875 12.77777778 4.46667E-05 3.01015E-05
89.96597222 12.77777778 4.46667E-05 2.81097E-05
96.23333333 12.77777778 4.46667E-05 2.55343E-05
0.004166667 12.77777778 3.53333E-05 6.5077E-05
0.861805556 12.77777778 3.53333E-05 6.47246E-05
3.901388889 12.77777778 3.53333E-05 6.34756E-05
7.11875 12.77777778 3.53333E-05 6.21535E-05
11.96597222 12.77777778 3.53333E-05 6.01616E-05
18.23333333 12.77777778 3.53333E-05 5.75862E-05
102.4069444 28.33333333 0.000158 0.000188426
105.2402778 29.44444444 0.000158 0.000199079
107.2194444 25.55555556 0.000158 0.000156908
112.0458333 23.33333333 0.000158 0.000131292
24.40694444 28.33333333 0.000273146 0.000220478
27.24027778 29.44444444 0.000244736 0.000231131
29.21944444 25.55555556 0.000228159 0.00018896
34.04583333 23.33333333 0.000195814 0.000163344
300 12.77777778 4.46667E-07 -5.81981E-05
300 25.81196581 0.00000158 8.04169E-0
```

MATLAB function file: “importdmap”

```
function importdmap(fileToRead1)
%IMPORTFILE(FILETOREAD1)
% Imports data from the specified file
% FILETOREAD1: file to read
```

```

% Auto-generated by MATLAB on 15-Sep-2012 02:50:12

% Import the file
rawData1 = importdata(fileToRead1);

% For some simple files (such as a CSV or JPEG files), IMPORTDATA might
% return a simple array. If so, generate a structure so that the output
% matches that from the Import Wizard.
[~,name] = fileparts(fileToRead1);
newData1.(genvarname(name)) = rawData1;

% Create new variables in the base workspace from those fields.
vars = fieldnames(newData1);
for i = 1:length(vars)
    assignin('base', vars{i}, newData1.(vars{i}));
end

```

### MATLAB script file: "Regress\_Plots201213\_3DSurface\_NoPoints"

```

%Multiple Linear Regression
%Example 15.2
%Use matrices from "2012 Bucket and 2013 Mesocoms Test" spreadsheet

%1. Adjust "Bucket Test Data" as desired
%2. Copy paste columns AU-AW into "Regress_Plots201213_3DSurface" script
%3. Run "Regress_Plots201213_3DSurface" script
%4. Use output C array to populate green cells below regression data
%5. Use "Flux Results" and update txt files used by
"Regress_Plots201213_3DSurface" script
%6. Run "Regress_Plots201213_3DSurface" script twice to get plot scales to
be the same.

%2012 matrices
ANO3N2012 = [
20.0000000 1547.9041667 360.3968254
1547.9041667 259404.0984057 30155.2119709
360.3968254 30155.2119709 7531.0216679
];

bNO3N2012 = [
0.047329198378
1.926151141626
0.963213609099
];

APO4P2012 = [
22.0000000 1093.9958333 366.6666667
1093.9958333 183117.4859404 21444.9699074
366.6666667 21444.9699074 7693.8271605
];

bPO4P2012 = [
0.012836593591
0.740772968750

```

```

0.302108421040
];

CNO3N2012 = ANO3N2012\bNO3N2012
CPO4P2012 = APO4P2012\bPO4P2012
AINO3N = inv(ANO3N2012);
AIPO4P = inv(APO4P2012);

%2013 matrices
ANO3N2013 = [
20.0000000 1547.9041667 360.3968254
1547.9041667 259404.0984057 30155.2119709
360.3968254 30155.2119709 7531.0216679
];

bNO3N2013 = [
0.009939131659
0.404491739742
0.202274857911
];

APO4P2013 = [
22.0000000 1693.9958333 405.2564103
1693.9958333 273117.4859404 33021.8929843
405.2564103 33021.8929843 8523.3563445
];

bPO4P2013 = [
0.002055881641
0.118997675000
0.048378130272
];

CNO3N2013 = ANO3N2013\bNO3N2013
CPO4P2013 = APO4P2013\bPO4P2013
AINO3N2013 = inv(ANO3N2013);
AIPO4P2013 = inv(APO4P2013);

%plot 2012 NO3-N and PO4-P flux

tempa = 5;
tempb = 30;
timea = 0;
timeb = 300;
coloraxisa = 0;
coloraxisb1 = 0.0015;
coloraxisb2 = 0.01;
coloraxisb3 = 0.0055;
res = .1;

time = linspace(timea,timeb);
temp1 = linspace(tempa,tempb);

NO3Nflux2012=CNO3N2012(1)+CNO3N2012(2).*time+CNO3N2012(3).*temp1;% NO3-N 2012
5-30 deg C

```

```

PO4Pflux2012=CPO4P2012(1)+CPO4P2012(2).*time+CPO4P2012(3).*temp1;% PO4-P 2012
5-30 deg C

%Plot 2013 NO3-N and PO4-P flux

%Using 2013 time/temp coefficients
NO3Nflux2013=CNO3N2013(1)+CNO3N2013(2).*time+CNO3N2013(3).*temp1;% NO3-N 2013
5-30 deg C
PO4Pflux2013=CPO4P2013(1)+CPO4P2013(2).*time+CPO4P2013(3).*temp1;% PO4-P 2013
5-30 deg C

%Creating meshgrids and grid data for surf command.

[XI,YI] = meshgrid (timea:res:timeb, tempa:res:tempb);

%2012
%N
Nflux2012 = CNO3N2012(1)+CNO3N2012(2).*XI+CNO3N2012(3).*YI;% Equation for
2012 NO3-N rate constant
importdmap('N2012.txt')
for n =1:20
    X2012N(n,1)=N2012(n,1);
    Y2012N(n,1)=N2012(n,2);
    Z2012BucketkN(n,1)=N2012(n,3);
    Z2012EquationkN(n,1)=N2012(n,4);

end

figure(1)
subplot(2,1,1)
hold on
ZIN2012 = griddata(XI, XI, Nflux2012,XI,YI);
surf(XI,YI,Nflux2012,'EdgeColor','none');
colorbar
shading interp
colormap jet
axis([timea timeb tempa tempb coloraxisa coloraxisb2])
caxis([coloraxisa coloraxisb3]) %Set range of colorbar. Use % to use auto
range for full spectrum.
%scatter3 (X2012N, Y2012N, Z2012EquationkN, 'o','MarkerEdgeColor','r',...
% X2012N, Y2012N, Z2012BucketkN,'x','MarkerEdgeColor','k');
scatter3 (X2012N, Y2012N, Z2012BucketkN,'o','MarkerEdgeColor','k');

xlabel 'Time (days)'
ylabel 'Temperature (Deg C)'
zlabel 'Rate Constant (1/day)'
title ('2012 NO3-N')

V=axis;
view(3)
grid on

```

```

%2013
%N
Nflux2013=CNO3N2013(1)+CNO3N2013(2).*XI+CNO3N2013(3).*YI;% Equation for 2013
NO3-N rate constant
importdmap('N2013.txt')
for n =1:20
    X2013N(n,1)=N2013(n,1);
    Y2013N(n,1)=N2013(n,2);
    Z2013BucketkN(n,1)=N2013(n,3);
    Z2013EquationkN(n,1)=N2013(n,4);
end

subplot(2,1,2)
hold on
ZIN2013 = griddata(XI, XI, Nflux2013,XI,YI);
surf(XI,YI,Nflux2013,'EdgeColor','none');
colorbar EastOutside
shading interp
colormap jet
axis([timea timeb tempa tempb coloraxisa coloraxisb1])
caxis([coloraxisa coloraxisb1]) %Set range of colorbar. Use % to use auto
range for full spectrum.
%scatter3 (X2013N, Y2013N, Z2013EquationkN, 'o','MarkerEdgeColor','r',...
% X2013N, Y2013N, Z2013BucketkN,'x','MarkerEdgeColor','k');
scatter3 (X2013N, Y2013N, Z2013BucketkN,'o','MarkerEdgeColor','k');

xlabel 'Time (days)'
ylabel 'Temperature (Deg C)'
zlabel 'Rate Constant (1/day)'
title ('2013 NO3-N')

axis(V);
view(3)
grid on

%2012
%P
Pflux2012 = CPO4P2012(1)+CPO4P2012(2).*XI+CPO4P2012(3).*YI;% Equation for
2012 PO4-P rate constant
importdmap('P2012.txt')
for n =1:22 %number of rows in .txt file
    X2012P(n,1)=P2012(n,1);
    Y2012P(n,1)=P2012(n,2);
    Z2012BucketkP(n,1)=P2012(n,3);
    Z2012EquationkP(n,1)=P2012(n,4);

end

figure(2)
subplot(2,1,1)
hold on
ZIP2012 = griddata(XI, XI, Pflux2012,XI,YI);
surf(XI,YI,Pflux2012,'EdgeColor','none');
colorbar EastOutside
axis([timea timeb tempa tempb coloraxisa coloraxisb1])
caxis([coloraxisa coloraxisb1]) %Set range of colorbar. Use % to use auto

```

```

range for full spectrum.
shading interp
colormap jet
%scatter3 (X2012P, Y2012P, Z2012EquationkP, 'o','MarkerEdgeColor','r',...
%   X2012P, Y2012P, Z2012BucketkP,'x','MarkerEdgeColor','k');
scatter3 (X2012P, Y2012P, Z2012BucketkP,'o','MarkerEdgeColor','k');

xlabel 'Time (days)'
ylabel 'Temperature (Deg C)'
zlabel 'Rate Constant (1/day)'
title ('2012 PO4-P')

V=axis;
view(3) %default for 3d plots
grid on

%2013
%P
Pflux2013=CPO4P2013(1)+CPO4P2013(2).*XI+CPO4P2013(3).*YI;% Equation for 2013
PO4-P rate constant

importdmmap('P2013.txt')
for n =1:22
    X2013P(n,1)=P2013(n,1);
    Y2013P(n,1)=P2013(n,2);
    Z2013BucketkP(n,1)=P2013(n,3);
    Z2013EquationkP(n,1)=P2013(n,4);
end

subplot(2,1,2)
hold on
ZIP2013 = griddata(XI, XI, Pflux2013,XI,YI);
surf(XI,YI,Pflux2013,'EdgeColor','none');
colorbar EastOutside
axis([timea timeb tempa tempb coloraxisa coloraxisb1])
caxis([coloraxisa coloraxisb1]) %Set range of colorbar. Use % to use auto
range for full spectrum.
shading interp
colormap jet

%scatter3 (X2013P, Y2013P, Z2013EquationkP, 'o','MarkerEdgeColor','r',...
%   X2013P, Y2013P, Z2013BucketkP,'x','MarkerEdgeColor','k');
scatter3 (X2013P, Y2013P, Z2013BucketkP,'o','MarkerEdgeColor','k');

xlabel 'Time (days)'
ylabel 'Temperature (Deg C)'
zlabel 'Rate Constant (1/day)'
title('2013 PO4-P')

axis(V);
view(3) %default for 3d plots
grid on

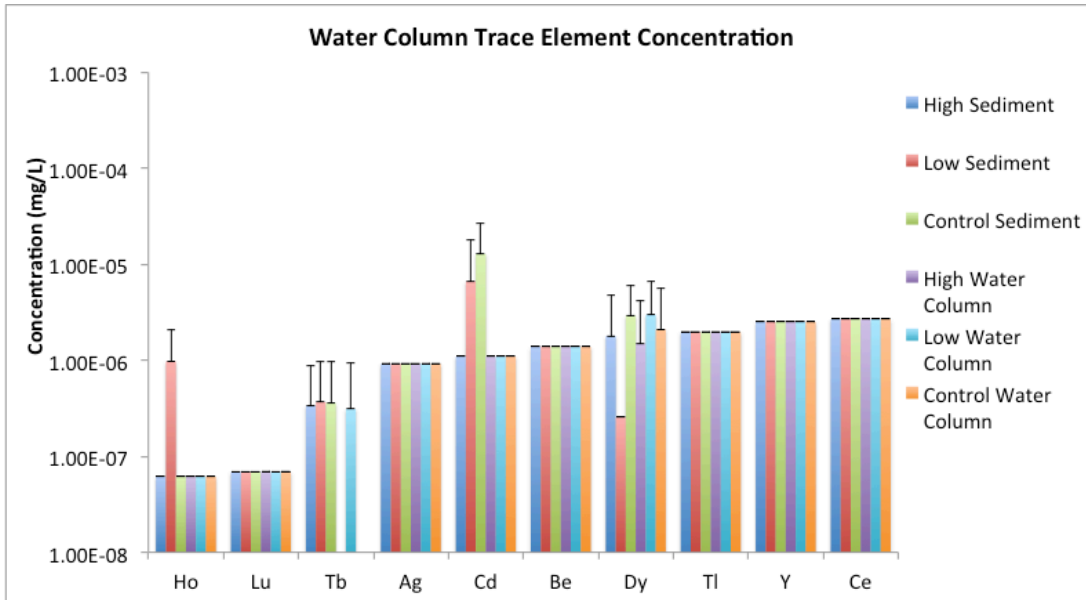
```



## A.3 Results

### A.3.1 2012 Surface Water

a.



b.

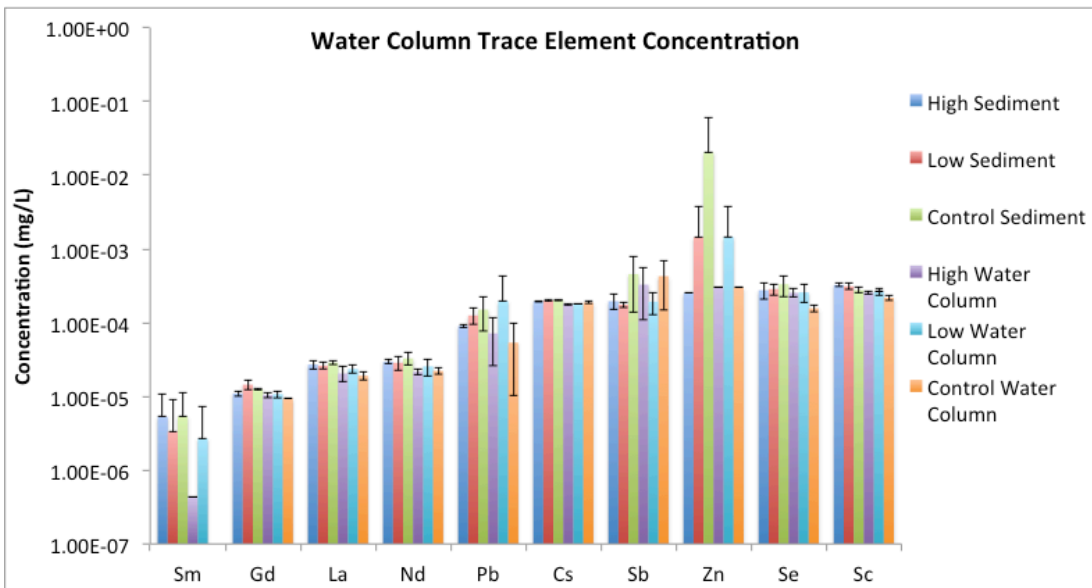
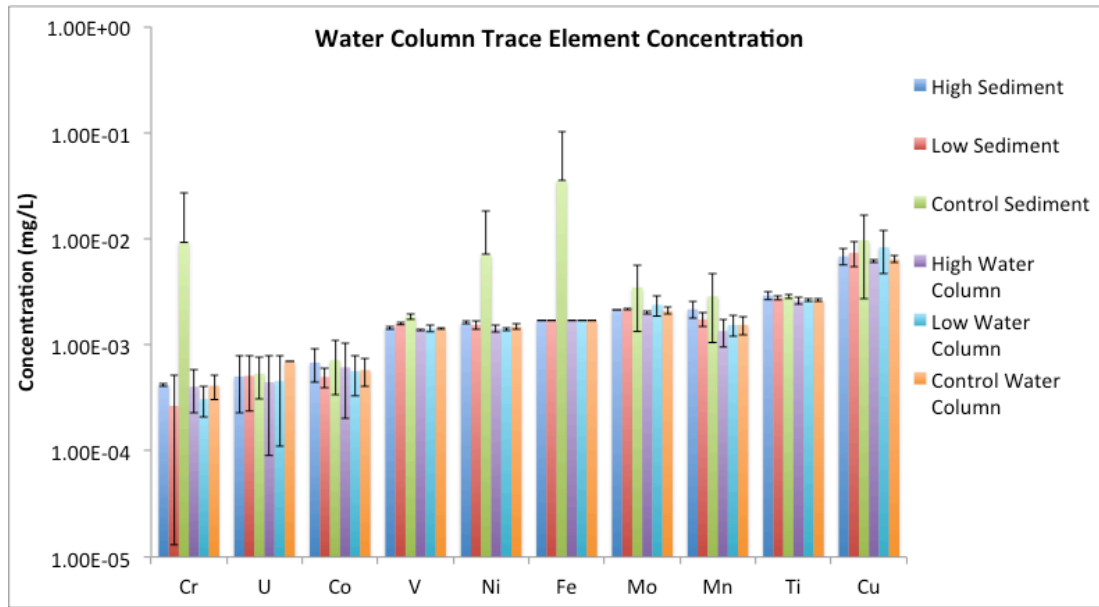


Figure A.3. Dissolved trace element concentrations in for all elements measured. Error bars represent one standard deviation ( $n=4$  excluding Control Water Column where  $n=3$ ).

C.



d.

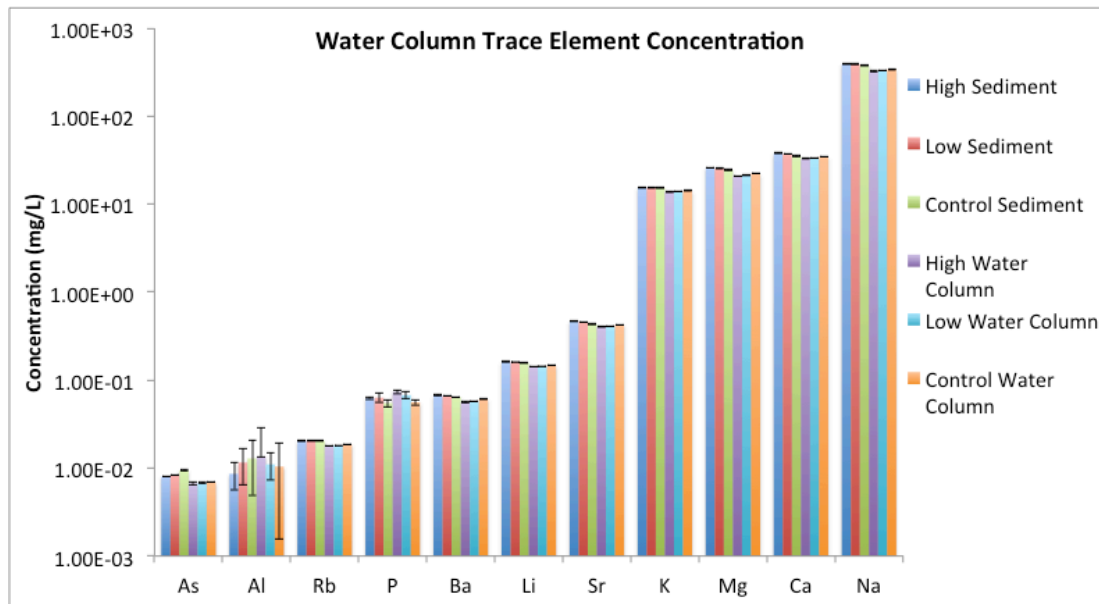


Figure A.3. Continued.

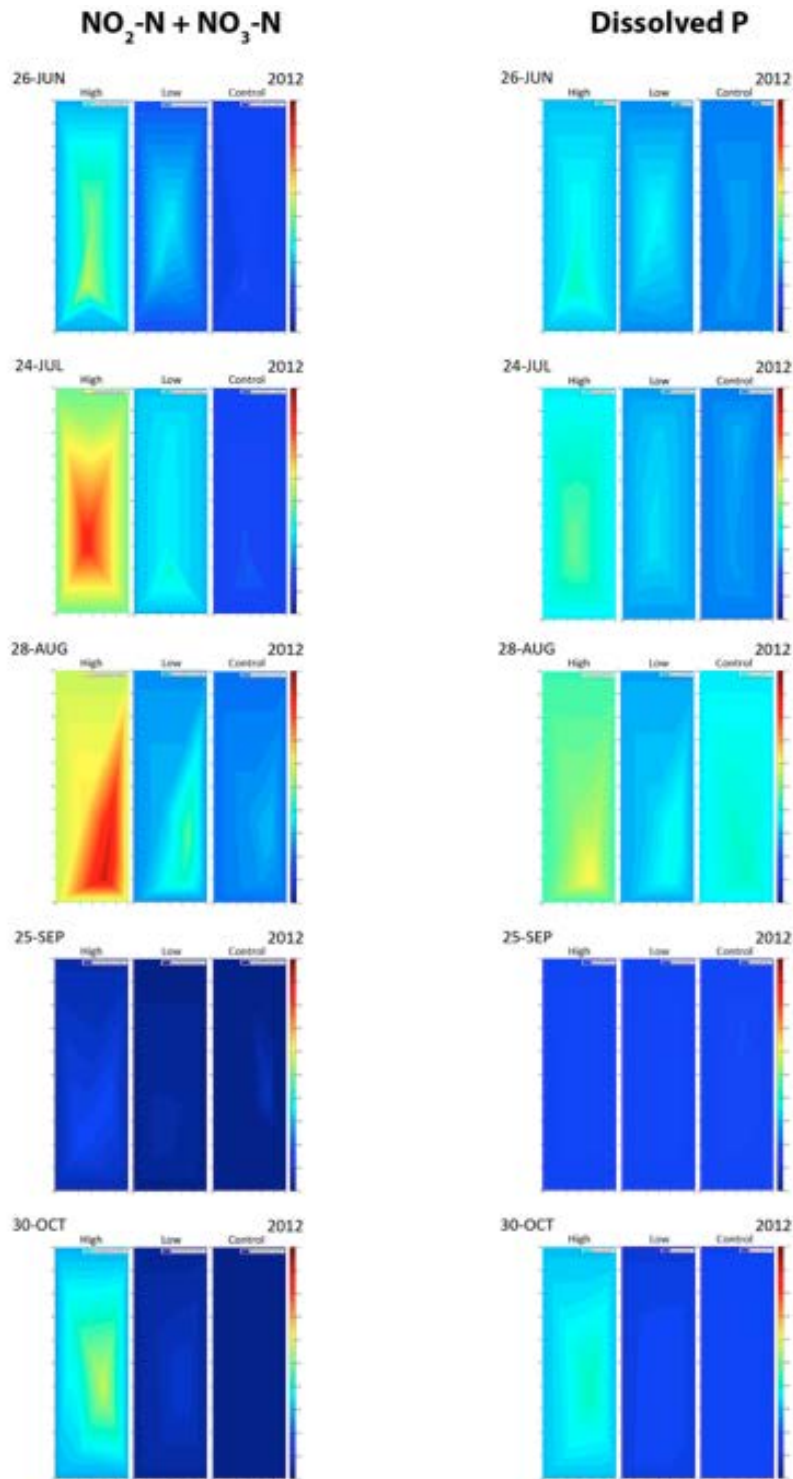


Figure A.4. Dissolved Nitrite + Nitrate and Dissolved P 2D plots for filtered surface water samples. Boundary values were set at 90% of lowest value measured in the plot ( $n=3$  except for June samples where  $n=4$ , excluding June Control Water Column where  $n=3$ ).

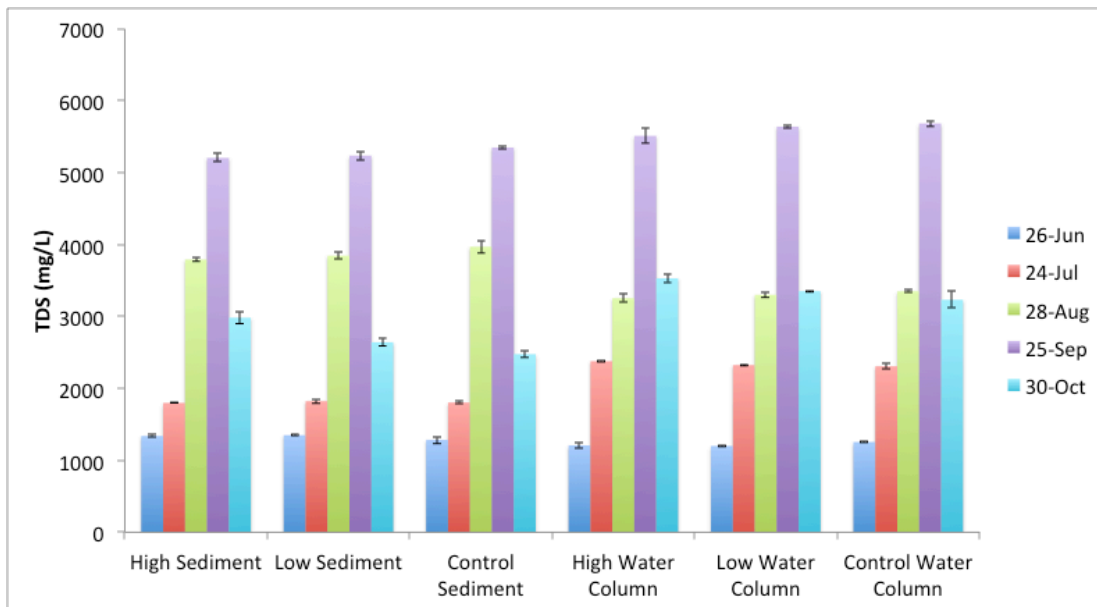


Figure A.5. Total Dissolved Solids for unfiltered surface water samples. Error bars represent one standard deviation ( $n=3$  except for June samples where  $n=4$ , excluding June Control Water Column where  $n=3$ ).

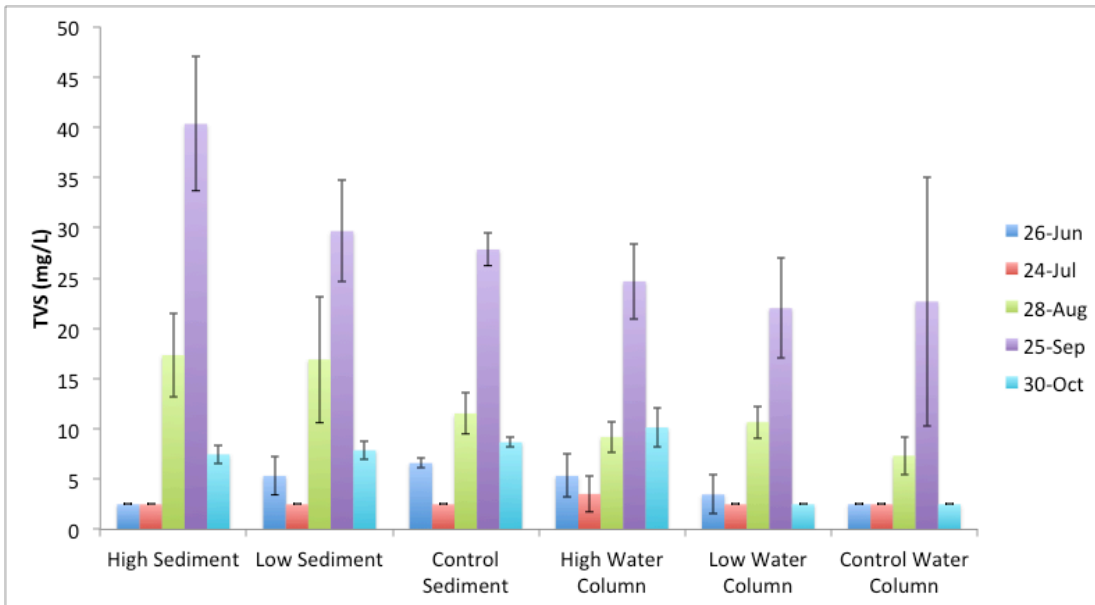


Figure A.6. Total Volatile Solids for unfiltered surface water samples. Error bars represent one standard deviation ( $n=3$  except for June samples where  $n=4$ , excluding June Control Water Column where  $n=3$ ).

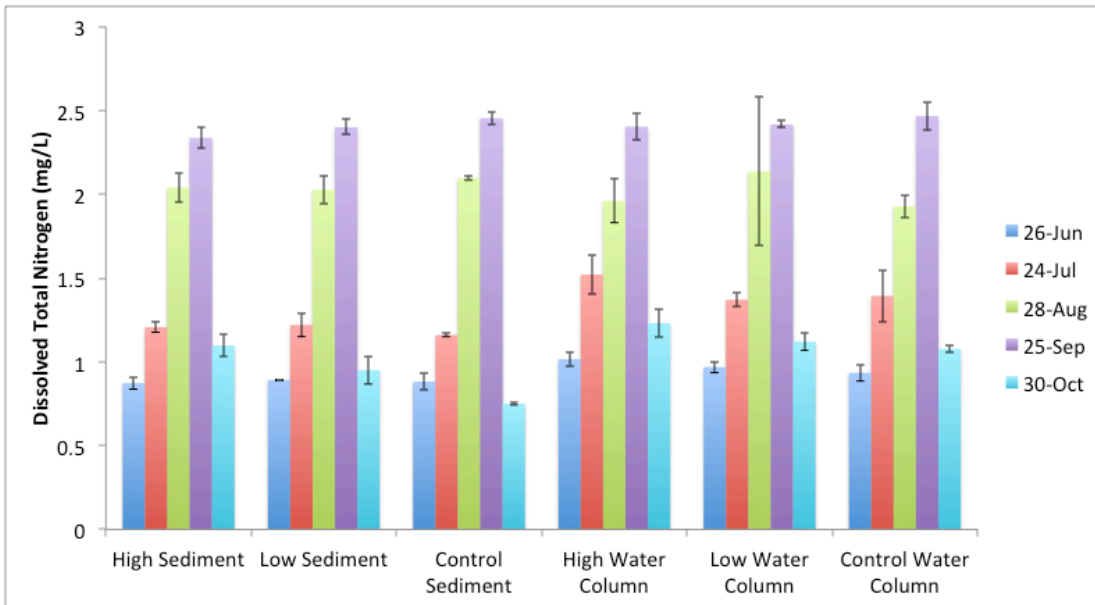


Figure A.7. Dissolved Total Nitrogen for filtered surface water samples. Error bars represent one standard deviation ( $n=3$  except for June samples where  $n=4$ , excluding June Control Water Column where  $n=3$ ).

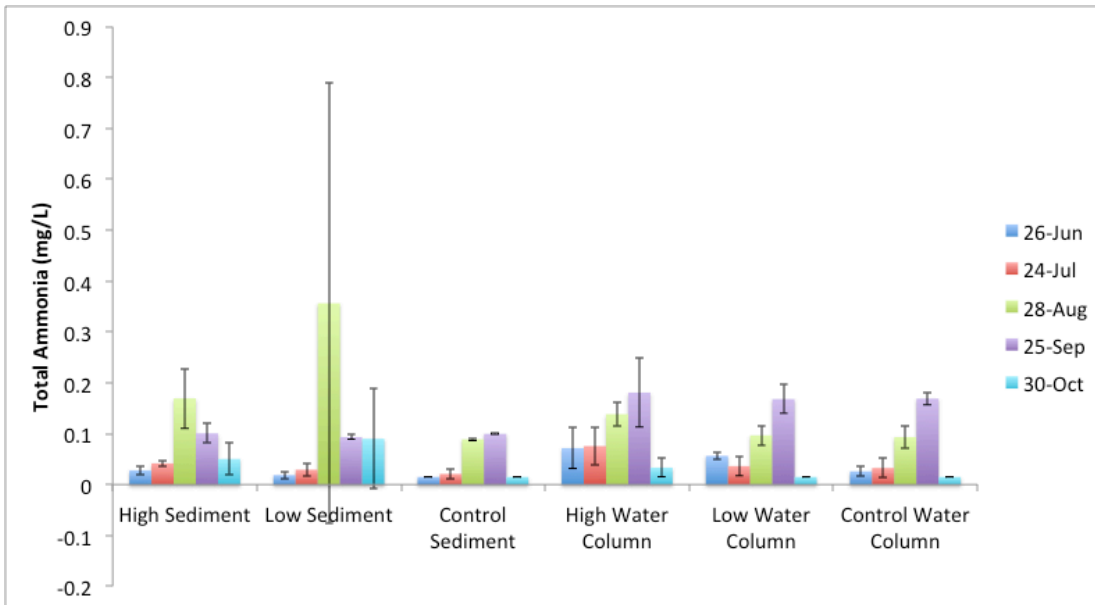


Figure A.8. Total ammonia for unfiltered surface water samples. Error bars represent one standard deviation ( $n=3$  except for June samples where  $n=4$ , excluding June Control Water Column where  $n=3$ ).

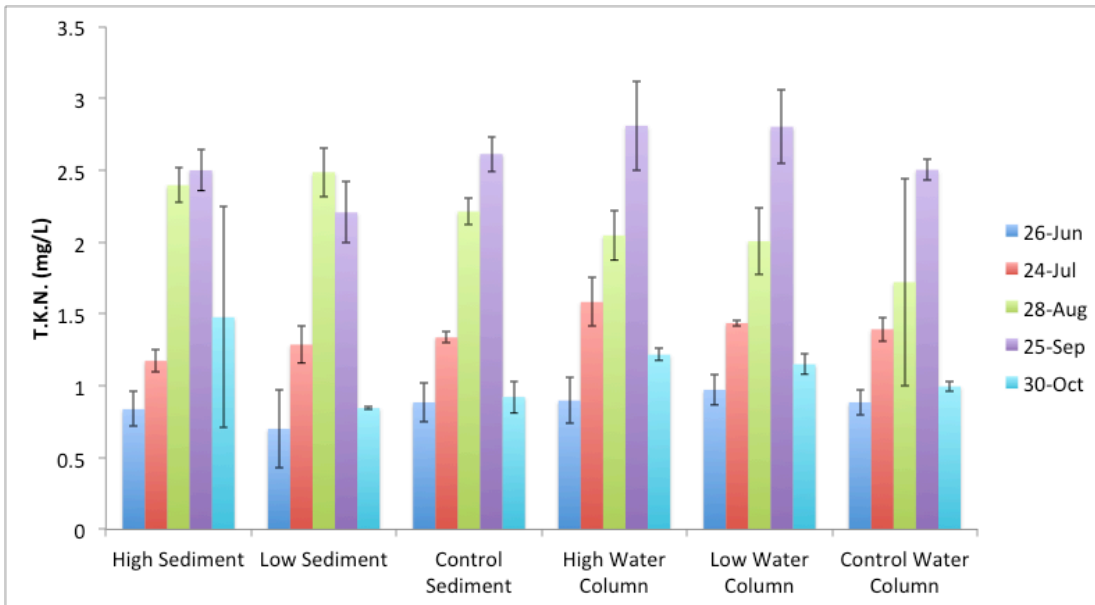


Figure A.9. TKN for unfiltered surface water samples. Error bars represent one standard deviation ( $n=3$  except for June samples where  $n=4$ , excluding June Control Water Column where  $n=3$ ).

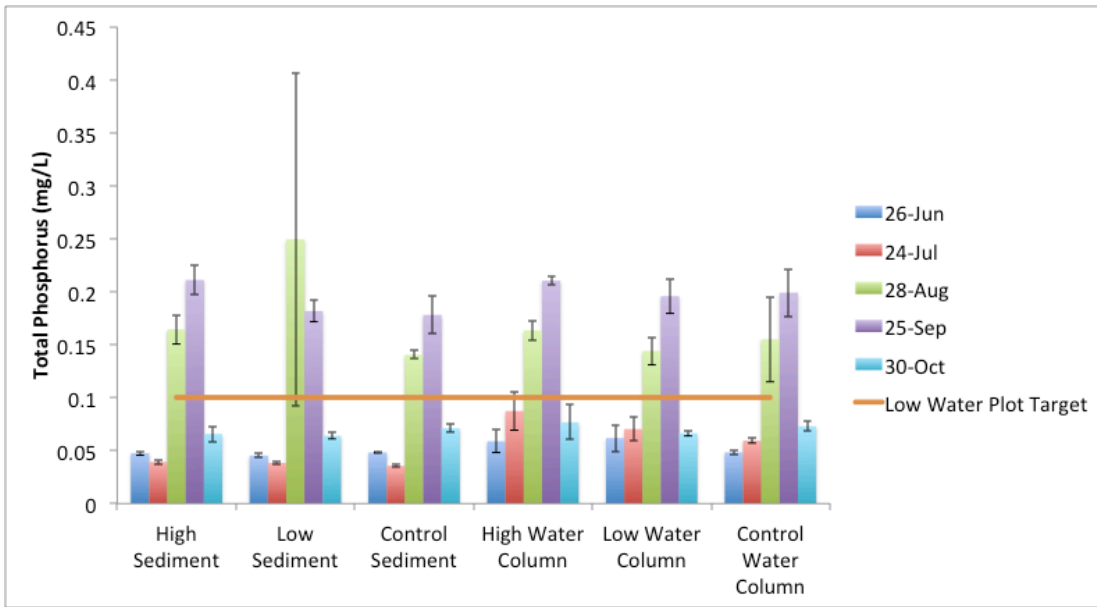
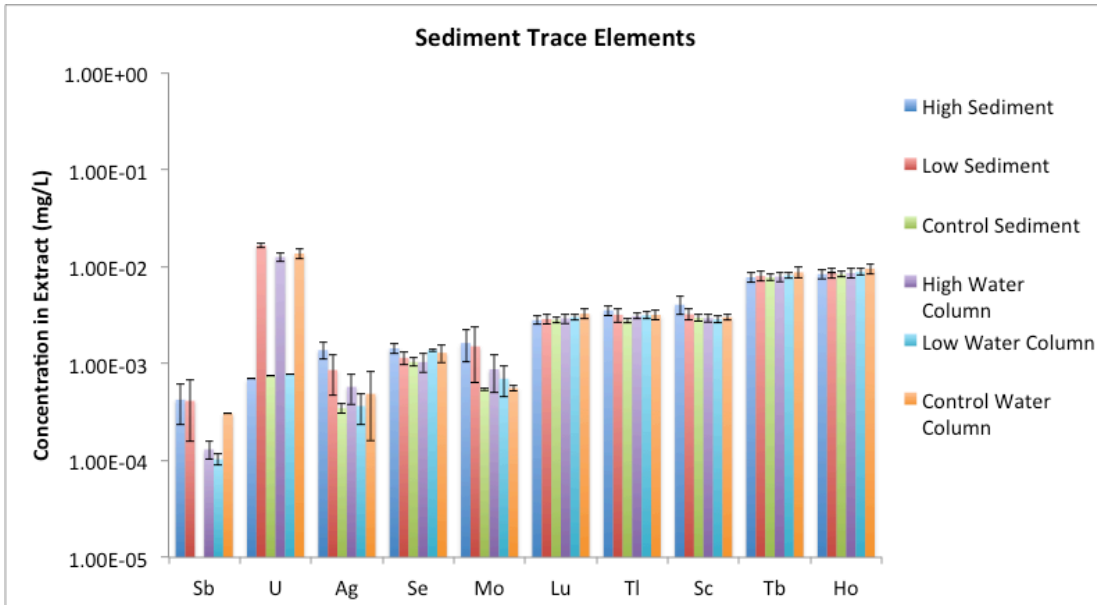


Figure A.10. Unfiltered total phosphate ( $n=3$  except for June samples where  $n=4$ , excluding June Control Water Column where  $n=3$ ).

### A.3.2 2012 Sediment Results

a.



b.

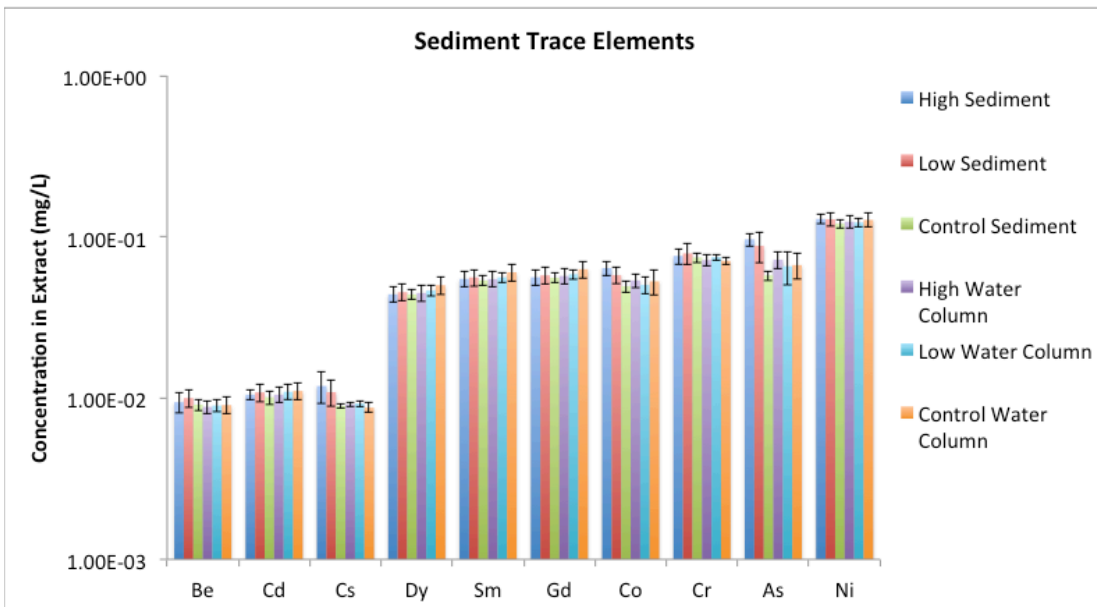
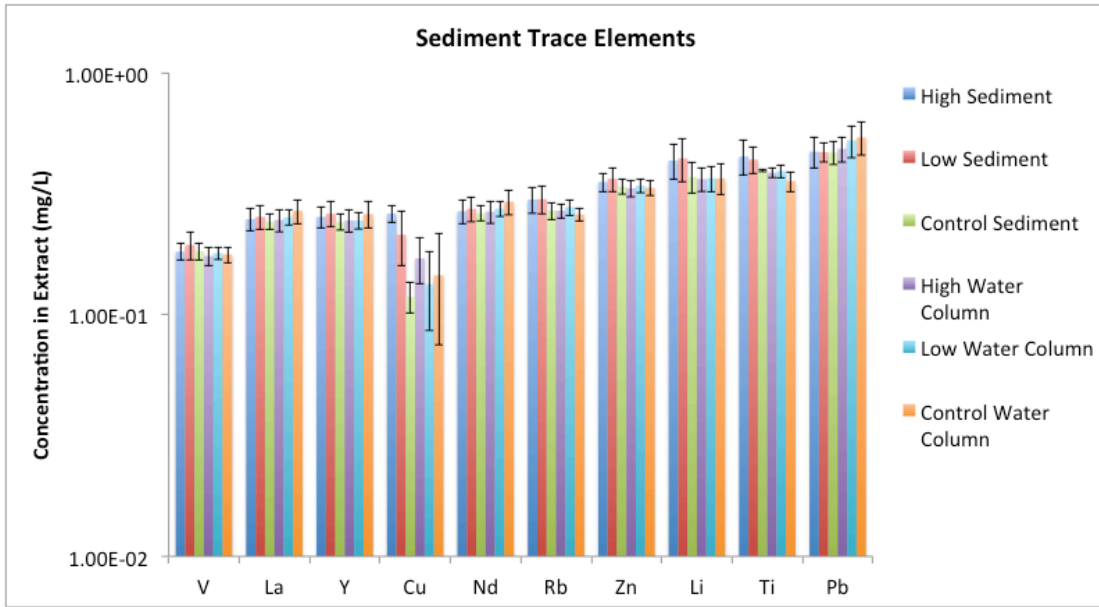


Figure A.11. Sediment trace metals represented by the concentration of trace elements in the extract. Error bars represent one standard deviation ( $n=3$ ).

C.



d.

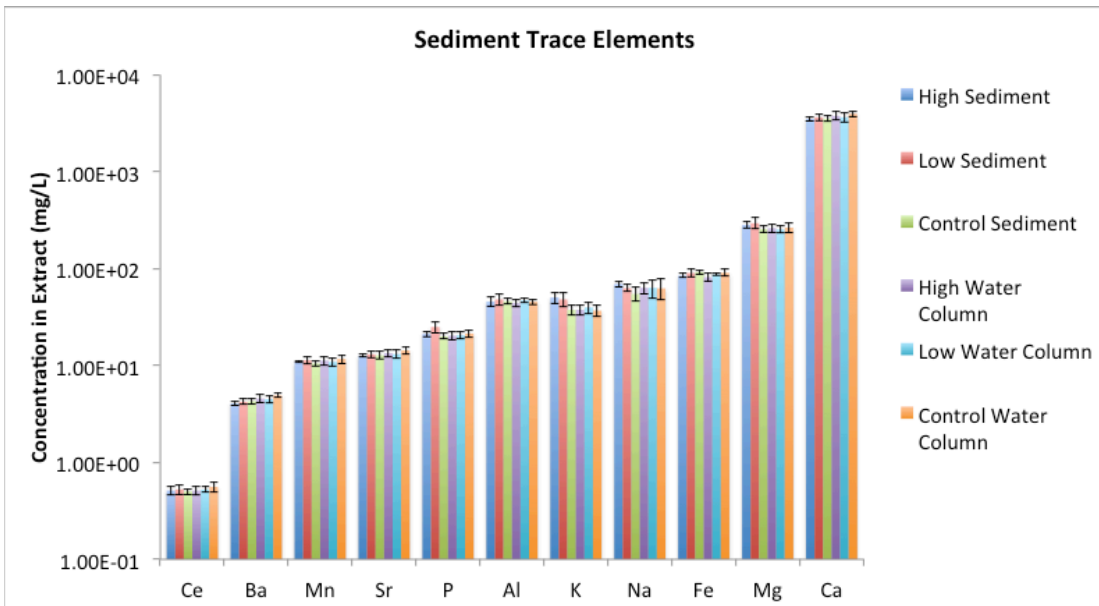


Figure A.11. Continued.

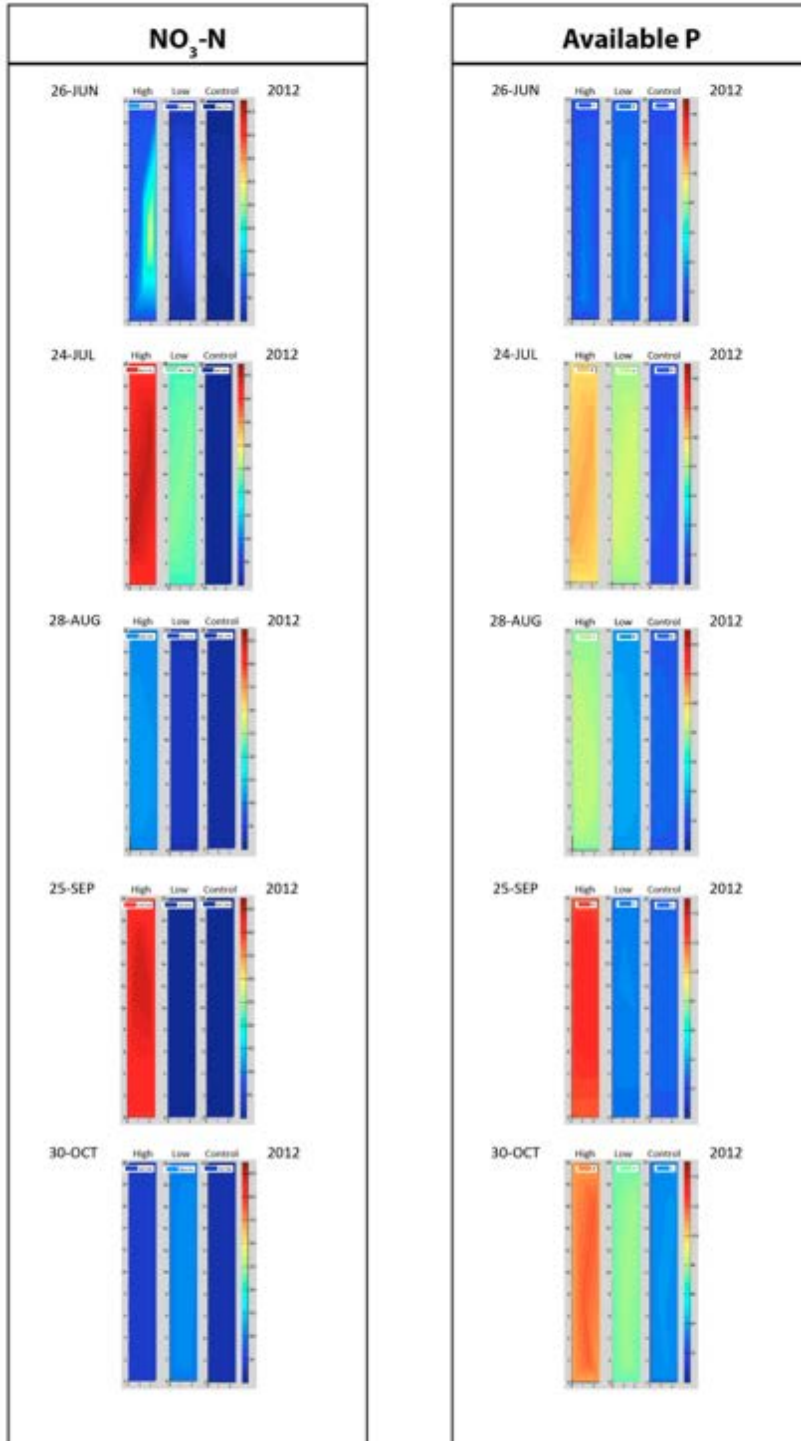


Figure A.12. Sediment nitrate and available phosphorus in amended sediment plots. Three samples were collected in random locations. Boundary values were set at 90% of lowest value measured in the plot ( $n=3$  except for June samples where  $n=4$ , excluding June Control Water Column where  $n=3$ ).

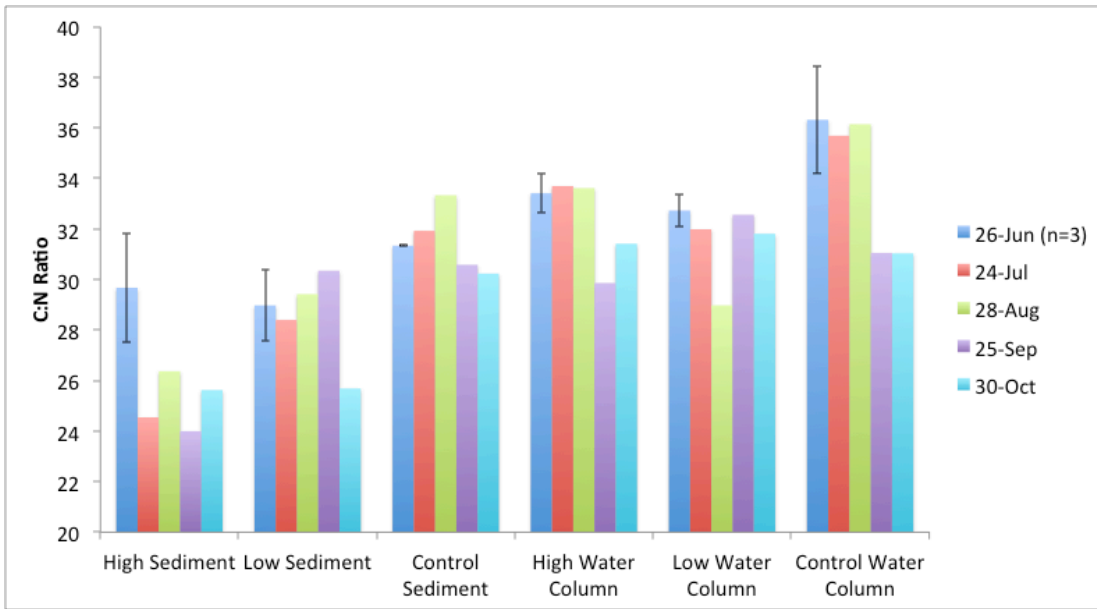


Figure A.13. Sediment C:N ratio. Error bars represent one standard deviation (n=3).

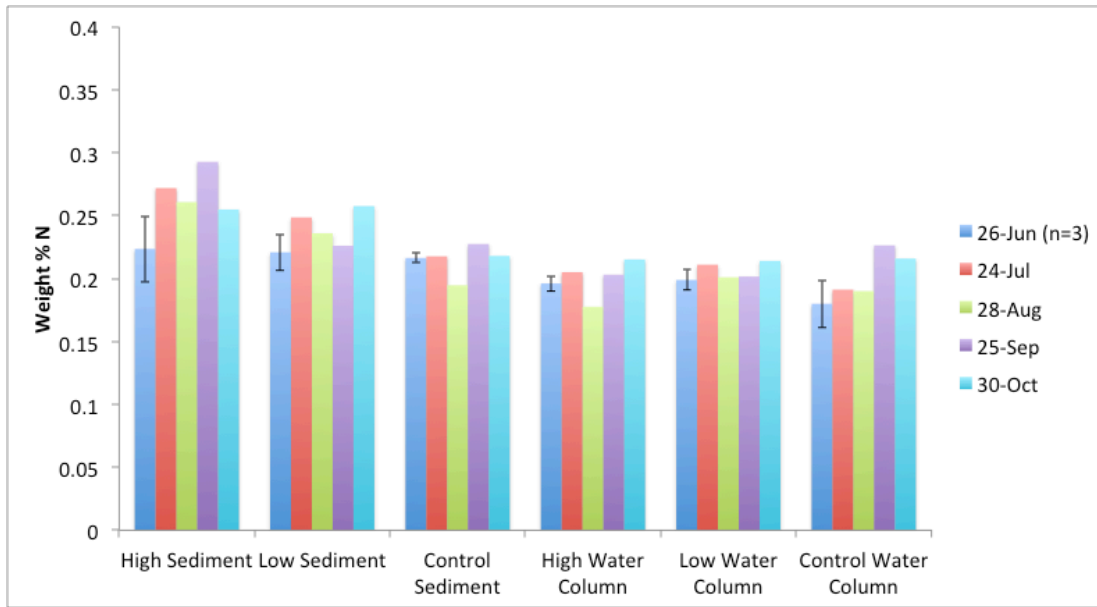


Figure A.14. Total weight percent nitrogen. Error bars represent one standard deviation (n=3).

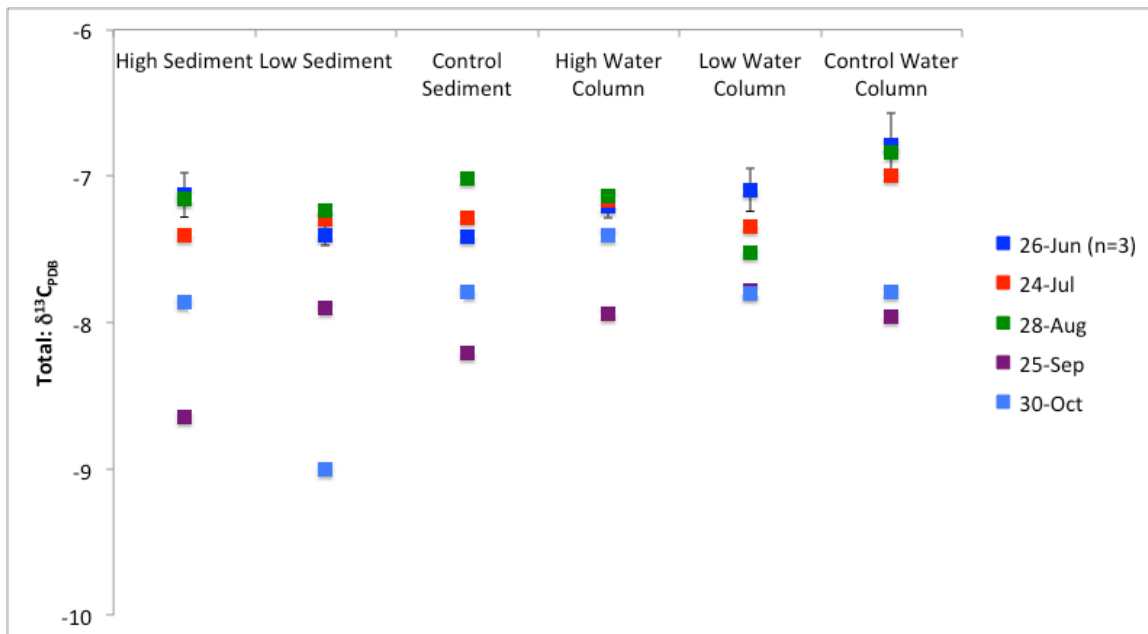


Figure A.15. Total  $\delta^{13}C_{PDB}$ . Error bars represent one standard deviation (n=3).

### A.3.3 2013 Surface Water

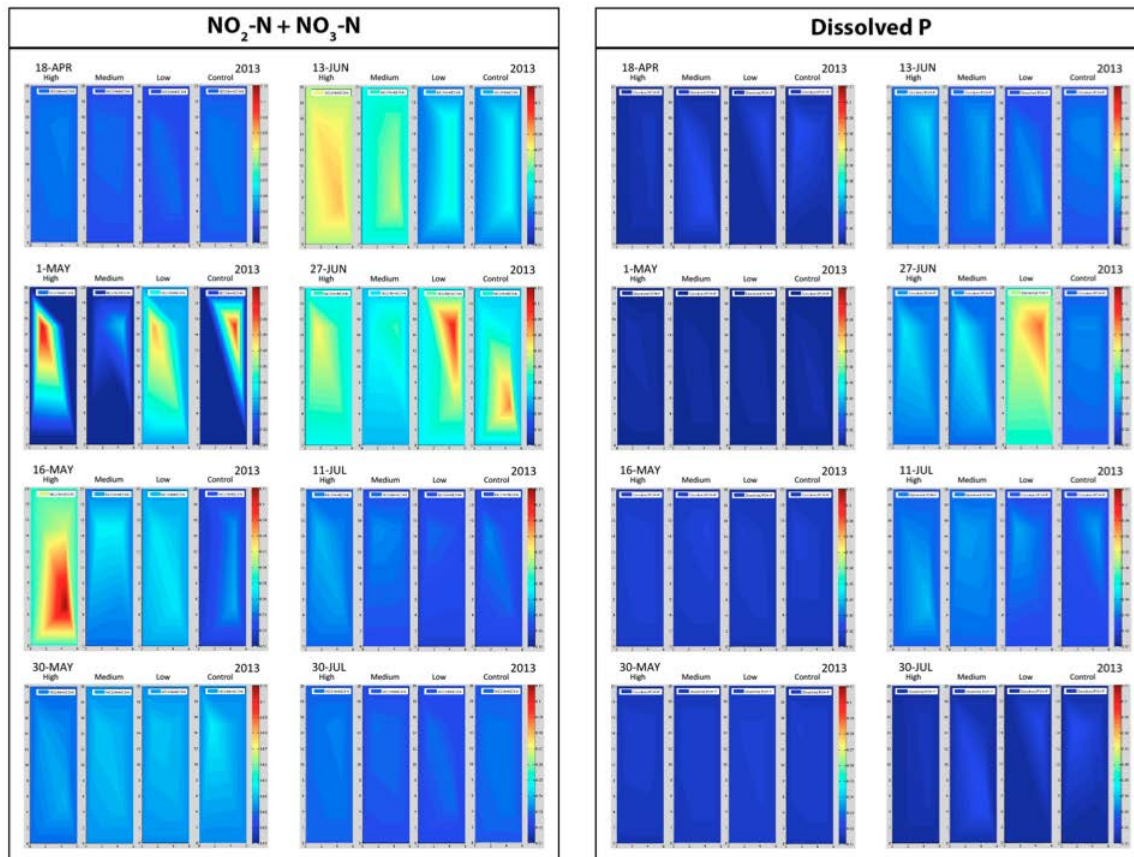


Figure A.16. Dissolved nitrite + nitrate and dissolved P 2D plots for filtered surface water samples. Error bars represent one standard deviation ( $n=3$  except for June samples where  $n=4$ , excluding June Control Water Column where  $n=3$ ).

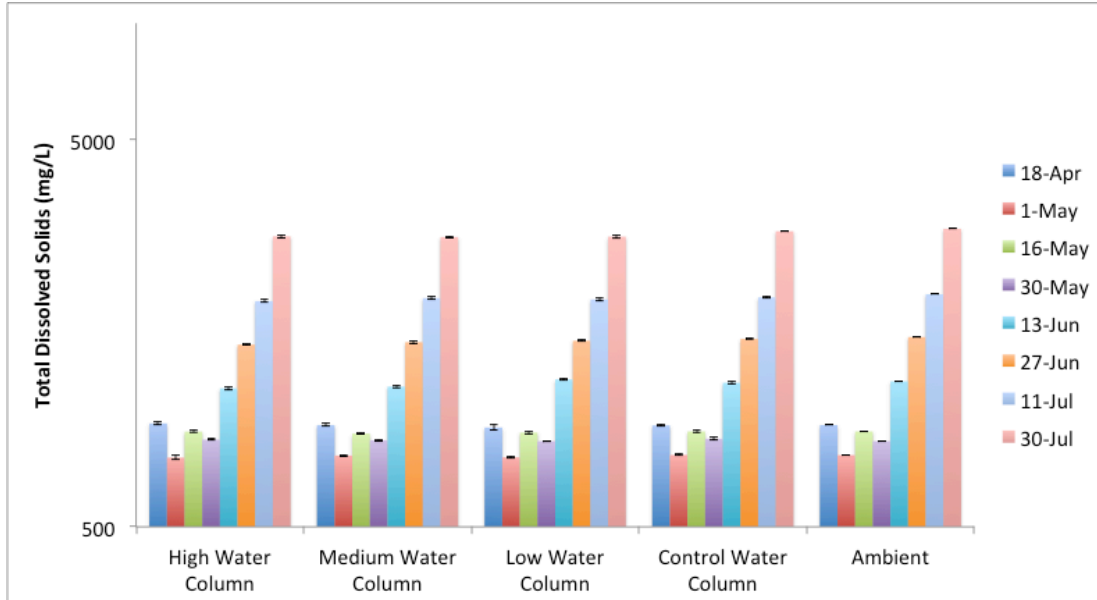


Figure A.17. Total Dissolved Solids for unfiltered surface water samples. Error bars represent one standard deviation ( $n=3$  except for June samples where  $n=4$ , excluding June Control Water Column where  $n=3$ ).

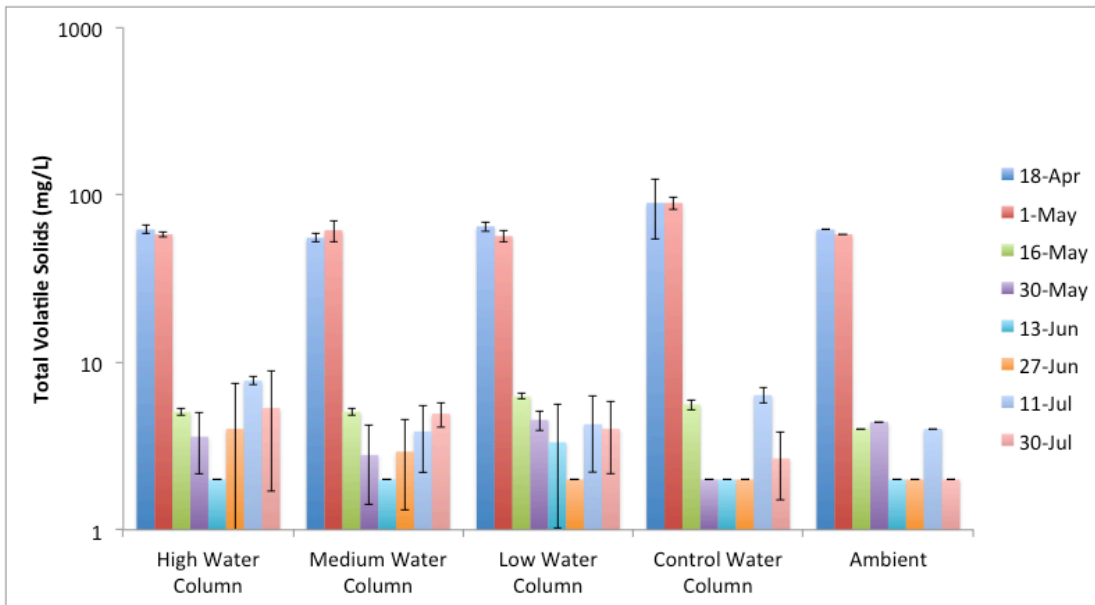


Figure A.18. Total Volatile Solids for unfiltered surface water samples. Error bars represent one standard deviation ( $n=3$  except for June samples where  $n=4$ , excluding June Control Water Column where  $n=3$ ).

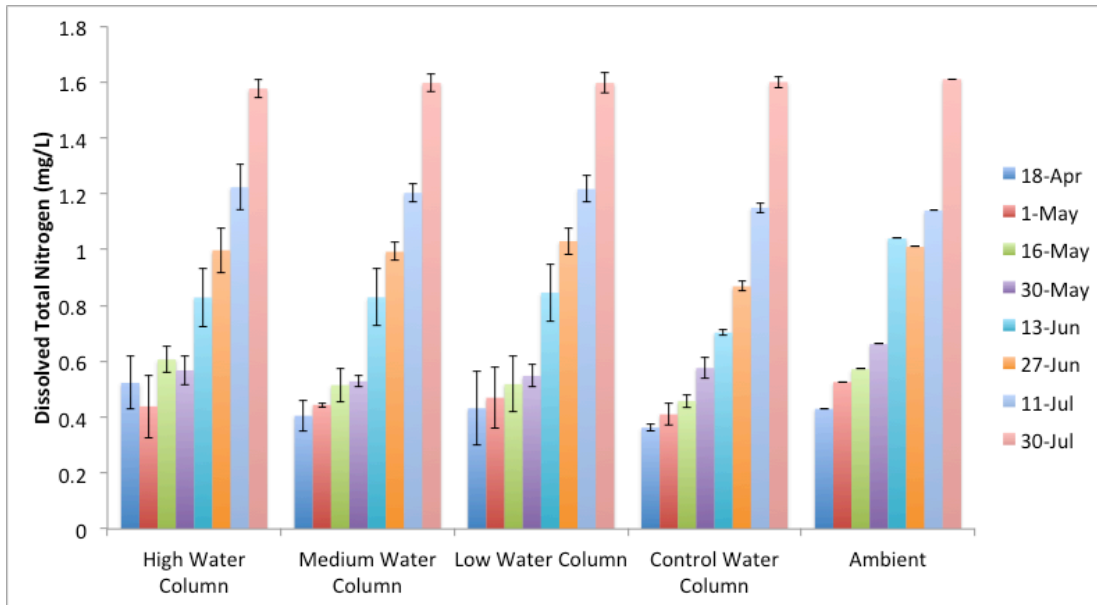


Figure A.19. Dissolved Total Nitrogen for filtered surface water samples. Error bars represent one standard deviation ( $n=3$  except for June samples where  $n=4$ , excluding June Control Water Column where  $n=3$ ).

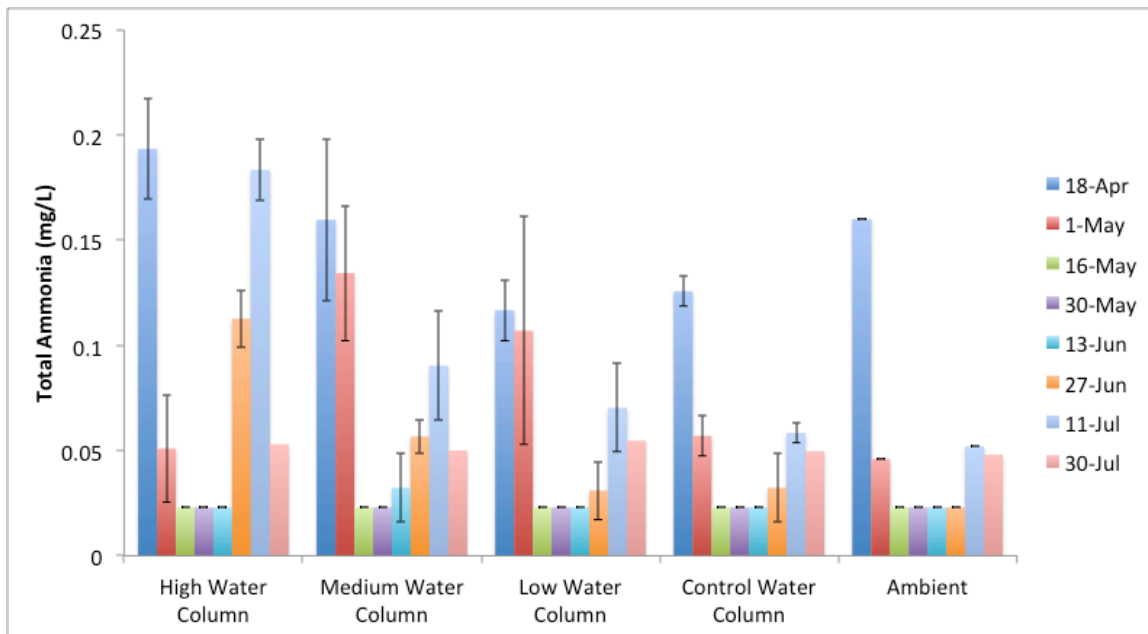


Figure A.20. Total ammonia for unfiltered surface water samples. Error bars represent one standard deviation ( $n=3$  except for June samples where  $n=4$ , excluding June Control Water Column where  $n=3$ ).

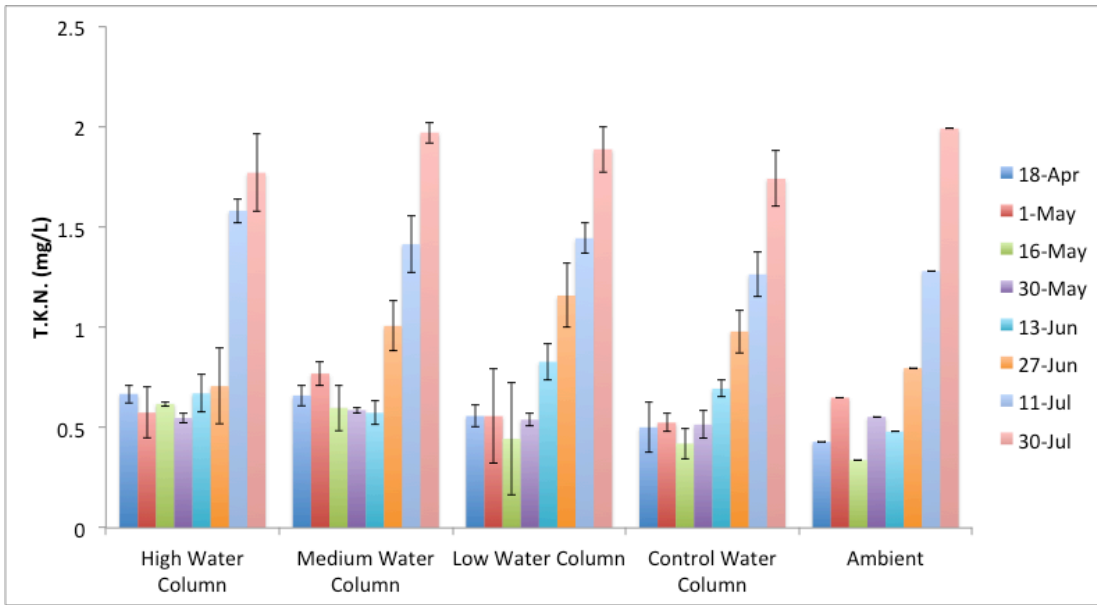


Figure A.21. TKN for unfiltered surface water samples. Error bars represent one standard deviation ( $n=3$  except for June samples where  $n=4$ , excluding June Control Water Column where  $n=3$ ).

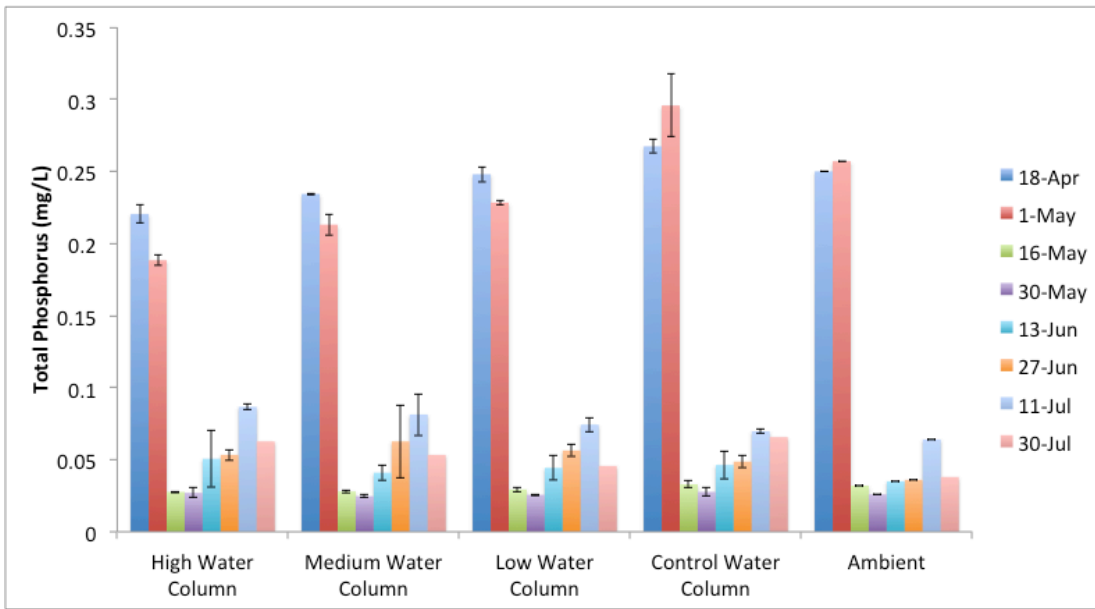


Figure A.22. Unfiltered total phosphate ( $n=3$  except for June samples where  $n=4$ , excluding June Control Water Column where  $n=3$ ).

### A.3.4 2013 Sediment Results

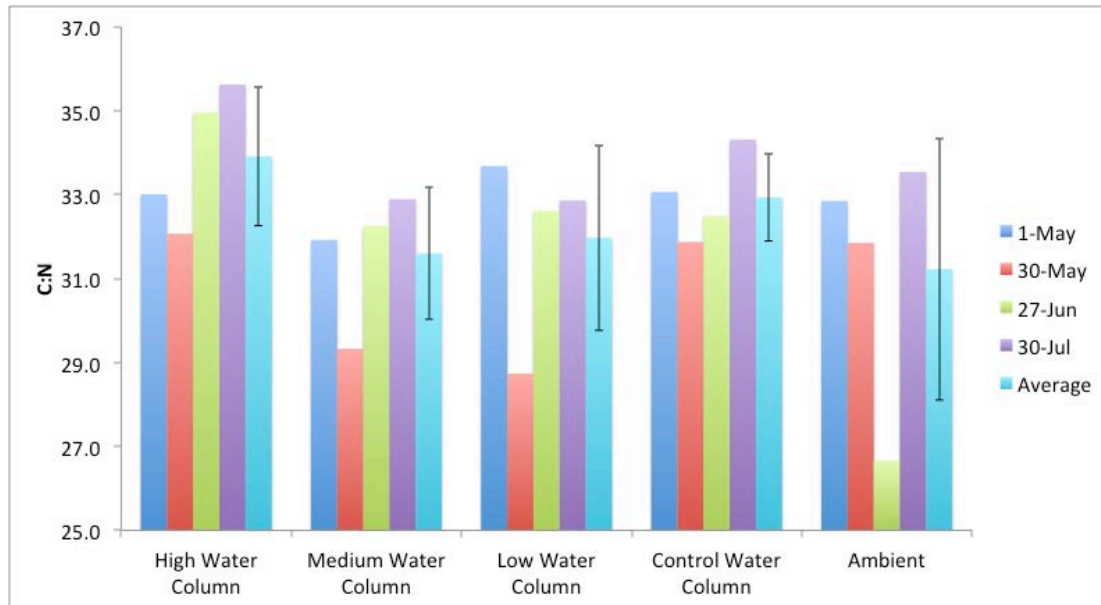


Figure A.23. Sediment C:N ratio. Error bars represent one standard deviation (n=3).

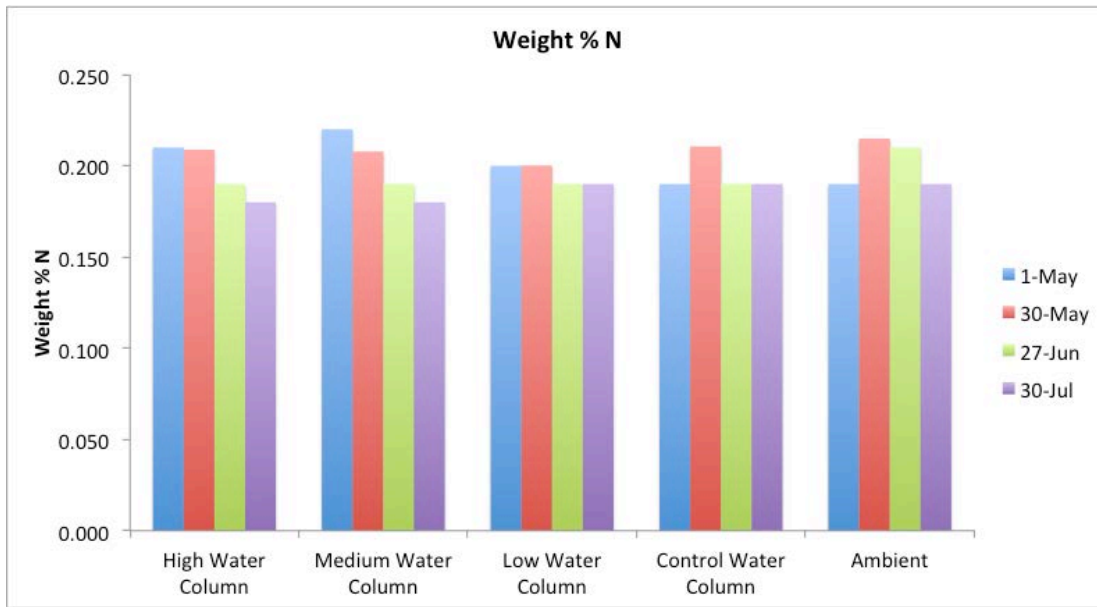


Figure A.24. Total weight percent nitrogen. Error bars represent one standard deviation (n=3).

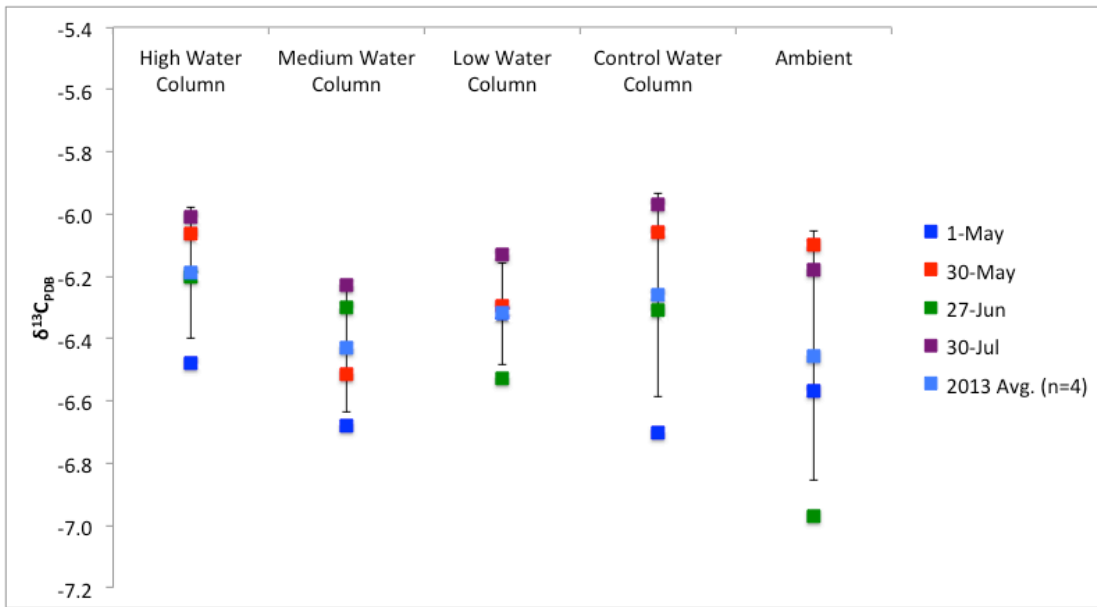


Figure A.25. Total  $\delta^{13}C_{PDB}$ . Error bars represent one standard deviation ( $n=3$ ).

## APPENDIX B. Nutrient spiking experiment using “Square Chambers” in Willard Spur

### B.1 Overall Objective

The overall objective of this short study was to evaluate the response of the water column and sediments at one site in Willard Spur Wetlands when spiked with known concentrations of nitrogen and phosphorus. This overarching objective was accomplished by installing Plexiglas square cross section chambers and spiking the contents of these chambers with known concentrations of nutrients. Following the spiking, the concentrations of major inorganic nitrogen species and orthophosphate were monitored in the water column.

### B.2 Chamber Details and Methodology

#### B.2.1 Chamber Details and installation

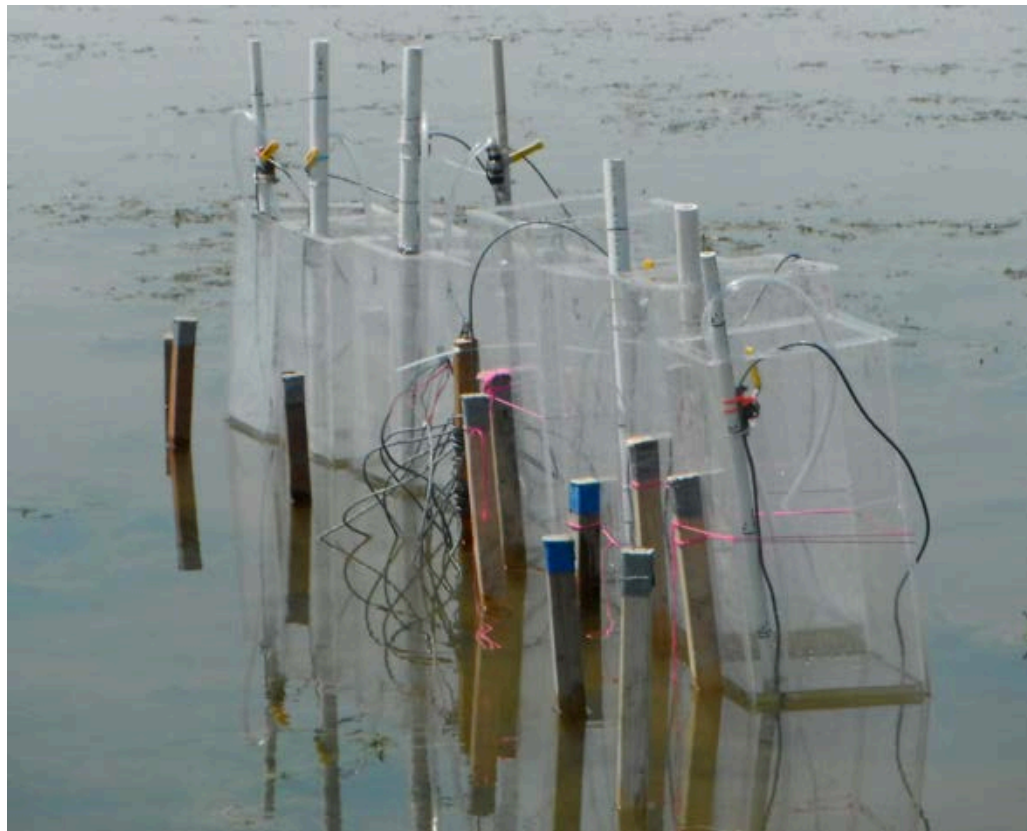
Each chamber was 10 inches square with 30 inches in height and, was made from transparent acrylic. At the selected site shown in [Figure B.1.A](#) below, a total of 8 chambers were placed about 300m from the shoreline of the Willard Spur near the nutrient amended experimental plots. Of the 8 chambers, 4 were water column chambers and the 4 were sediment chambers. The only difference between the water column and the sediment chamber was that the sediment chamber was open at the bottom to allow sediment-water column interactions. The water column chambers were closed at the bottom to separate the water column from the sediments.



Figure B.1. Site and Chamber Details; (A) site location, (B) sample photo showing installed chambers (WC chamber tied to stake to prevent falling over due to wind (left) and sediment chamber (right))

Figure B.2 below provides a photograph of all eight chambers installed. The four sediment chambers are in the back left of the photo and the WC chambers are located in the front right. The line of stakes

running parallel to the chambers acts as a bulwark to protect the chambers from being bumped by the canoe during windy and nighttime conditions. The sediment chambers were placed in areas having no SAV, therefore sediment disturbances associated with removing SAV were not encountered.



*Figure B.2. Chambers installed for daytime and nighttime sampling*

In case of 4 sediment chambers, two chambers (duplicate) were spiked with nutrients and the other two (duplicate) were not spiked with nutrients to monitor ambient conditions. Likewise, two of the water column chambers were spiked with nutrients and the other two were not. Hence, for each variable in terms of nutrient spiking (i.e ambient versus spiked), duplicate chambers were employed. Furthermore, to avoid/minimize the effect of submerged vegetation on the spiked nutrients, the chambers were installed in an area that was clear of plant growth (submerged aquatic vegetation). Once the first round of spiking was finished (includes the low concentration spike during light and dark conditions), the chambers were moved to a new nearby location with fresh sediment to evaluate the effect of high nutrient concentration spiking. In summary, the set of 8 chambers was installed twice to evaluate the effect of low and high concentration nutrient spikes. Additionally, the monitoring was conducted during the daylight and at night to understand the fate of nutrients in chambers under light and dark conditions.

### B.2.2 Spiked nutrient concentrations

Tables B.1 & B.2 below show the experimental matrix for nutrient spiking. Table B.1 shows low concentrations and Table B.2 shows high concentrations.

*Table B.1. Matrix of experiments with low concentrations of nutrients (Total 8 chambers)*

Type of chamber	Amendment	Target Concentration	Comment	Chamber ID
Sed+WC	None	Background (Non spiked)	In duplicate	SD-C1 & SD-C2
WC only	None	Background (Non spiked)	In duplicate	WC-C1 & WC-C2
Sed+WC	(N+P)- low	0.1 mg P/l+0.5 mg-NH <sub>3</sub> -N+0.5 NO <sub>3</sub> <sup>-</sup> N/L	In duplicate	SD-S1 & SD-S2
WC only	(N+P)- low	0.1 mg P/l+0.5 mg-NH <sub>3</sub> -N+0.5 NO <sub>3</sub> <sup>-</sup> N/L	In duplicate	WC-S1 & WC-S2

**Note\*:** WC and SD stand for water column and sediment respectively. C's (i.e C1, C2) and S's (i.e S1,S2) stand for control and spike respectively.

*Table B.2: Matrix of experiments with high concentrations of nutrients (total 8 chambers)*

Type of chamber	Amendment	Target Concentration	Comment	Chamber ID
Sed+WC	None	Background (Non spiked)	In duplicate	SD-C1 & SD-C2
WC only	None	Background (Non spiked)	In duplicate	WC-C1 & WC-C2
Sed+WC	(N+P)- high	0.5 mg P/l+2.5 mg-NH <sub>3</sub> -N+2.5 NO <sub>3</sub> <sup>-</sup> N/L	In duplicate	SD-S1 & SD-S2
WC only	(N+P)- high	0.5 mg P/l+2.5 mg-NH <sub>3</sub> -N+2.5 NO <sub>3</sub> <sup>-</sup> N/L	In duplicate	WC-S1 & WC-S2

**Note\*:** WC and SD stand for water column and sediment respectively. C's (i.e C1, C2) and S's (i.e S1,S2) stand for control and spike respectively.

The water column was spiked with combined concentrations of both nitrogen (N) and phosphorus (P). The target N was supplied as equal concentrations of ammonia (NH<sub>4</sub>Cl) and nitrate (NaNO<sub>3</sub>), calculated as N. KHPO<sub>4</sub> was used to supplement P in the chambers.

### B.2.3 Sample collection and analysis

Each chamber had a submersible pump installed 2-3 inches above the sediment-water interface to ensure complete mixing from bottom to top of the chambers. Water quality samples were collected every two hours over a 12-hour period to capture both light and dark conditions. Before collecting each water sample, the submersible pumps were turned on for 10 minutes to internally circulate the water in the chamber to create well-mixed conditions. The samples were immediately filtered (0.45µm) after collection and stored on ice until they were transported to lab for further analysis. All laboratory analysis was completed within 48-hours following the sample collection. Water depth in each water chamber was also measured and the volume of water in each chamber was then calculated using the cross sectional area of chamber. All anions were measured on a Metrohm Ion Chromatogram (EPA 300.0 revision 2.1, 1993). For each analysis, a new calibration curve for each anion was created using HACH premade standards. In this way, any human error associated with making analytical stock

solutions to create standard calibration curves was minimized. Ammonia nitrogen was measured using low range ammonia HACH kits (TNTplus 830, Method 10205).

Steps during the sampling event and sample analysis were taken for proper quality assurance and control. Field blanks were taken into the field and treated in the same manner as the samples collected, along with a spike solution containing  $\text{NO}_3\text{-N}$ ,  $\text{NH}_4\text{-N}$ , and  $\text{PO}_4\text{-P}$ . Duplicates and the placement of the chambers (side by side) allowed for us to compare the nutrient concentrations within samples, assuring our methods were producing consistent results. The mixing of the water within each chamber occurred at a low speed and prevented stratification while providing a representative sample. Samples were taken using the tube from the pump to prevent any contamination from handling the sample. The filtering equipment and collection vials were thoroughly rinsed with deionized water between each filtration and sampling collection time. During laboratory sample analysis, blanks and check standard were analyzed between every 10 samples.

### B.3 Results and Discussion

In general, wetland specialists and plant ecologists focus on processes occurring in the water column that affect nutrient dynamics. However, a significant part of the driving mechanisms take place at the sediment-water interface and, below this interface in wetland plant root zone in shallow water bodies. Estimating the fate of nutrients in terms of their partitioning to various pathways is imperative to conduct the ecosystem assessment and to understand the ecosystem resiliency in terms of handling of excess loads of nutrients. One methodology to evaluate the response of wetland ecosystems towards the availability of nutrients is to conduct short-term nutrient spiking experiments in which case a controlled volume (i.e water column) of the wetland is spiked with nitrogen and phosphorus to achieve target concentrations in the water column and then monitor the spiked water column.

In this current study, nutrient spike experiments were conducted at one site to see the response of the Willard Spur Wetland system and more importantly to establish a protocol for future experiments. The experimental site was located in the vicinity of nutrient amendment plots put by the University of Utah research team in Willard Spur. After spiking, the monitoring was conducted during daylight and nighttime hours.

To facilitate the discussion, we have calculated the nutrient fluxes in terms of  $\text{g/m}^2/\text{day}$  for sediments (hereafter referred as  $\text{SED}_{\text{net flux}}$ ) and  $\text{g/m}^3/\text{day}$  for the water column only chambers. It is also worth mentioning that the sediment flux values account for nutrient concentration changes in the water column and is calculated as follows.

$\text{SED}_{\text{net flux}} = (\text{Conc. change in sediment chamber} - \text{average conc. change in water column chamber}) * \text{water depth}$

In this calculation, when calculating  $\text{SED}_{\text{net flux}}$  in sediment control chambers (i.e unspiked), the average concentration change in the control water column was considered. Likewise, to calculate  $\text{SED}_{\text{net flux}}$  in sediment spiked chambers, the average concentration change in the control water column was considered. Furthermore, the daylight and nighttime fluxes were also calculated separately.

Furthermore, for water column concentration changes, these are expressed as rates ( $\text{g}/\text{m}^3/\text{day}$ ) rather than fluxes to account for the whole water column.

Figure B.3 shows  $\text{NH}_3\text{-N}$  dynamics in chambers spiked with low and high concentrations (see Tables B.1 & B.2 above) of nutrients and during day light and night hours. The fluxes with positive values represent that the respective nutrient concentration increased in the water column. Likewise, the negative values show removal from the water column.

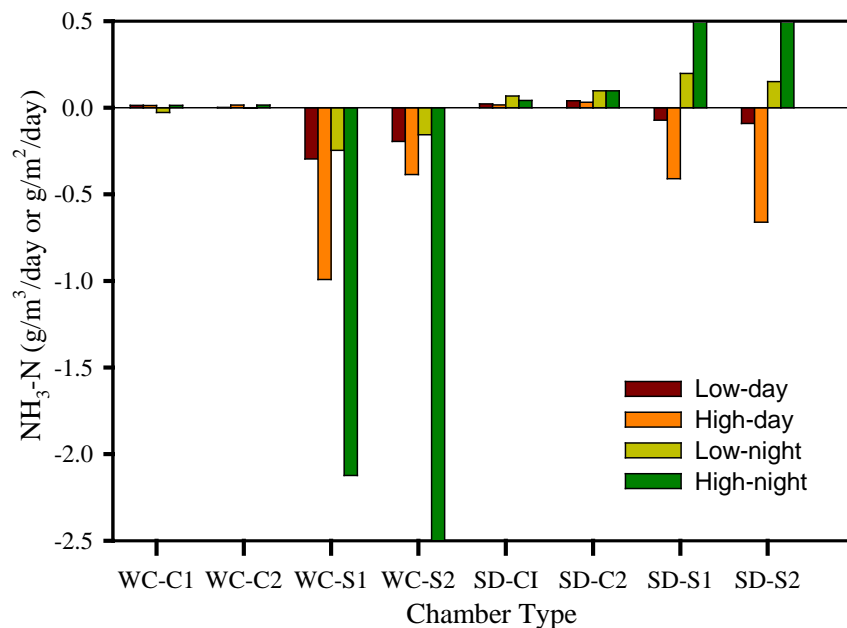


Figure B.3.  $\text{NH}_3\text{-N}$  expressed as  $\text{g}/\text{m}^3/\text{day}$  for water column and as  $\text{g}/\text{m}^2/\text{day}$  for sediments in all chambers under low and high spikes.

As evident from Figure B.3, a minimal flux values were recorded in control (unspiked) water column chambers (WC-C1 and WC-C2). The water column spiked chambers (WC-S1 and WC-S2) showed negative rates of  $\text{NH}_3\text{-N}$ , which means  $\text{NH}_3\text{-N}$  was consumed in the water column. Furthermore, it is also interesting to note that  $\text{NH}_3\text{-N}$  removal in terms of  $\text{g}/\text{m}^3/\text{day}$  in the water column was relatively more for “high nutrient spiked” chambers than the same chambers when spiked with low concentrations. On the contrary,  $\text{NH}_3\text{-N}$  was added to the water column in unspiked sediment chambers (i.e control sediment chambers, SD-C1 and SD-C2). In the spiked sediment chambers (SD-S1 & SD-S2), negative fluxes of  $\text{NH}_3\text{-N}$ , i.e removal from the water column, was recorded during day hours but positive fluxes of  $\text{NH}_3\text{-N}$  were observed during the night hours. Based on spiked water column and sediment chamber results, it appears that the water column is a sink of  $\text{NH}_3\text{-N}$ . Since all chambers were placed at a site locally devoid of submerged aquatic vegetation, it is impossible that the  $\text{NH}_3\text{-N}$  was consumed for the plant growth. Other factors which could have contributed to the  $\text{NH}_3\text{-N}$  loss in the water column include aerobic nitrification, volatilization to the air, sorption to the suspended particles and walls of chamber and assimilation by phytoplankton. Aerobic nitrification should result in the simultaneous increase of nitrite and/or nitrate nitrogen, but the data does not show such increase in the water column for  $\text{NO}_3\text{-N}$  (Figure B.3) and  $\text{NO}_2\text{-N}$  (data not included). Positive fluxes of  $\text{NH}_3\text{-N}$  in

unspiked sediment chambers indicate  $\text{NH}_3\text{-N}$  was generated in sediments possibly through decay of matter and/or dissimilatory nitrate reduction.

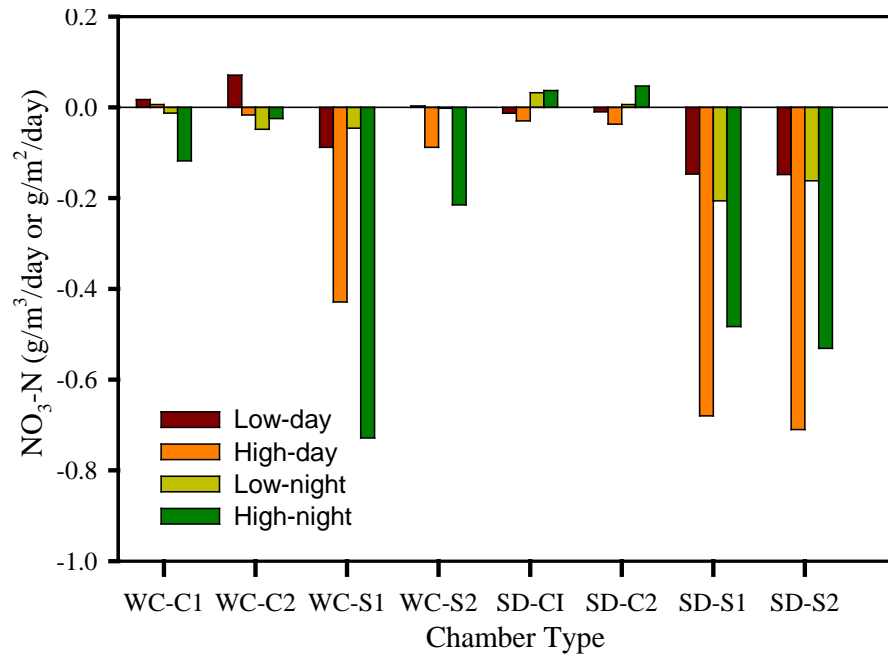


Figure B.4.  $\text{NO}_3\text{-N}$  expressed as  $\text{g/m}^3/\text{day}$  for water column and as  $\text{g/m}^2/\text{day}$  for sediments in all chambers under low and high spikes.

$\text{NO}_3\text{-N}$  fluxes under all conditions are presented in Figure B.4. In general, except at few occasions (i.e. night time in sediment control chambers and day time during low spiking water column control chambers), negative fluxes of  $\text{NO}_3\text{-N}$  were calculated based on the measured concentration data in all chambers. Nitrate loss in spiked sediment chambers (SD-S1 & SD-S2) possibly means that  $\text{NO}_3\text{-N}$  was undergoing denitrification in the sediments and/or was consumed through other activities in the water column.  $\text{NO}_3\text{-N}$  loss in spiked water column chambers (WC-S1 & WC-S2) especially under “high spiked condition” and under both day light (orange bar) and night hours (green bar) is interesting and difficult to explain except to speculate that denitrification in the water column, sorption to suspended sediments and to chamber walls could have contribute to  $\text{NO}_3\text{-N}$  loss in the water column. Sorption to suspended sediments is also less likely because care was taken as not to resuspend sediments during the sampling and, the visual inspection also indicated clear but greenish water column.  $\text{NO}_2\text{-N}$  fluxes in all chambers were almost negligible except at few occasions. For example,  $\text{NO}_2\text{-N}$  fluxes during night hours in case of low spiked experiment were measured estimated to be undetectable.

Figure B.5 shows  $\text{PO}_4\text{-P}$  fluxes in all chambers. Like in the case of nitrogen species (ammonia and nitrate), mostly negative fluxes which means sink of  $\text{PO}_4\text{-P}$  was recorded in water column and sediment spiked chambers. However, for  $\text{PO}_4\text{-P}$ , low flux values relative to those obtained for  $\text{NH}_3\text{-N}$  and  $\text{NO}_3\text{-N}$  were obtained (note the scale of y-axis). Positive  $\text{PO}_4\text{-P}$  fluxes were associated with unspiked sediment chambers corresponding to day time low spike and, unspiked water column chamber especially during night time hours.

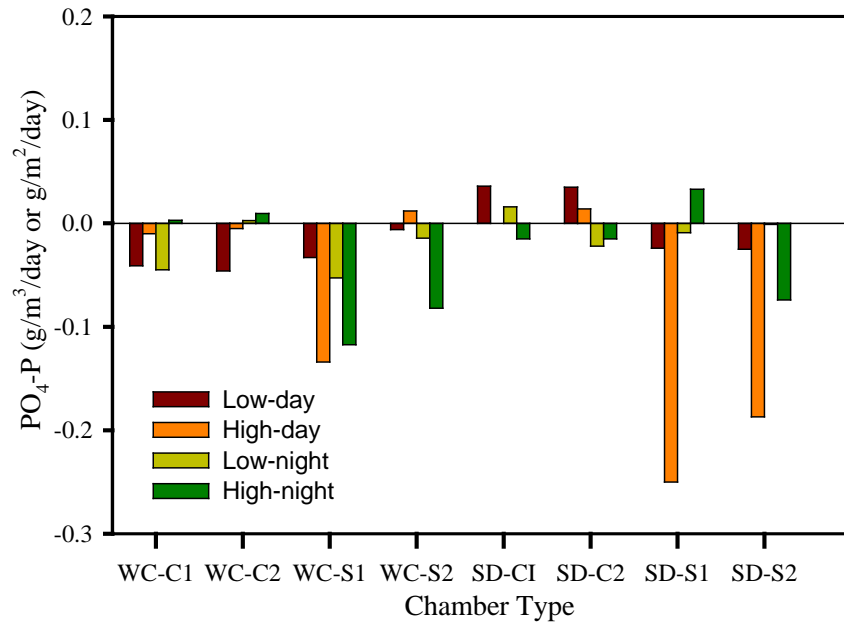


Figure B.5. PO<sub>4</sub>-P expressed as g/m<sup>3</sup>/day for water column and as g/m<sup>2</sup>/day for sediments in all chambers under low and high spikes.

#### B.4 Conclusions

In wetlands, several factors can contribute to the fate of nutrients. Ammonia, nitrate and nitrite nitrogen are interlinked as the fate of one affects the fate of others. However, the fate of phosphorus is independent of inorganic nitrogen species and is primarily determined through plant uptake, pH dependent chemistry and physical processes such as sorption. The bacteria mediated main biological processes that contributes to the fate nitrogen in wetlands include aerobic ammonia oxidation to nitrite and then to nitrate, denitrification of nitrite and nitrate, dissimilatory nitrate reduction to ammonia, nitrogen fixation and anaerobic ammonia oxidation. Nitrogen consumed by biota and plants forms another important pathway for nitrogen loss in wetlands. Physical sorption to plant tissues and sediments of nitrogen species and pH dependent volatilization of ammonia can also contribute to nitrogen losses from the bulk water column. The inputs of nitrogen and phosphorus include anthropogenic sources, internal cycling such as release from sediments and the atmospheric deposition.

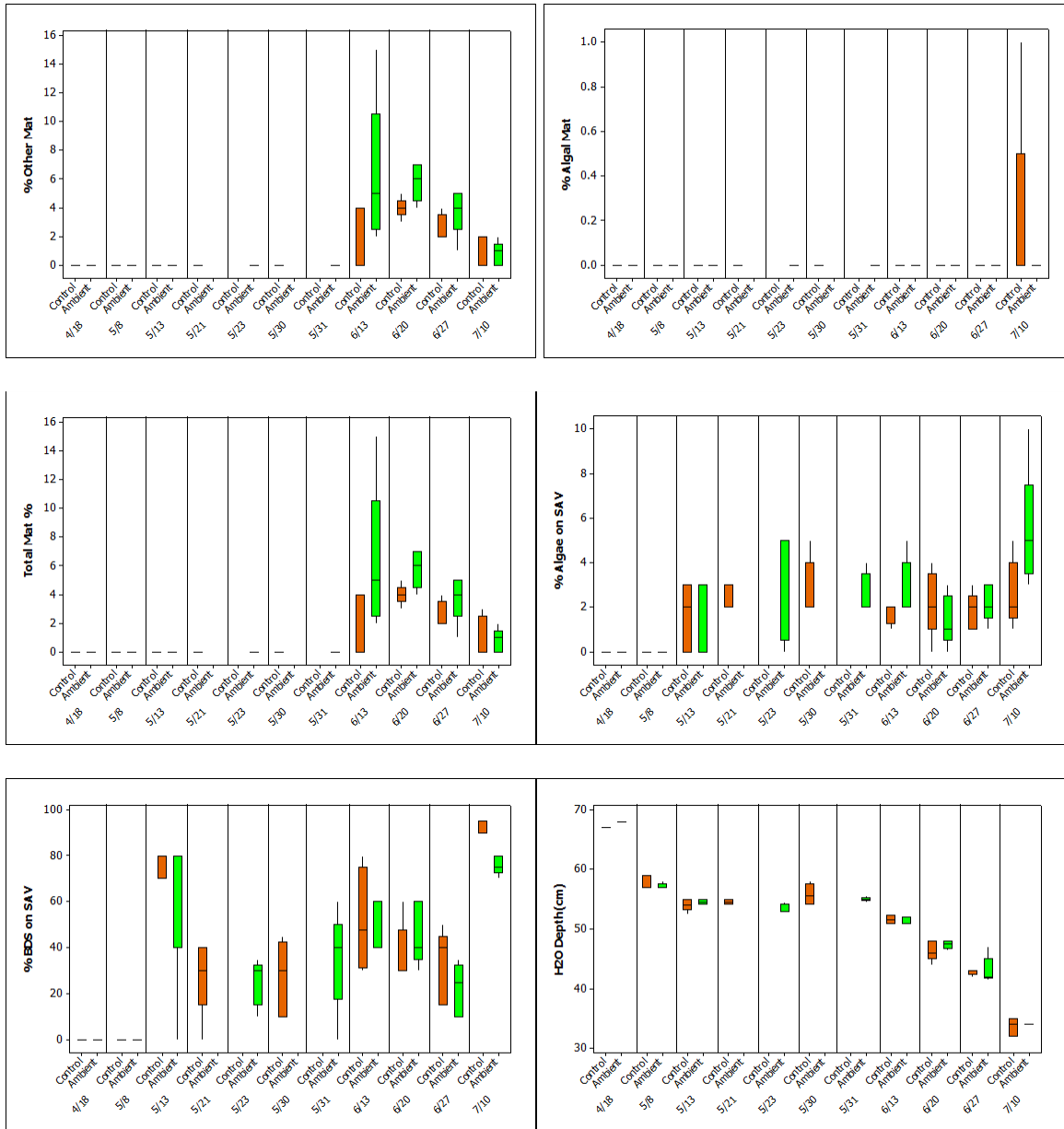
In the current study, although a trend was recorded in terms of the fate of NH<sub>3</sub>-N, NO<sub>3</sub>-N and PO<sub>4</sub>-P, the factors contributing to the fate could not be ascertained. For example, if aerobic ammonia oxidation was one of the pathways for ammonia disappearance from the water column that should have resulted in corresponding increases in NO<sub>3</sub>-N and/or NO<sub>2</sub>-N concentrations in the water column. However, such trend was missing. Instead, decrease in NO<sub>3</sub>-N concentration resulting in negative fluxes was recorded at many occasions. Nevertheless, the possibility of simultaneous ammonia oxidation (i.e nitrification) and nitrate/nitrite reduction (denitrification) cannot be ruled out.

Another important observation was relatively greater negative fluxes of  $\text{NH}_3\text{-N}$  and  $\text{NO}_3\text{-N}$  as compared to the fluxes for  $\text{PO}_4\text{-P}$ . Although, more experiments such as determining the composition of primary producers are needed, it appears that the water column is nitrogen limited. Some important observations on the data are summarized below.

1. *In water column chambers spiked with nutrients*; The  $\text{NH}_3\text{-N}$ ,  $\text{NO}_3\text{-N}$  and  $\text{PO}_4\text{-P}$  were consumed in spiked water column chambers under all conditions. Several factors could have contributed to the fate of these nutrients of which, the role of primary producers seems prominent based on the nutrient data. The dissolved oxygen concentrations under daytime ambient conditions were recorded to be well above saturation levels indicating significant primary production in the water column. Nevertheless, the presence of simultaneous nitrification and denitrification and, the role of other physical factors such as volatilization and sorption cannot be ruled out as well.
2. *In sediment chambers spiked with nutrients*;  $\text{NH}_3\text{-N}$  removal during the day light hours (i.e negative flux) indicating consumption in the water column and sink to sediment and addition during night hours (i.e positive flux) indicating organic matter decay and/or dissimilatory nitrate reduction to ammonia were observed.  $\text{NO}_3\text{-N}$  was removed during both day light and night hours possibly through a combination of nitrate reduction through biological denitrification, dissimilatory nitrate reduction and other processes.  $\text{PO}_4\text{-P}$  was removed from the water column possibly due to consumption by planktonic and benthic phytoplankton, sorption to sediments or simply sedimentation.
3. *In sediment control chambers (unspiked with nutrients)*;  $\text{NH}_3\text{-N}$  was added to the water column (i.e positive fluxes) indicating a combination of processes possibly decaying in sediments, nitrate reduction to ammonia, nitrogen fixation from the atmosphere.  $\text{NO}_3\text{-N}$  was removed during daylight hours but was added during nighttime. However, for  $\text{PO}_4\text{-P}$  the opposite was observed in which case, it was added to the water column during daylight hours but removed during nighttime.

In summary, the chamber experiments established a useful protocol for future experiments. However, these experiments must be supplemented with additional experiments such as sampling of biota, sediments, measurement of chlorophyll a and determination of N-partitioning through stable isotope experiments.

## APPENDIX C. Box plots of control and ambient metrics and H2O depth at eleven sampling dates 2013.



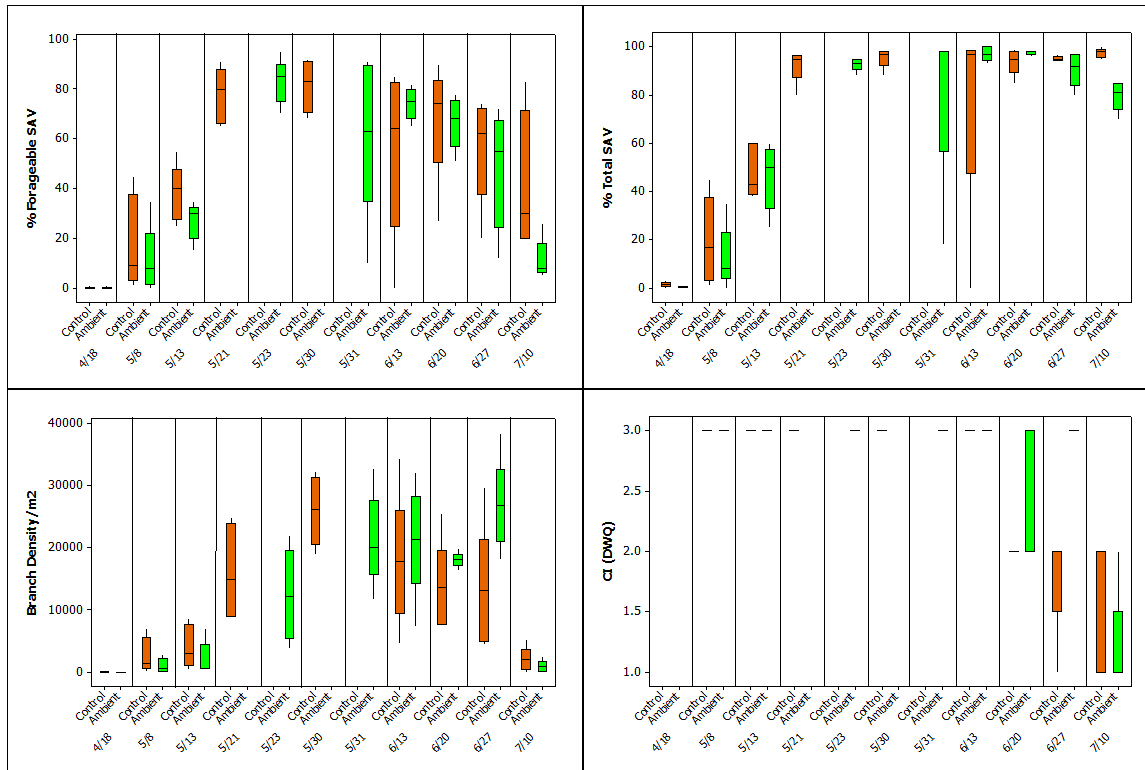


Figure C.1 Box plots of control and ambient metrics and H2O depth at eleven sampling dates 2013.

## APPENDIX D. Metric Evaluation

Table D.1. Kruskal-Wallis Tests for SAV and isotope metrics\* (Date = Julian Date; Treatment = High, Medium, Low, and Control; DF = degrees of freedom; alpha = 0.05). Note: calendar dates are shown in Table D.2.

<i>Metric</i>	<i>Factor</i>	<i>DF</i>	<i>K (observed)</i>	<i>K (critical)</i>	<i>p-value</i>
<b>SAV</b>					
<b>Branch Density</b>	Date	5	61.52	12.59	< 0.01
	Treatment	3	17.90	7.82	< 0.01
<b>% Total SAV</b>	Date	3	1.04	7.82	0.79
	Treatment	3	32.89	7.82	< 0.01
<b>% Total Mat</b>	Date	2	0.05	5.99	0.98
	Treatment	3	3.60	7.82	0.31
<b>% Forageable SAV</b>	Date	7	83.59	14.07	< 0.01
	Treatment	3	3.81	7.82	0.28
<b>% BDS on SAV</b>	Date	6	57.22	12.59	< 0.01
	Treatment	3	41.48	7.82	< 0.01
<b>% Algae on SAV</b>	Date	6	26.56	12.59	< 0.01
	Treatment	3	27.08	7.82	< 0.01
<b>%Algae + BDS on SAV</b>	Date	6	19.54	11.07	< 0.01
	Treatment	3	56.42	7.82	< 0.01
<b>DWQ Condition Index</b>	Date	2	44.15	7.82	< 0.01
	Treatment	3	9.93	7.82	< 0.01
<b>Leaf Nutrients &amp; Isotopes</b>					
<b>15N/14NAIR</b>	Date	2	0.44	5.99	0.80
	Treatment	3	26.49	7.82	< 0.01
<b>13C/12CPDB</b>	Date	2	31.14	5.99	< 0.01
	Treatment	3	0.74	7.82	0.86
<b>Wt% N</b>	Date	2	20.06	5.99	< 0.01
	Treatment	3	6.99	7.82	0.07
<b>Wt% C</b>	Date	2	12.43	5.99	< 0.01
	Treatment	3	12.98	7.82	< 0.01
<b>C:N ratio</b>	Date	2	11.13	5.99	< 0.01
	Treatment	3	17.52	7.82	< 0.01
<b>P SAV Leaves</b>	Date	2	2.88	5.99	0.24
	Treatment	3	13.72	9.49	0.10
<b>Algal Nutrients &amp; Isotopes</b>					
<b>15N/14NAIR</b>	Treatment	3	2.77	9.49	0.60
<b>13C/12CPDB</b>	Treatment	3	4.98	9.49	0.29
<b>Wt% N</b>	Treatment	3	8.44	9.49	0.08
<b>Wt% C</b>	Treatment	3	7.91	9.49	0.10
<b>C:N ratio</b>	Treatment	3	11.12	9.49	0.03
<b>P Algae</b>	Treatment	2	10.42	9.49	0.03

\* The Conover-Iman two-tailed non-parametric test for multiple pairwise comparisons of algal treatment data was used because sample sizes were small.)

*Table D.2. Multiple pairwise comparisons of treatment dates, 2013 on all metrics examined using the Steel-Dwass-Critchlow-Fligner (1984) two tailed test No algae comparisons were possible because there was only one collection date. (If upper case letters are the same then there was no significant difference between treatments at alpha = 0.05. If letters are different then there were significant differences. All metrics that were measured as percentages were arcsine transformed and Branch Density m<sup>2</sup> was log + 1 transformed prior to comparisons).*

<i>SAV</i>							
Metric	Date						
	5/13	5/21	5/29	6/13	6/20	6/27	7/10
Branch Density m <sup>2</sup>	A	B	D	D	CD	BC	
% Total SAV				A	A	A	A
% Total Mat				A	A	A	
% Forageable SAV	A	BC	C	BC	BC	B	
% BDS on SAV	A	AB	B	AB	B	B	C
% Algae on SAV	A	B	B	B	AB	B	B
% Algae + %BDS on SAV	A	AB	AB	AB	AB	B	
Modified Condition Index				A	B	B	C
DWQ Condition Index				A	B	B	C
<i>Leaf Nutrients &amp; Isotopes</i>							
	5/13	5/21	5/29	6/13	6/20	6/27	7/10
15N/14NAIR		A	A	A			
13C/12CVPDB		A	B	C			
Wt% N		A	A	B			
Wt% C		A	A	B			
C:N ratio		A	AB	B			
P SAV Leaves		A	A	A			

Table D.3. Multiple pairwise comparisons of the 2013 four nutrient treatments; high, medium, low, and control on all metrics examined using the Steel-Dwass-Critchlow-Fligner (1984) two-tailed test (If upper case letters are the same then there was no significant difference between treatments at alpha = 0.05. If letters are different then there were significant differences. All metrics that were measured as percentages were arcsine transformed and Branch Density/m<sup>2</sup> was log + 1 transformed prior to comparisons.)

Metric	Group			
	High	Medium	Low	Control
<i>SAV</i>				
Branch Density/m <sup>2</sup>	A	A	B	AB
% Total SAV	A	B	B	B
% Total Mat	A	A	A	A
% Forageable SAV	A	A	A	A
% BDS on SAV	A	B	C	C
% Algae on SAV	A	A	AB	B
% Algae + %BDS on SAV	A	B	C	D
Modified Condition Index	A	AB	B	AB
DWQ Condition Index	A	B	B	AB
<i>Leaf Nutrients &amp; Isotopes</i>				
15N/14NAIR	A	B	C	C
13C/12CVPDB	A	A	A	A
Wt% N	A	A	A	A
Wt% C	A	B	B	B
C:N ratio	A	AB	BC	C
P SAV Leaves	A	B	B	B
<i>Algal Nutrients &amp; Isotopes</i>				
15N/14NAIR	A	A	A	A
13C/12CVPDB	A	A	A	A
Wt% N	A	AB	AB	B
Wt% C	A	A	A	A
C:N ratio	A	AB	B	C
P Algae	AB	B	AB	A

## APPENDIX E. Comparison between cumulative degree days and Julian Date

Table E.1 Comparison between cumulative degree days and Julian Date. Lower Threshold was set at 10 °C.

Weekly JD	Date	Cumulative	
		Degree WS2	Days WS6
108	4/18/2013	0.96	0.56
126	5/6/2013	2.37	1.66
133	5/13/2013	2.83	2.04
141	5/21/2013	3.25	2.42
149	5/29/2013	3.6	2.78
164	6/13/2013	4.05	3.31
171	6/20/2013	4.17	3.48
178	6/27/2013	4.28	3.64
191	7/10/2013	4.76	4.11

Table E.2. Pearson's correlation matrix of cumulative degree days vs. weekly Julian date

Variables	WS2	WS6	AVG	Weekly JD
WS2	<b>1</b>	<b>0.995</b>	<b>0.999</b>	<b>0.965</b>
WS6	<b>0.995</b>	<b>1</b>	<b>0.999</b>	<b>0.987</b>
AVG	<b>0.999</b>	<b>0.999</b>	<b>1</b>	<b>0.977</b>
Weekly JD	<b>0.965</b>	<b>0.987</b>	<b>0.977</b>	<b>1</b>

## APPENDIX F. Correlation matrix (Pearson) of CART chemical and physical parameters of surface water samples

Table F.1 Correlation matrix (Pearson) of CART chemical and physical parameters of surface water samples

Variables	OrthoP	Dis_NO2+NO3	T_NO2+NO3	Tot_TKN	T P	DIS TN	T D S	Tot Alk	Weekly JD	Temp	NO3-N Flux	PO4-P Flux	H2O Depth
Dis_OrthoP_mg/l	<b>1.00</b>	<b>0.50</b>	<b>0.32</b>	<b>0.60</b>	<b>0.62</b>	<b>0.65</b>	<b>0.59</b>	<b>0.33</b>	<b>0.65</b>	<b>0.51</b>	<b>0.47</b>	<b>0.54</b>	<b>-0.46</b>
Dis_NO2+N O3(mg/l)	<b>0.50</b>	<b>1.00</b>	<b>0.72</b>	<b>0.18</b>	<b>0.20</b>	<b>0.28</b>	<b>0.23</b>	<b>0.32</b>	<b>0.24</b>	<b>0.13</b>	<b>0.38</b>	<b>0.43</b>	<b>-0.08</b>
T_NO2+NO3(mg/l)	<b>0.32</b>	<b>0.72</b>	<b>1.00</b>	0.11	0.12	0.11	0.07	0.16	0.07	0.05	<b>0.47</b>	<b>0.50</b>	0.02
Tot_TKN(mg/l)	<b>0.60</b>	<b>0.18</b>	0.11	<b>1.00</b>	<b>0.88</b>	<b>0.91</b>	<b>0.92</b>	<b>0.57</b>	<b>0.92</b>	<b>0.68</b>	<b>0.29</b>	<b>0.40</b>	<b>-0.84</b>
T P	<b>0.62</b>	<b>0.20</b>	0.12	<b>0.88</b>	<b>1.00</b>	<b>0.92</b>	<b>0.92</b>	<b>0.55</b>	<b>0.93</b>	<b>0.51</b>	<b>0.30</b>	<b>0.41</b>	<b>-0.83</b>
DIS TN	<b>0.65</b>	<b>0.28</b>	0.11	<b>0.91</b>	<b>0.92</b>	<b>1.00</b>	<b>0.97</b>	<b>0.65</b>	<b>0.98</b>	<b>0.61</b>	<b>0.32</b>	<b>0.43</b>	<b>-0.83</b>
TDS	<b>0.59</b>	<b>0.23</b>	0.07	<b>0.92</b>	<b>0.92</b>	<b>0.97</b>	<b>1.00</b>	<b>0.68</b>	<b>0.99</b>	<b>0.62</b>	<b>0.23</b>	<b>0.36</b>	<b>-0.88</b>
Tot Alk	<b>0.33</b>	<b>0.32</b>	0.16	<b>0.57</b>	<b>0.55</b>	<b>0.65</b>	<b>0.68</b>	<b>1.00</b>	<b>0.64</b>	<b>0.01</b>	<b>0.33</b>	<b>0.44</b>	<b>-0.33</b>
Weekly JD	<b>0.65</b>	<b>0.24</b>	0.07	<b>0.92</b>	<b>0.93</b>	<b>0.98</b>	<b>0.99</b>	<b>0.64</b>	<b>1.00</b>	<b>0.66</b>	<b>0.28</b>	<b>0.40</b>	<b>-0.86</b>
Temperature (deg C)	<b>0.51</b>	0.13	0.05	<b>0.68</b>	<b>0.51</b>	<b>0.61</b>	<b>0.62</b>	0.01	<b>0.66</b>	<b>1.00</b>	0.12	0.15	<b>-0.72</b>
NO3-N Flux	<b>0.47</b>	<b>0.38</b>	<b>0.47</b>	<b>0.29</b>	<b>0.30</b>	<b>0.32</b>	<b>0.23</b>	<b>0.33</b>	<b>0.28</b>	<b>0.12</b>	<b>1.00</b>	<b>0.98</b>	0.01
PO4-P Flux	<b>0.54</b>	<b>0.43</b>	<b>0.50</b>	<b>0.40</b>	<b>0.41</b>	<b>0.43</b>	<b>0.36</b>	<b>0.44</b>	<b>0.40</b>	<b>0.15</b>	<b>0.98</b>	<b>1.00</b>	<b>-0.11</b>
H2O Depth(cm)	<b>-0.46</b>	<b>-0.08</b>	0.02	<b>-0.84</b>	<b>-0.83</b>	<b>-0.83</b>	<b>-0.88</b>	<b>-0.33</b>	<b>-0.86</b>	<b>-0.72</b>	0.01	<b>-0.11</b>	<b>1.00</b>

Values in bold are different from 0 with a significance level  $\alpha=0.05$

## REFERENCES

- Aldrich, T.W. and Paul, D.S., 2002. Avian ecology of Great Salt Lake. Great Salt Lake: An Overview of Change. Special publication of the Utah Department of Natural Resources, Salt Lake City, Utah: 343-374.
- Baggett, L.P., Heck Jr, K.L., Frankovich, T.A., Armitage, A.R., and Fourqurean, J.W., 2010. Nutrient enrichment, grazer identity, and their effects on epiphytic algal assemblages: field experiments in subtropical turtlegrass *Thalassia testudinum* meadows.
- Bakker, E.S., E. Van Donk, S.A.J. Declerck, N.R. Helmsing, B. Hidding, and B.A. Nolet. 2010. Effect of macrophyte community composition and nutrient enrichment on plant biomass and algal blooms. *Basic and Allied Ecology* 11:432-439.
- Bellrose, F.C. and Low, J.B., 1978. Advances in waterfowl management research. *Wildlife Society Bulletin*: 63-72.
- BUHAN, E., H.M. DOĞAN, S. DİRİM BUHAN, S. ÖZDEMİR, F. POLAT, Ç.N. DOĞAN. 2013. Investigating phosphorus and turbidity removal efficiencies of main aquatic vegetation species in the Lower Kelkit Basin of Turkey. *Turkish Journal of Botany* 37:744-752.
- Carling, G.T., Richards, D. C., Hoven, H., Miller, T., Fernandez, D. P., Rudd, A., Pazmino, E., and Johnson, W. P., 2013. Relationships of surface water, pore water, and sediment chemistry in wetlands adjacent to Great Salt Lake, Utah, and potential impacts on plant community health. *Science of The Total Environment*, 443: 798-811.
- Carpenter S.R. & D.M. Lodge. 1986. Effects of submersed macrophytes on ecosystem processes. *Aquatic Botany* 341-370.
- Cloern, J.E., E.A. Canuel, & D. Harris. 2002. Stable carbon and nitrogen isotope composition of aquatic and terrestrial plants of the San Francisco Bay estuarine system. *Limnol. Oceanogr.*, 47(3):713–729.
- Conover W.J. and Iman (1999). *Practical Nonparametric Statistics*, 3rd edition, Wiley.
- DEMARS, B. O. L. and EDWARDS, A. C. (2007), Tissue nutrient concentrations in freshwater aquatic macrophytes: high inter-taxon differences and low phenotypic response to nutrient supply. *Freshwater Biology*, 52:2073–2086.
- Denbleyker, Jeff. "Hydrology and Nutrient Loads." Utah Division of Water Quality: Science Panel Meetings. Utah Division of Water Quality, 29 01 2013. Web. 10 Oct 2013. <<http://www.willardspur.utah.gov/panel/meetings.htm>>.
- Denbleyker, Jeff. "Plant effluent." Message to Joel Pierson. 28 10 2013. E-mail.
- Downing, J.A., 2010. Emerging global role of small lakes and ponds: little things mean a lot. *Limnetica*, 1(29): 9-24.

- Dunn O.J. (1964). Multiple Comparisons Using Rank Sums. *Technometrics*, 6(3):241-252.
- DWQ 2011. Standard operating procedure for determining percent cover of aquatic vegetation in wetlands; Willard Spur 2011 monitoring activities. State of Utah Department of Environmental Quality, Division of Water Quality; 09092011\_WS.doc.
- Esteves, B. dos S. & M.S. Suzuki. 2010. Limnological variables and nutritional content of submerged aquatic macrophytes in a tropical lagoon. *Acta Limnologica Brasiliensia* 22(2):187-198.
- Farquhar, G.D., J.R. Ehleringer, & K.T. Hubick. 1989. Carbon isotope discrimination and photosynthesis. *Annual Review of Plant Physiology and Plant Molecular Biology*. 40:503-37. Gross, E.M., C. Feldbaum, & A. Graf. 2003. Epiphyte biomass and elemental composition on submersed macrophytes in shallow eutrophic lakes. *Hydrobiologia* 506-509:559-565.
- Furman, B.T. and Heck, K., 2008. Effects of nutrient enrichment and grazers on coral reefs: an experimental assessment. *Mar Ecol Prog Ser*, 363: 89-101.
- Gorrell, J.V., Andersen, M. E., Bunnell, K. D., Canning, M. F., Clark, A. G., Dolsen D. E., and Howe F. P., 2005. Utah comprehensive wildlife conservation strategy (CWCS). Utah Division of Wildlife Resources Salt Lake City, UT.
- Heaton, T., 1986. Isotopic studies of nitrogen pollution in the hydrosphere and atmosphere: a review. *Chemical Geology*, 59(1): 87-102.
- Heck, K.L., Jr., Pennock, J.R., Valentine, J.F., Coen, L.D., and Sklenar, S.A., 2000. Effects of Nutrient Enrichment and Small Predator Density on Seagrass Ecosystems: An Experimental Assessment. *Limnology and Oceanography*, 45(5): 1041-1057.
- Hollander M. and Wolfe D. A. (1999). *Nonparametric Statistical Methods*, Second Edition. John Wiley and Sons, New York.
- Horppila J. & L. Nurminen. 2003. Effects of submerged macrophytes on sediment resuspension and internal phosphorus loading in Lake Hiidenvesi (southern Finland). *Water Research* 37:4468–4474.
- Hoven, H.M. 2010. The 2009 Report on SAV Condition in Farmington Bay and other Impounded wetlands of Great Salt Lake. The Institute for Watershed Sciences, Kamas, Utah. 39 pp.
- Hoven, H.M. and Miller, T.G., 2009. Developing vegetation metrics for the assessment of beneficial uses of impounded wetlands surrounding Great Salt Lake, Utah, USA. *Natural Resources and Environmental Issues*, 15(1): 11.
- Hoven, H., W. Johnson, D. Richards, S. Rushforth, S. Rushforth, R. Goel, J. Pierson, M. Hogsett, R. Nasrabadi, & S. Kissell. 2013a. Willard Spur Nutrient Cycling Report January 2013 to the Willard Spur Science Panel.

- Hoven, H.M., D. Richards, W.P. Johnson & G.T. Carling 2011. Plant Metric Refinement for Condition Assessment of Great Salt Lake Impounded Wetlands, Final Report: June 7, 2011. IWSciences, Kamas, Utah. 44pp.
- Hoven, H.M., D. Richards, & W.P. Johnson. 2013b. Comparison of assessment metrics for impounded wetlands of Farmington Bay, Great Salt Lake. The Institute for Watershed Sciences, Kamas, Utah. 69 pp.
- Hoven, H.M. , Johnson, W.P., Goel, R.K., Richards, D.C., and Rushforth S.. In preparation.
- Howard-Williams, C. 1981. Studies on the ability of a *Potamogeton pectinatus* community to remove dissolved nitrogen and phosphorus compounds from lake water. *Journal of Applied Ecology*, 18(2) 619-637.
- Howard-Williams, C. & B. R. Allanson. 1981. Phosphorus cycling in a dense *Potamogeton pectinatus* L. Bed. *Oecologia* 49(1): 56-66.
- Huebert, D.B. & P.R. Gorham. 1983. Biphasic mineral nutrition of the submerged aquatic macrophyte *Potamogeton pectinatus* L. *Aquatic Botany* 16:269-284.
- Hurlbert, S. H. 1984. Pseudoreplication and the Design of Ecological Field Experiments. *Ecological Monographs* 54:187–211.
- James, W. F. 2007. *Experimental effects of lime application on aquatic macrophytes:4. Growth response of three species*. APCRP Technical Notes Collection (ERDC/TN APCRP-EA-14). Vicksburg, MS: U.S. Army Engineer Research and Development Center.
- Johnson, A.M., 2008. Food abundance and energetic carrying capacity for wintering waterfowl in the Great Salt Lake wetlands.
- Kadlec, J.A., 2002. Avian botulism in Great Salt Lake marshes: perspectives and possible mechanisms. *Wildlife Society Bulletin*, 30(3): 983-989.
- Keeley, J.E. 1989. Stable carbon isotopes in vernal pool aquatics of differing photosynthetic pathways. In: *Stable Isotopes in Ecological Research*, Ecological Studies Volume 68; P.W. Rundel, J.R. Ehleringer, and K.A. Nagy, eds., Springer-Verlag, New York; pp. 77-81.
- Keeley, J.E. 1991. Interactive role of stresses on structure and function in aquatic plants. In: *Response of Plants to Multiple Stresses*; H.A. Mooney, W.E. Winner, E.J. Pell, & E. Chu., eds. Academic Press., Inc. pp. 329-343.
- Keeley, J.E., L.O. Sternberg, & M.J. Deniro. 1986. The use of stable isotopes in the study of photosynthesis in freshwater plants. *Aquatic Botany* 26:213-223.
- Keeley, J.E. & D.R. Sandquist. 1992. Carbon: freshwater plants. *Plant, Cell and Environment* 15:1021-1035.

- Li, W., T. Cao, L. Ni, X. Zhang, G. Zhu, P. Xie. 2013. Effects of water depth on carbon, nitrogen and phosphorus stoichiometry of five submersed macrophytes in an in situ experiment. *Ecological Engineering* 61:358– 365.
- Lucas, W. J. 1983. Photosynthetic assimilation of exogenous  $\text{HCO}_3^-$  by aquatic plants. *Annu. Rev. Plant Physiol.* 34:71-104.
- McCormick, P.V. and Laing, J.A., 2003. Effects of increased phosphorus loading on dissolved oxygen in a subtropical wetland, the Florida Everglades. *Wetlands Ecology and Management*, 11(3): 199-216.
- Naftz, D., Angerth, C., Kenney, T., Waddell, B., Darnall, N., Silva, S., Perschon C., and Whitehead, J., 2008. Anthropogenic influences on the input and biogeochemical cycling of nutrients and mercury in Great Salt Lake, Utah, USA. *Applied Geochemistry*, 23(6): 1731-1744.
- O'Leary, M.H. 1981. Review: Carbon isotope fractionation in plants. *Phytochemistry*; 20(4):553-567.
- Ozimek T., R.D. Gulati, & E. van Donk. 1990. Can macrophytes be useful in biomanipulation of lakes? The Lake Zwemlust example. *Hydrobiologia* 200/201:399-407.
- Ostermiller, Jeff. "Hydrology & Nutrient Loads." Utah Division of Water Quality: Science Panel Meetings. Utah Division of Water Quality, 05 04 2012. Web. 15 Sep 2013. <<http://www.willardspur.utah.gov/panel/meetings.htm>>.
- Ostermiller, Jeff. "Water Chemistry." Utah Division of Water Quality: Science Panel Meetings. Utah Division of Water Quality, 29 01 2013. Web. 15 Sep 2013. <<http://www.willardspur.utah.gov/panel/meetings.htm>>.
- Paul, D.S., and A.E. Manning. 2002. Great Salt Lake Waterbird Survey Five-Year Report (1997–2001). Publication Number 08-38. Utah Division of Wildlife Resources, Salt Lake City.
- Poulton, P., Johnston, A., and White, R., 2012. Plant, available soil phosphorus. Part I: the response of winter wheat and spring barley to Olsen P on a silty clay loam. *Soil Use and Management*.
- Sand-Jensen, K. 1982. Photosynthetic carbon sources of stream macrophytes. *Journal of Experimental Biology* 34(2):198-210.
- Sand-Jensen, K., T. Riis, O. Vestergaard, & S.E. Larsen. 2000. Macrophyte decline on Danish lakes and streams over the past 100 years. *Journal of Ecology* 88: 1030-1040.
- Søndergaard, M. 1988. Photosynthesis of aquatic plants under natural conditions. In: *Vegetation of Inland Waters: Handbook of vegetation science*. J.J. Symoens, ed. Kluwer Academic Publishers. pp. 63 – 113.
- Steel R. G. D. (1961). Some rank sum multiple comparison tests. *Biometrics*, 17:539-552.
- Twilley, R.R., W.M. Kemp, K.W. Staver, J.C. Stevenson, & W.R. Boynton. 1985. Nutrient enrichment of

- estuarine submersed plant communities. 1. Algal growth and effects on production of plants and associated communities. *Marine Ecology Progress Series*, 23:179-191.
- Utah. Division of Water Quality. Willard Spur: willardspurgenerallocation. 2013. Photograph. willardspur.utah.gov, Salt Lake City. Web. 12 Sep 2013. <<http://www.willardspur.utah.gov/images/maps/willardspurgenerallocation.jpg>>.
- Vahtera, E., Conley, D. J., Gustafsson, B. G., Kuosa, H., Pitkanen, H., Savchuk, O. P., Tamminen, T., Viitasalo, M., Voss, M., and Wasmund N., 2007. Internal ecosystem feedbacks enhance nitrogen-fixing cyanobacteria blooms and complicate management in the Baltic Sea. *AMBIO: A journal of the Human Environment*, 36(2): 186-194.
- Vest, J.L., Conover, and M.R., 2011. Food habits of wintering waterfowl on the Great Salt Lake, Utah. *Waterbirds*, 34(1): 40-50.
- Waddell, K.M. and Giddings, E.M., 2004. Trace elements and organic compounds in sediment and fish tissue from the Great Salt Lake basins, Utah, Idaho, and Wyoming, 1998, 1999. *Water Resources Investigations Report 03-4283*.
- Westlake, D.F. 1967. Some effects of low velocity currents on the metabolism of aquatic macrophytes. *Journal of Experimental Botany*. 18:187-205.
- "Wildlife and Habitat." Bear River Migratory Bird Refuge: Wildlife and Habitat. U.S. Fish and Wildlife Service. Web. 19 Jan 2014. <<http://www.fws.gov/refuges/profiles/WildHabitat.cfm?ID=65530>>.
- Winter, K. 1978. Short-term fixation of <sup>14</sup>Carbon by the submerged aquatic angiosperm *Potamogeton pectinatus*. *Journal of Experimental Botany* 29(112):1169-1172.
- Wurts, W.A. & R.M. Durborow. 1992. Interactions of pH, Carbon Dioxide, Alkalinity and Hardness in Fish Ponds. SRAC Pub. No. 464.
- Vymazal, J. 1995. *Algae and element cycling in wetlands*. CRC Press, Boca Raton.
- Zhu, M., Zhu, G., Li, W., Zhang, Y., Zhao, L., and Gu, Z., 2013. Estimation of the algal-available phosphorus pool in sediments of a large, shallow eutrophic lake (Taihu, China) using profiled SMT fractional analysis. *Environmental Pollution*, 173(0): 216-223.